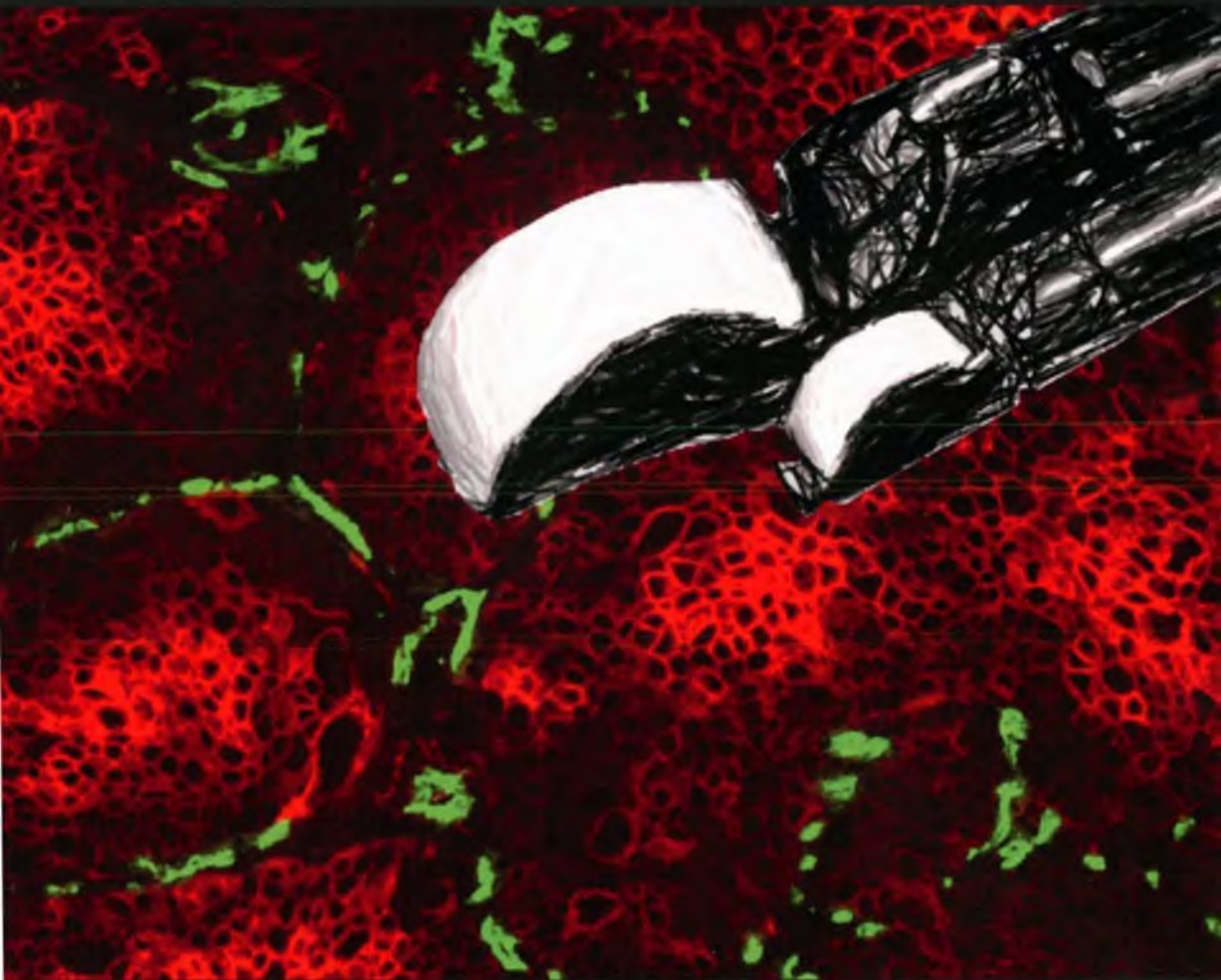# Tumour microenvironment and clinical diagnostic approach in lung cancer patients

Olga CJ Schuurbiers

Tumour microenvironment and clinical diagnostic approach in lung cancer patients

Olga CJ Schuurbiers

O.C.J. Schuurbiers-Siebers

Tumour microenvironment and clinical diagnostic approach in lung cancer patients.

Thesis Radboud University Nijmegen Medical Centre, with summary in Dutch.

Tumour microenvironment and clinical diagnostic approach in lung cancer patients

Een wetenschappelijke proeve op het gebied van de

Medische Wetenschappen

Proefschrift

ter verkrijging van de graad van doctor

aan de Radboud Universiteit Nijmegen

op gezag van de rector magnificus prof. Mr. S.C.J.J. Kortmann

volgens besluit van het College van Decanen

in het openbaar te verdedigen op woensdag 18 december 2013

om 14.30 uur precies

door

Olga Cornelia Johanna Schuurbiers

geboren op 28 april 1970

te Nijmegen

Promotoren

Prof. dr. J.H.A.M. Kaanders

Prof. dr. W.J.G. Oyen

Prof. dr. P.N.R. Dekhuijzen

Copromotoren

Dr. J. Bussink

Dr. H.F.M. van der Heijden

Manuscriptcommissie:

Prof. dr. M. Prokop (voorzitter), radiologie, UMC St Radboud

Prof. dr. W.T.A. van der Graaf, medische oncologie, UMC St Radboud

Prof. dr. M.A.G.G. Vooijs, moleculaire biologie, Maastricht UMC

Contents

Chapter 1

Introduction and outline

∞

Introduction

Lung cancer is the leading cause of cancer related death worldwide.[1] According to the World Health Organization (WHO) nearly 6 million people die from tobacco-related causes every year. More than 5 million are smokers and ex-smokers and more than 600.000 are nonsmokers exposed to second-hand smoke. Tobacco use is the most important risk factor for cancer causing 22% of global cancer deaths and 71% of global lung cancer deaths.[2]

Lung cancer is classified into two groups: non-small cell lung cancer (NSCLC) which is accountable in 87% of cases and 10-15% concerns small cell lung cancer (SCLC).[3] Treatment options in NSCLC patients mainly depend on TNM stage.[4] At the time of diagnosis NSCLC is often locally or systemically advanced resulting in an overall 5-year survival of only 16%. Approximately 25% of patients are potentially curable with surgery but half of those die due to recurrent disease.[5]

In the past 20 years stage migration has occurred due to improved staging techniques such as [18]fluorodeoxyglucose positron emission tomography ([18]FDG-PET) and endoscopic ultrasound-guided biopsy techniques like esophageal ultrasound-guided fine-needle aspiration (EUS-FNA) and endobronchial ultrasound transbronchial needle aspiration (EBUS-TBNA) but also due to changes in the TNM classification system.[6-12] [18]FDG-PET is recommended as standard work-up of potentially curable lung cancer patients according to the American College of Chest Physicians (ACCP) guidelines and the dutch national guideline on NSCLC staging and treatment.[13] With the implementation of [18]FDG-PET in 10-20% of cases distant metastasis are detected.[13-15] For mediastinal staging [18]FDG-PET is usefull to localize potentially involved mediastinal lymph nodes or to a certain extent exclude metastases. EUS and EBUS have proven to be superior techniques to obtain material for definite histologic proof of metastases. The value of endoscopic ultrasound techniques in mediastinal staging has been demonstrated[6,8] and prevents futile mediastinoscopies or thoracotomies in 70% of cases.[16] Complete mediastinal staging with combined EUS and EBUS, if negative followed by cervical mediastinoscopy in comparison to cervical mediastinoscopy alone results in a sensitivity of 94% vs 80% and a negative predictive value of 93% vs 86% for detection of lymph node metastasis.[17]

A prognostic factor provides information on the outcome of disease for a particular group of patients. Predictive factors prospectively determine or predict the outcome after a certain therapy, for example the presence of an EGFR mutation which is predictive for the response to treatment with tyrosine kinase inhibitors (TKI) that block EGFR signalling.[18] Prognostic factors provide information about tumor characteristics that are associated with a better or worse prognosis but can be – to a certain extent – dependent on treatment strategies.[19] To date the TNM classification still is the most important prognostic factor and essential for treatment guidance. However, this staging system is not always able to explain differences in relapse and survival between individual patients with the same disease stage, since the

TNM staging system does not provide information about the biologic behavior of the tumor cells.[20]

Emerging evidence suggests that histology might be prognostic or predictive for clinical outcome as was reviewed by Hirsch and coworkers. A consistent link between histology and treatment outcome was established between expression of epidermal growth factor receptor (EGFR) mutations (more frequent in adenocarcinoma) and outcome of EGFR-TKI treatment.[21] Significant differences in survival with respect to histology have also been shown in first line chemotherapy with pemetrexed.[22,23] Pemetrexed is an antifolate that acts by disrupting several folate-dependent metabolic processes essential for cell replication through inhibition of thymidylate synthase and other enzymes.[24] Overexpression of thymidylate synthase correlated with reduced sensitivity to pemetrexed in preclinical studies.[25,26] Baseline thymidylate synthase expression in chemo-naïve NSCLCs is higher in squamous cell carcinoma compared to adenocarcinoma and correlates with poor prognosis in NSCLC.[27,28] A meta-analysis (5 studies) confirmed this treatment-by-histology interaction for pemetrexed.[29]

Biological behavior of cancer cells is not only determined by tumor cell characteristics but is also dependent of the tumor microenvironment. In malignant tumors metabolism is influenced by hypoxia as with growing mass and abnormal vasculature, areas with low oxygen supply arise. In normal tissue energy production is mainly via aerobic oxidative phosphorylation: After glycolysis, pyruvate is oxidated in the mitochondria to produce energy (ATP). In cancer cells, however, a high rate of anaerobic glycolysis is observed also in the presence of oxygen and is associated with selective growth and tumor cell survival (Warburg effect)[30]. Hypoxia is a feature of most tumors and is a negative prognostic and predictive factor due to its role in angiogenesis, invasiveness, metastasis, resistance to cell death, altered metabolism and genomic instability.[31] Hypoxia, anaerobic metabolism and intracellular acidosis are associated with more aggressive tumor behavior and impaired response to radiotherapy and chemotherapy.[31-37] The higher rate of glycolysis with the consequential higher glucose consumption of tumor cells is one of the reasons why [18]FDG-PET is useful as an imaging biomarker in solid tumors.[38] Glucose transporters (GLUT) are considered to be the most important mechanism for glucose influx into cells.[39] The anaerobic glucose metabolism in tumor cells provides less energy than normal aerobic glycolysis and thus more glucose uptake is required. As anaerobic glycolysis leads to substantial more lactate production, this may lead to intracellular acidosis. The intracellular pH is regulated amongst others by CAIX (carbonic anhydrase IX) and passive transport of lactate by MCT-4 (monocarboxyl transporter 4).[37] Under aerobic conditions lactate can be used by tumor cells for oxidative metabolism.[40]

In the field of lung cancer research and also in daily management of lung cancer patients, there is growing awareness that treatment of lung cancer patients is more and more individualized. Besides clinical studies to the effect of certain treatment approaches further insight in histology specific tumor behavior and the tumor microenvironment may

contribute to improved treatment outcome. This thesis focuses on multimodality diagnostics and the tumor microenvironment, which both may contribute to further insight in lung cancer behavior and can provide us valuable information for multimodality and/or multidisciplinary lung cancer treatment.

Outline of this thesis

The phosphatidylinositol-3-kinase (PI3-K)/protein kinase B (AKT) pathway is associated with all three major radiation resistance mechanisms: intrinsic radiosensitivity, tumor cell proliferation, and hypoxia. In cell signaling cascades, the PI3-K/AKT signaling pathway is a key regulator of normal and cancerous growth and cell fate decisions by processes such as proliferation, invasion, apoptosis, and induction of hypoxia-related proteins. Activation of this pathway can be the result of stimulation of receptor tyrosine kinases such as epidermal growth factor receptor or vascular endothelial growth factor receptor or from mutations or amplification of PI3-K or AKT itself which are frequently found in NSCLC. Furthermore, several treatment modalities such as radiotherapy can activate this survival pathway. Monitoring and manipulation of this signal transduction pathway may have important implications for the management of NSCLC. For this purpose studies concerning the PI3K-AKT pathway in non-small cell lung cancer in relation to radiation resistance were reviewed in **chapter 2**.

In **chapter 3 and 4** correlations between metabolic markers, their relation to FDG-PET and the association with recurrence and survival in curatively resected stage I, II and limited stage III NSCLC patients were studied. Differences in glucose metabolism between adeno- and squamous cell lung carcinomas were quantified using the hypoxia and glycolysis-related markers GLUT1, MCT1, MCT4, CAIX, vascular density and ^{18}FDG-PET imaging in patients with curatively resected stage I-IIIA NSCLC. Furthermore, the associations of these differences with treatment and survival were analyzed.

Staging procedures in lung cancer patients include ^{18}FDG-PET as a first step towards defining the stage of disease. Based on outcome of ^{18}FDG-PET choices are made for further cytological or histological confirmation. In a subset of patients with (suspected) lung cancer the presence of another tumor or suspicion of metastasis can be detected by ^{18}FDG-PET. Histological proof of a pulmonary metastasis of another primary tumor or a synchronic lung tumor can be essential for further management. Sometimes invasive procedures such as video assisted thoracoscopic surgery or thoracotomy are necessary to provide tissue. ^{18}FDG-PET might provide metabolic information that could be used to differentiate between synchronous tumors and metastatic disease. This potential role of ^{18}FDG-PET is investigated in **chapter 5**.

With the introduction of EUS-FNA and EBUS-TBNA further progress has been made in staging procedures. EUS-FNA prevented 70% of scheduled surgical interventions in patients with (suspected) lung cancer because of the demonstration of mediastinal metastases or tumor invasion (69%) or by establishing an alternative diagnosis (1%).[16] A complete mediastinal staging is possible with combined EUS and EBUS.[6-8,12,41] Among patients with (suspected) NSCLC, a staging strategy combining endosonography and surgical staging compared with surgical staging alone resulted in greater sensitivity for mediastinal nodal metastases and fewer unnecessary thoracotomies.[17,42] Adrenal glands are a predilection side for metastatic spread in lung cancer patients. Due to a limited positive predictive value of both CT and PET-CT for the assessment of adrenal gland metastases tissue proof can be important for further treatment management. Former reports about EUS-FNA for the assessment of left adrenal gland (LAG) metastases in lung cancer patients are limited and rarely take [18]FDG-PET findings into account. The aim of the study described in **chapter 6** was to investigate the sensitivity of EUS-FNA in detecting LAG metastasis in lung cancer patients with a suspect LAG on [18]FDG-PET/CT.

EGFR and KRAS mutation analysis is used to select patients who may benefit from treatment with TKIs.[43-46] Tissue samples are not only needed for diagnosis but also for further characterization of tumor biology on which treatment decisions can be based. In advanced lung cancer diagnostic procedures not always provide histological samples for further analysis. Many patients are characterized as stage III/IV based on cytological punctures such as EUS and EBUS. For this purpose the feasibility of EGFR/KRAS mutation analysis in trans-esophageal ultrasound- and endobronchial ultrasound-guided fine needle aspirates was studied in **chapter 7**.

12

References

1.   Jemal A, Bray F, Center MM, Ferlay J, Ward E, Forman D. Global cancer statistics. CA Cancer J Clin 2011;61(2):69-90.

2.   WHO. WHO report on the global tobacco epidemic. 2011.

3.   Devesa SS, Bray F, Vizcaino AP, Parkin DM. International lung cancer trends by histologic type: male:female differences diminishing and adenocarcinoma rates rising. Int J Cancer 2005;117(2):294-9.

4.   Goldstraw P, Ball D, Jett JR, Le CT, Lim E, Nicholson AG, et al. Non-small-cell lung cancer. Lancet 2011;378(9804):1727-40.

5.   Chansky K, Sculier JP, Crowley JJ, Giroux D, Van MJ, Goldstraw P. The International Association for the Study of Lung Cancer Staging Project: prognostic factors and pathologic TNM stage in surgically managed non-small cell lung cancer. J Thorac Oncol 2009;4(7):792-801.

6.   Adams K, Shah PL, Edmonds L, Lim E. Test performance of endobronchial ultrasound and transbronchial needle aspiration biopsy for mediastinal staging in patients with lung cancer: systematic review and meta-analysis. Thorax 2009;64(9):757-62.

7.   Gu P, Zhao YZ, Jiang LY, Zhang W, Xin Y, Han BH. Endobronchial ultrasound-guided transbronchial needle aspiration for staging of lung cancer: a systematic review and meta-analysis. Eur J Cancer 2009;45(8):1389-96.

8.   Micames CG, McCrory DC, Pavey DA, Jowell PS, Gress FG. Endoscopic ultrasound-guided fine-needle aspiration for non-small cell lung cancer staging: A systematic review and metaanalysis. Chest 2007;131(2):539-48.

9.   Mountain CF. Revisions in the International System for Staging Lung Cancer. Chest 1997;111(6):1710-7.

10.   Pieterman RM, van Putten JW, Meuzelaar JJ, Mooyaart EL, Vaalburg W, Koeter GH, et al. Preoperative staging of non-small-cell lung cancer with positron-emission tomography. N Engl J Med 2000;343(4):254-61.

11.   Tinteren van H., Hoekstra OS, Smit EF, van den Bergh JH, Schreurs AJ, Stallaert RA, et al. Effectiveness of positron emission tomography in the preoperative assessment of patients with suspected non-small-cell lung cancer: the PLUS multicentre randomised trial. Lancet 2002;359(9315):1388-93.

12.   Varela-Lema L, Fernandez-Villar A, Ruano-Ravina A. Effectiveness and safety of endobronchial ultrasound-transbronchial needle aspiration: a systematic review. Eur Respir J 2009;33(5):1156-64.

13.   Niet-kleincellig longcarcinoom. Landelijke richtlijn. Versie 2.0. 2011.

14.   Silvestri GA, Gould MK, Margolis ML, Tanoue LT, McCrory D, Toloza E, et al. Noninvasive staging of non-small cell lung cancer: ACCP evidenced-based clinical practice guidelines (2nd edition). Chest 2007;132(3 Suppl):178S-201S.

15. Schrevens L, Lorent N, Dooms C, Vansteenkiste J. The role of PET scan in diagnosis, staging, and management of non-small cell lung cancer. Oncologist 2004;9(6):633-43.

16. Annema JT, Versteegh MI, Veselic M, Voigt P, Rabe KF. Endoscopic ultrasound-guided fine-needle aspiration in the diagnosis and staging of lung cancer and its impact on surgical staging. J Clin Oncol 2005;23(33):8357-61.

17. Annema JT, van Meerbeeck JP, Rintoul RC, Dooms C, Deschepper E, Dekkers OM, et al. Mediastinoscopy vs endosonography for mediastinal nodal staging of lung cancer: a randomized trial. JAMA 2010;304(20):2245-52.

18. Maemondo M, Inoue A, Kobayashi K, Sugawara S, Oizumi S, Isobe H, et al. Gefitinib or chemotherapy for non-small-cell lung cancer with mutated EGFR. N Engl J Med 2010;362(25):2380-8.

19. Thunnissen FB, Schuurbiers OC, den Bakker MA. A critical appraisal of prognostic and predictive factors for common lung cancers. Histopathology 2006;48(7):779-86.

20. In: Goldstraw P, editor. Staging manual in thoracic oncology. An International Association for the study of Lung Cancer Publication. 2009.

21. Hirsch FR, Spreafico A, Novello S, Wood MD, Simms L, Papotti M. The prognostic and predictive role of histology in advanced non-small cell lung cancer: a literature review. J Thorac Oncol 2008;3(12):1468-81.

22. Hanna N, Shepherd FA, Fossella FV, Pereira JR, De MF, von PJ, et al. Randomized phase III trial of pemetrexed versus docetaxel in patients with non-small-cell lung cancer previously treated with chemotherapy. J Clin Oncol 2004;22(9):1589-97.

23. Scagliotti GV, Parikh P, von PJ, Biesma B, Vansteenkiste J, Manegold C, et al. Phase III study comparing cisplatin plus gemcitabine with cisplatin plus pemetrexed in chemotherapy-naive patients with advanced-stage non-small-cell lung cancer. J Clin Oncol 2008;26(21):3543-51.

24. Rollins KD, Lindley C. Pemetrexed: a multitargeted antifolate. Clin Ther 2005;27(9):1343-82.

25. Giovannetti E, Mey V, Nannizzi S, Pasqualetti G, Marini L, Del TM, et al. Cellular and pharmacogenetics foundation of synergistic interaction of pemetrexed and gemcitabine in human non-small-cell lung cancer cells. Mol Pharmacol 2005;68(1):110-8.

26. Sigmond J, Backus HH, Wouters D, Temmink OH, Jansen G, Peters GJ. Induction of resistance to the multitargeted antifolate Pemetrexed (ALIMTA) in WiDr human colon cancer cells is associated with thymidylate synthase overexpression. Biochem Pharmacol 2003;66(3):431-8.

27. Ceppi P, Volante M, Saviozzi S, Rapa I, Novello S, Cambieri A, et al. Squamous cell carcinoma of the lung compared with other histotypes shows higher messenger RNA and protein levels for thymidylate synthase. Cancer 2006;107(7):1589-96.

28. Nakagawa T, Otake Y, Yanagihara K, Miyahara R, Ishikawa S, Fukushima M, et al. Expression of thymidylate synthase is correlated with proliferative activity in non-small cell lung cancer (NSCLC). Lung Cancer 2004;43(2):145-9.

29. Al-Saleh K, Quinton C, Ellis PM. Role of pemetrexed in advanced non-small-cell lung cancer: meta-analysis of randomized controlled trials, with histology subgroup analysis. Curr Oncol 2012;19(1):e9-e15.

30. Warburg O, Posener K, Negelein E. Ueber den stoffwechsel der tumoren, on metabolism of tumors. In: Warburg O, editor. Constable, London.; 1930.

31. Wilson WR, Hay MP. Targeting hypoxia in cancer therapy. Nat Rev Cancer 2011;11(6):393-410.

32. Bristow RG, Hill RP. Hypoxia and metabolism. Hypoxia, DNA repair and genetic instability. Nat Rev Cancer 2008;8(3):180-92.

33. Brizel DM, Schroeder T, Scher RL, Walenta S, Clough RW, Dewhirst MW, et al. Elevated tumor lactate concentrations predict for an increased risk of metastases in head-and-neck. Int J Radiat Oncol Biol Phys 2001;51(2):349-53.

34. Lunt SJ, Chaudary N, Hill RP. The tumor microenvironment and metastatic disease. Clin Exp Metastasis 2009;26(1):19-34.

35. Walenta S, Salameh A, Lyng H, Evensen JF, Mitze M, Rofstad EK, et al. Correlation of high lactate levels in head and neck tumors with incidence of metastasis. Am J Pathol 1997;150(2):409-15.

36. Walenta S, Wetterling M, Lehrke M, Schwickert G, Sundfor K, Rofstad EK, et al. High lactate levels predict likelihood of metastases, tumor recurrence, and restricted patient survival in human cervical cancers. Cancer Res 2000;60(4):916-21.

37. Milosevic MF. Hypoxia, anaerobic metabolism and interstitial hypertension. In: Siemann DW, editor. Tumormicroenvironment. 1st ed. John Wiley and Sons, Ltd; 2011. p. 183-206.

38. Busk M, Horsman MR, Jakobsen S, Bussink J, van der KA, Overgaard J. Cellular uptake of PET tracers of glucose metabolism and hypoxia and their linkage. Eur J Nucl Med Mol Imaging 2008;35(12):2294-303.

39. Younes M, Brown RW, Stephenson M, Gondo M, Cagle PT. Overexpression of Glut1 and Glut3 in stage I nonsmall cell lung carcinoma is associated with poor survival. Cancer 1997;80(6):1046-51.

40. Sonveaux P, Vegran F, Schroeder T, Wergin MC, Verrax J, Rabbani ZN, et al. Targeting lactate-fueled respiration selectively kills hypoxic tumor cells in mice. J Clin Invest 2008;118(12):3930-42.

41. Wallace MB, Pascual JM, Raimondo M, Woodward TA, McComb BL, Crook JE, et al. Minimally invasive endoscopic staging of suspected lung cancer. JAMA 2008;299(5):540-6.

42. Annema JT, Versteegh MI, Veselic M, Welker L, Mauad T, Sont JK, et al. Endoscopic ultrasound added to mediastinoscopy for preoperative staging of patients with lung cancer. JAMA 2005;294(8):931-6.

43. Mok TS, Wu YL, Thongprasert S, Yang CH, Chu DT, Saijo N, et al. Gefitinib or carboplatin-paclitaxel in pulmonary adenocarcinoma. N Engl J Med 2009;361(10):947-57.

44. Rosell R, Moran T, Queralt C, Porta R, Cardenal F, Camps C, et al. Screening for epidermal growth factor receptor mutations in lung cancer. N Engl J Med 2009;361(10):958-67.

45. Shepherd FA, Rodrigues PJ, Ciuleanu T, Tan EH, Hirsh V, Thongprasert S, et al. Erlotinib in previously treated non-small-cell lung cancer. N Engl J Med 2005;353(2):123-32.

46. Shepherd FA, Tsao MS. Epidermal growth factor receptor biomarkers in non-small-cell lung cancer: a riddle, wrapped in a mystery, inside an enigma. J Clin Oncol 2010;28(6):903-5.

Chapter 2

The PI3-K/AKT-pathway and radiation resistance mechanisms in non-small cell lung cancer*

Olga CJ Schuurbiers

Johannes HAM Kaanders

Henricus FM van der Heijden

Richard PN Dekhuijzen

Wim JG Oyen

Johan Bussink

Abstract

The phosphatidylinositol-3-kinase (PI3-K)/protein kinase B (AKT) pathway is associated with all three major radiation resistance mechanisms: intrinsic radiosensitivity, tumor cell proliferation and hypoxia. In cell signalling cascades, the PI3-K/AKT signaling pathway is a key regulator of normal and cancerous growth and cell fate decisions by processes such as proliferation, invasion, apoptosis and induction of hypoxia-related proteins. Activation of this pathway can be the result of stimulation of receptor tyrosine kinases (TK) such as EGFR or VEGFR or from mutations or amplification of PI3-K or AKT itself which are frequently found in non-small cell lung cancer (NSCLC). Furthermore, several treatment modalities such as radiotherapy can stimulate this survival pathway. Monitoring and manipulation of this signal transduction pathway may have important implications for the management of NSCLC.

Strong and independent associations were found between expression of *activated* AKT (pAKT) and treatment outcome in clinical trials. Direct targeting and inhibition of this pathway may increase radiosensitivity by antagonizing the radiation induced cellular defense mechanisms especially in tumors that have activated the PI3-K/AKT cascade. To successfully implement these treatments in daily practice, there is a need for molecular predictors of sensitivity to inhibitors of PI3-K/AKT activation.

In conclusion, the PI3K/AKT pathway plays a crucial role in cellular defense mechanisms. Therefore, quantification of the activation status is a potential parameter for predicting treatment outcome. More importantly, specific targeting of this pathway in combination with radiotherapy or chemotherapy may enhance tumor control in non-small cell lung cancer by antagonizing cellular defense in response to treatment.

Introduction

Lung cancer is one of the most lethal forms of cancer, frequently presenting in advanced stages. Despite combined treatment modalities prognosis is poor with 5-year survival rates of 10-15%. In combined modality treatment the phosphatidylinositol-3-kinase (PI3-K)/protein kinase B (AKT) pathway (Figure 1) is involved in resistance mechanisms for radiotherapy as well as for chemotherapy. The PI3-K/AKT cascade can be upregulated by radiotherapy and plays a central role in the three major radiotherapy resistance mechanisms in non-small cell lung cancer and other tumors: intrinsic radiosensitivity, tumor proliferation and tumor cell hypoxia.[1] Understanding this pathway offers opportunities to unravel mechanisms of radioresistance. Furthermore, specifically targeting this pathway can potentially enhance the efficacy of combined treatment modalities. In this review we discuss the potential effects of inhibition of the PI3-K/AKT pathway in the light of the tumor microenvironment, more specifically, what the effect may be on tumor cell hypoxia, proliferation and DNA-repair in non-small cell lung cancer.

Strategies for increasing responsiveness to radiotherapy

Modifications in fractionation schedules have been developed to overcome radiation resistance. Hyperfractionation is designed to overcome intrinsic radioresistance and exploits the difference in the fractionation sensitivity between rapidly and slowly renewing tissues, i.e., a higher total dose can be given when the dose per fraction is reduced. However, in unresectable locally advanced NSCLC patients (95% stage III disease) hyperfractionated radiotherapy failed to demonstrate improvement over conventional radiotherapy.[2] Clinical studies have shown the relevance of tumor cell repopulation on tumor control and survival after radiotherapy in NSCLC. Delays exceeding 5 days beyond planned radiation treatment duration led to pronounced reduction in 2- (33% and 15 %) and 5-year survival rates (14% and 0%) for locally advanced NSCLC.[3, 4] Accelerated fractionation aims to counteract compensatory tumor cell repopulation by reducing the overall treatment time. A multicentre randomized controlled trial of continuous hyperfractionated accelerated radiotherapy (CHART) versus conventional radiotherapy was conducted in 563 inoperable NSCLC patients (61% stage III disease). With this treatment strategy an improvement of 2-year survival from 20% to 29% was achieved.[5] This illustrates the importance of proliferation because this improvement was obtained despite a reduction of the total dose by 10%.

Another approach to increase radiosensitivity is to combine radiotherapy with chemotherapy. Randomized trials report modest improvements in survival for concurrent chemoradiotherapy: 5-year survival of 17% for concurrent versus 6% for sequential chemoradiotherapy in the CALGB trial.[6] Data from three trials were used in a meta-analysis comparing concurrent versus sequential chemoradiotherapy. The results showed a

significant reduction (14%) in the two year risk of death if chemotherapy was given together with radiotherapy (RR 0.86; 95% CI 0.78-0.95; p=0.003).[7]

The third radioresistance mechanism, hypoxia, can be overcome by combining radiotherapy with treatments such as hyperoxic gas breathing, nitroimidazole radiosensitizers or hypoxic cytotoxins.[8] Although these approaches were successful in head and neck cancer and cervical cancer, data from patients with lung cancer are limited.[8] In advanced NSCLC a randomized trial of tirapazamine, a hypoxic cytotoxin, with cisplatin versus cisplatin alone showed significantly improved overall response rate (28% vs. 14%) and 1-year survival rate (34% vs. 23%) for the combination.[9]

The PI3-K/AKT-pathway

PI3-K is a cytosolic complex and consists of an 85 kDa regulatory subunit and a 110 kDa catalytic subunit (p110α). Upon ligand-mediated activation of receptor TK the p85-p110 complex is recruited to the receptor where it is activated and generates phosphatidylinositol 3,4,5-triphosphate (PIP3). PIP3 functions as a second messenger and recruits AKT to the cell membrane where it binds by its pleckstrin-homology (PH)-domain.[10-12] At the membrane, AKT is phosphorylated (pAkt) at threonine 308 (Thr308) by 3-phosphoinositide-dependent protein kinase-1 (PDK1) and thereby activated.[13] Full activation requires additional phosphorylation at serine 473 (Ser473) by PDK2. After activation, AKT translocates to the cytosol and nucleus to phosphorylate its substrates.[14]

PI3-K/AKT is one of the major downstream targets of the ErbB tyrosine kinase receptor family (Figure1). Activation of this pathway is not only achieved after activation of the epidermal growth factor receptor (EGFR) but also, and more effectively through other members of the ErbB-membrane receptor family. The four members of this family, ErbB1 (EGFR), ErbB2 (HER-2/neu), ErbB3 (HER-3), and ErbB4 (HER-4) are activated upon ligand-induced (e.g. epidermal growth factor or tumor growth factor α) receptor homo- and heterodimerization.[15] Upon heterodimerization, the cytoplasmatic domain of ErbB-3 undergoes tyrosine phosphorylation and activates PI3-K. EGFR itself is a weak direct activator of PI3-K but in particular connects to the RAS/PI3-K/AKT pathway or collaborates with ErbB-3. It has been demonstrated that PI3-K/AKT signaling is tightly regulated by EGFR in some tumors[16] but this is not a general feature and EGFR overexpression is not necessarily associated with PI3-K/AKT activation.[15, 17]

Furthermore, receptor TK independent activation of the PI3-K/AKT pathway is commonly observed in many cancers as well, and can occur through multiple mechanisms, such as mutation or amplification of PI3-K, amplification of AKT, activation of oncogenes upstream (e.g. *RAS*), or mutation or decreased expression of the tumor suppressor protein Phosphatase and TENsin homolog (PTEN).[18] The PTEN tumor suppressor gene is the central negative regulator of the PI3-K/AKT pathway by dephosphorylation of PIP3 at the plasma membrane. It was demonstrated that loss of PTEN in EGFR expressing tumor cells

Figure 1. The PI3-K/AKT pathway and other major downstream targets of the ErbB tyrosine-kinase receptor.
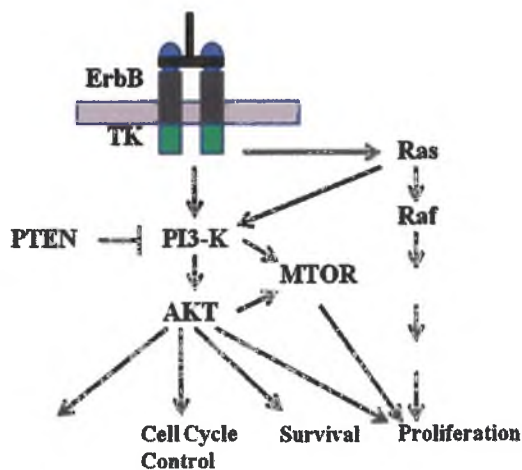
TK=tyrosine kinase. PI3-K=phosphatidylinositol-3-kinase. AKT=protein-kinase B. PTEN=phosphatase and TENsin homologue. mTOR=mammalian target of rapamycine. MAPK=mitogen-activated protein kinase.

counteracts the anti-tumor action of EGFR inhibitors by permitting AKT activity independent of receptor TK inputs.[19] PTEN is also located in the nucleus and maintains chromosomal stability through association with centromere protein in a phosphatase independent manner and through control of DNA double strand break repair mechanisms.[20, 21]

The PI3-K/AKT pathway is frequently over-activated in many solid tumors such as NSCLC.[11, 12, 17] PI3-K/AKT activation triggers a cascade of responses, which has consequences for all major cancer-cell growth mechanisms: survival, proliferation and cell growth. Additional effects involve DNA double strand break repair and tumor angiogenesis through hypoxia-inducible factor 1α (HIF-1α) and vascular endothelial growth factor (VEGF).[12]

The PI3-K/AKT-pathway and radiation resistance

The PI3-K/AKT pathway and intrinsic radiosensitivity

Radiation induced activation of multiple signaling pathways, depends at least in part on the expression of the EGF-receptor. In general, this radiation induced signaling will lead to radioprotective signals.[1] Ionizing radiation produces complex multiple, and potentially lethal, DNA double strand breaks by direct energy deposition or generation of reactive oxygen species (Figure 2). The main DNA double strand break repair mechanisms make use of homologous recombination (HR) or non- homologous endjoining (NHEJ). HR takes place

during S- and G2-phase of the cell cycle and is responsible for repair of approximately 20% of all DNA double strand breaks.[22]

The more error prone repair by NHEJ is responsible for repair of the majority of DNA double strand breaks caused by irradiation and is therefore potentially more important for treatment outcome.[22, 23] EGFR/PI3-K/AKT signaling is directly involved in the activation of the catalytic subunit of DNA-dependent protein kinase (DNA-PK$_{cs}$) regulating DNA double strand break repair by NHEJ in K-RAS mutated cells and blockage of this pathway leads to significant impairment of DNA repair.[24] EGFR activation, in a ligand independent manner or through up regulation of autocrine ligands, is responsible for EGFR internalization. This is foliowed by nuclear translocation of EGFR together with DNA-PK$_{cs}$ which leads to an increase of the DNA-PK$_{cs}$ dependent NHEJ.[25] Das et al showed that DNA-PK$_{cs}$ plays a critical role in EGFR-mediated radioresistance: in DNA-PK$_{cs}$ deficient cells the radioprotective effect is lost.[26] Somatic mutations in the TK domain of EGFR in NSCLC cell lines significantly delayed DNA double strand break repair and reduced clonogenic survival in response to radiation by preventing nuclear transport of EGFR and/or association with DNA-PK$_{cs}$.[26, 27] Targeting of EGFR and downstream pathways by either the specific TK inhibitor BIBX1382BS (BIBX) or the PI3-K inhibitor LY294002 enhanced radiation sensitivity in K-RAS mutated human tumor cells.[28, 29] EGFR inhibition by cetuximab, an IgG1 monoclonal antibody against the ligand-binding domain of the EGFR, can modulate the balance between cytoplasmic and nuclear DNA-PK$_{cs}$ and thereby reduces DNA repair.[30, 31]

Activated RAS signaling to the PI3-K/AKT pathway leads to prolonged tumor cell survival after DNA damage has been inflicted, and hence radioresistance. This is irrespective whether RAS activation results from mutation of *RAS* or mutation or over-expression of receptor TK. This was illustrated by selective inhibition of either PI3-K or AKT in tumor cells with active RAS signaling resulting in increased radiosensitivity.[32] in the majority of NSCLC cell lines AKT was constitutively active, independent of histological subtype and *p53, Rb* or *K-RAS* status. Inhibition of AKT activity in these tumor cell lines by pharmacological or genetic approaches resulted in enhanced cellular responsiveness to chemotherapy and irradiation.[11] RAS activation by mutation or by receptor TK activity is a frequent event in human tumors indicating that PI3-K/AKT mediated DNA damage repair pathway plays an important role in radioresistance in the clinical situation.

The PI3-K/AKT pathway and tumor cell proliferation

Tumor cell proliferation is influenced by several factors such as differentiation status, cell cycle gene regulation and microenvironmental factors including oxygen and nutrient availability. Under hypoxic conditions progression of the tumor cell through the cell cycle is delayed, which may allow rapid repopulation under improved reoxygenated conditions.[33] PI3-K/AKT is mainly a survival pathway but involvement of the PI3-K/AKT pathway in tumor cell proliferation was shown by its signaling to cyclin D-dependent kinases which regulate the cell-cycle G1/S phase transition.[34] Preclinical data showed that G1 arrest as a result of inhibition of the EGF receptor prevented repopulation during radiotherapy.[35]

Figure 2. A mouse adenocarcinoma treated with radiotherapy
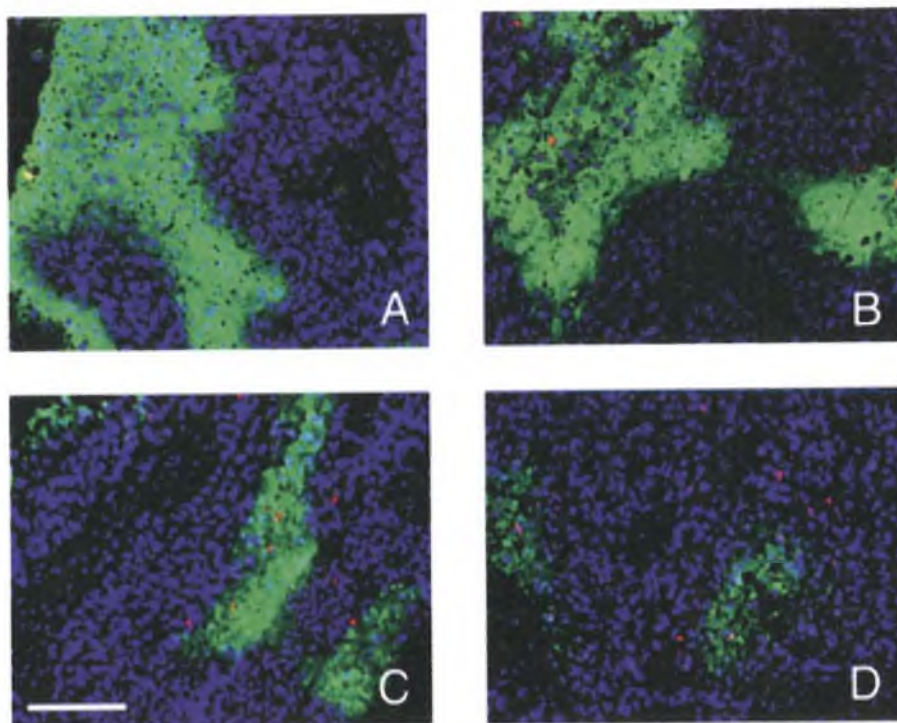
A=control B=0.5 Gy C=1 Gy D=2 Gy

Mouse adenocarcinoma treated with radiotherapy. Hypoxic areas are green (pimidazole). DNA double strand breaks are visualized after immunohistochemical staining of γH2AX. Nuclei are blue (Hoechst 33342). A dose dependent increase in γH2AX-foci is observed with more double strand breaks in normoxic tumor areas, indicating increased radioresistance of hypoxic tumor cells.

Accelerated tumor cell proliferation as a response to fractionated radiotherapy is linked to EGFR in a ligand independent manner. Irradiation leads to EGFR tyrosine phosphorylation, irrespective of the levels of EGFR expression, and through PIP3 activation of downstream pathways such as the RAF/Mitogen-activated protein kinase (MAPK) pathway to subsequent enhanced proliferation.[36]

Alternately, the inducible expression of a dominant negative EGFR led to decreased proliferation of tumor cells in response to irradiation. Combined inhibition of EGFR and ErbB2 further decreased AKT activity and proliferation in response to radiation.[37]

Another mechanism to influence response to radiation is combination treatment with the monoclonal antibody cetuximab. Inhibition of EGFR with cetuximab in human lung cancer cell lines and NSCLC xenografts showed marked inhibition of tumor growth when cetuximab was combined with radiation which can be explained by a shift to the G0/G1 phase of the cell cycle and reduced EGF induced phosphorylation of EGFR and ErbB2.[38] In FaDu cells

(human hypopharyngeal squamous cell carcinoma line) fractionated irradiation combined with cetuximab decreased repopulation and improved reoxygenation both contributing to local control. Underlying mechanisms for this improved reoxygenation may be rapid tumor regression and reduced oxygen consumption.[39] These data provide a rationale for clinical studies to investigate the effect of combinating cetuximab with radiation in NSCLC.

The PI3-K/AKT pathway and hypoxia

Hypoxia is an important phenomenon in solid tumors leading to genetic instability and creation of more aggressive phenotypes causing resistance to chemotherapy and radiotherapy.

Cancer cells have the ability to undergo genetic and adaptive changes in response to hypoxia that allow them to survive and even proliferate under hypoxic conditions. HIF-1 is a key transcription factor induced by hypoxia which modulates expression of genes and their protein products involved in tumor growth and apoptosis.[40, 41] Upon activation HIF-1 leads to upregulation of many gene products, including vascular endothelial growth factor (VEGF), the glucose transporters (GLUT-1 and GLUT-3) and carbonic anhydrase IX (CAIX).[42] Under normoxic conditions HIF-1α is rapidly deactivated by binding to the von Hippel Lindau protein (VHL) or by factor inhibiting HIF-1 (FIH-1) preventing further transcription. However under hypoxic conditions transcriptional activity is regulated through the PI3-K/AKT pathway.[41] Activation of this pathway results in increased transcription and expression of HIF-1. This is illustrated in human prostate cancer cells: HIF-1 transcription was blocked in the absence of AKT or PI3-K, and stimulated by constitutively active AKT or in dominant negative PTEN.[43] Also in breast cancer cell lines, interruption of the PI3K/AKT pathway by the selective PI3K inhibitor, LY294002, inhibited HIF-1α induction resulting in a reduction of VEGF expression by 50%.[44] The close interaction between hypoxia, angiogenesis and radiosensitivity was shown in lung carcinoma xenografts. In these tumors AKT signaling was inhibited by the protease inhibitor nelfinavir resulting in a decrease of both VEGF and HIF-1α expression. This led to both a reduction of angiogenesis and a decrease in hypoxia in response to radiation.[45]

The PI3-K/AKT pathway, hypoxia and VEGF

One of the important mechanisms by which EGFR inhibition enhances tumor oxygenation is by VEGF regulation. VEGF is crucial in tumor induced endothelial cell proliferation and vascular permeability leading to neo-angiogenesis. Prevention of neo-angiogenesis can result in a normalization of the vasculature and improved perfusion leading to a reduction of tumor cell hypoxia. VEGF is one of the most widely studied hypoxia-inducible proteins.[46] Two distinct pathways, one through HIF-1α translation and one HIF-independent, have been recognized by which VEGF expression is regulated, both involving PI3-K and AKT.[45, 47] VEGF is one of the genes under control of HIF-1α in hypoxic conditions but it is also activated in normoxic conditions through the PI3-K/AKT pathway by EGFR or loss of PTEN.[42, 48] The EGFR/PI3-K/AKT pathway can control expression of VEGF either in a paracrine manner

through EGF or through downstream signaling through the PI3-K/AKT pathway. In vitro and in vivo experiments showed that PI3-K inhibition leads to reduced VEGF expression. Also, pAKT counteracts the down regulation of VEGF activity by TK inhibition indicating that PI3-K/AKT operates immediately downstream of the TK receptor controlling VEGF expression. [49] Morelli et al. showed that angiogenesis can be decreased by VEGF-A blocking through EGFR inhibition.[50] Cell growth was significantly inhibited by small molecule TK inhibition (gefitinib), by anti-EGFR blocking monoclonal antibodies (cetuximab) and by vandetanib, a TK inhibitor (TKI) that inhibits both VEGFR-2 and EGFR. This growth inhibiting effect was more pronounced when combinations were used of TKIs (gefitinib or vandetanib) and cetuximab that could be explained by effects on EGFR and downstream signaling to proliferation and survival pathways. The combination of cetuximab and vandetanib resulted in an almost complete suppression of phosphorylated EGFR, 50-70% reduction in EGFR protein levels and almost complete suppression of pAKT and MAPK. VEGF blockage through EGFR-inhibition in xenografts of human non-small cell lung adenocarcinoma (A549), significantly reduced angiogenesis. Microvessel density was decreased both by cetuximab and vandetanib and combined, the two agents led to a significant decrease in angiogenesis.[50] This study showed that an optimal inhibition of EGFR can be obtained with concomitant inhibition of the extra-cellular ligand binding domain and the intra-cellular TK domain. Furthermore, an enhanced and more persistent control of tumor cell proliferation and angiogenesis was achieved by the combined inhibition of the two distinct but related signaling pathways (the EGFR pathway and the VEGFR pathway).[50] These findings highlight the close relation of EGFR and VEGF and downstream signaling to the PI3-K/AKT pathway.

Clinical relevance of PI3-K/AKT activation in non-small cell lung cancer

EGFR and PI3-K/AKT activation

EGFR is expressed in a variety of solid tumors including breast, prostate, colorectal, head and neck and NSCLC. EGFR amplification occurs in up to 80% of NSCLC patients and initial reports suggested a poor prognosis. However, a meta-analysis failed to identify any association between EGFR expression and survival in lung cancer patients.[51] Only a minority of EGFR positive tumors demonstrate a clinically meaningful response to EGFR inhibition.[52-54]

In order to increase response, targeting EGFR in combination with radiotherapy seems an attractive therapeutic strategy. The TKI erlotinib has shown to modulate response to radiotherapy in human non-small cell lung cancer both in vitro and in vivo. Erlotinib enhanced radiation induced apoptosis, inhibited radiation induced activation of the EGFR receptor and attenuated radiation induced expression of RAD51, a measure of DNA double strand break repair. Tumor response of non-small cell lung cancer xenografts to radiotherapy was improved when combined with erlotinib.[55] Gefitinib also enhanced the cytotoxic effects of radiotherapy in NSCLC cell lines. Cellular repair of radiation-induced DNA

double strand breaks was suppressed at pharmacologically achievable levels.[56] This underlines the strong involvement of the EGFR/PI3-K/AKT signaling pathway regulating DNA double strand break repair through DNA-PK$_{cs}$. In NSCLC preclinical data suggest a synergistic effect for cetuximab or EGFR TK inhibitors in combination with radiotherapy.[55-59] In unresectable stage III NSCLC the role of cetuximab in combination with chemoradiotherapy is currently evaluated by the Radiation Therapy Oncology Group, by the ongoing Cancer and Leukemia Group B 30407 trial and others.[58, 60]

For cancer cells to be successfully inhibited by anti-EGFR, EGFR must be a critical driving force for its growth and survival and thus control PI3-K activity. Potential mechanisms for lack of response to EGFR-inhibition include constitutive activation of signaling pathways independent of EGFR, as well as EGFR-independent activation of signaling pathways through a number of stimuli such as hypoxic stress, RAS-activation or PTEN-inhibition.[38, 48] Additionally, the potential of cells to develop resistance to TK inhibition was shown by Engelman et al. In this study resistance was caused by amplification of the MET proto-oncogene, not through EGFR but through ErbB3 stimulation of the PI3-K pathway.[61] Inhibition of AKT phosphorylation with LY294002 and wortmannin (Akt inhibitor) increased apoptosis but only in cells with activated AKT (pAKT). In cells with high pAKT, inhibition of pAKT in combination with either chemotherapy or irradiation led to increased apoptosis. Modulation of pAKT activity has shown to alter cellular responsiveness to chemotherapy and irradiation in NSCLC and offers opportunities for further research in clinical studies in patients with high levels of pAkt.[11] Therefore, molecular predictors of sensitivity to EGFR directed therapy should not only assess the EGFR status but need to be extended to quantify the EGFR-activation status and key markers of the activated downstream signaling pathways.[62]

PI3-K/AKT activation as a prognostic factor in non-small cell lung cancer

Preclinical data showed pAKT positivity, using immunoblotting, in 80% of NSCLC cell lines independent of tumor histology.[11] Clinical data using immunohistochemical staining to measure activated pAKT in pretreatment tumor specimens varied from 50% (Stage I-III) to 84% (stage III) of patients.[17, 63] Importantly, there was a discrepancy between pAKT expression and EGFR expression.[17] These findings are consistent with previous findings in head and neck cancers.[18] This suggests that, in the clinical situation, EGFR-independent activation or down regulation of the PI3-K/AKT pathway could be a frequent event. (Figure 3)

In patients who underwent surgical resection for NSCLC with lymph node metastasis, pAKT correlated with poor prognosis (5-year survival roughly 20% vs. 60% for pAKT negative patients). No association was found with other clinical characteristics.[64] Although in this study survival data may be confounded because of a lack of consistence for adjuvant therapy it clearly shows the clinical importance of activated signaling through the AKT pathway and its impact on treatment outcome and prognosis.

Figure 3. Fluorescent microscopic images of an undifferentiated non-small cell lung tumor (fine needle biopsy).
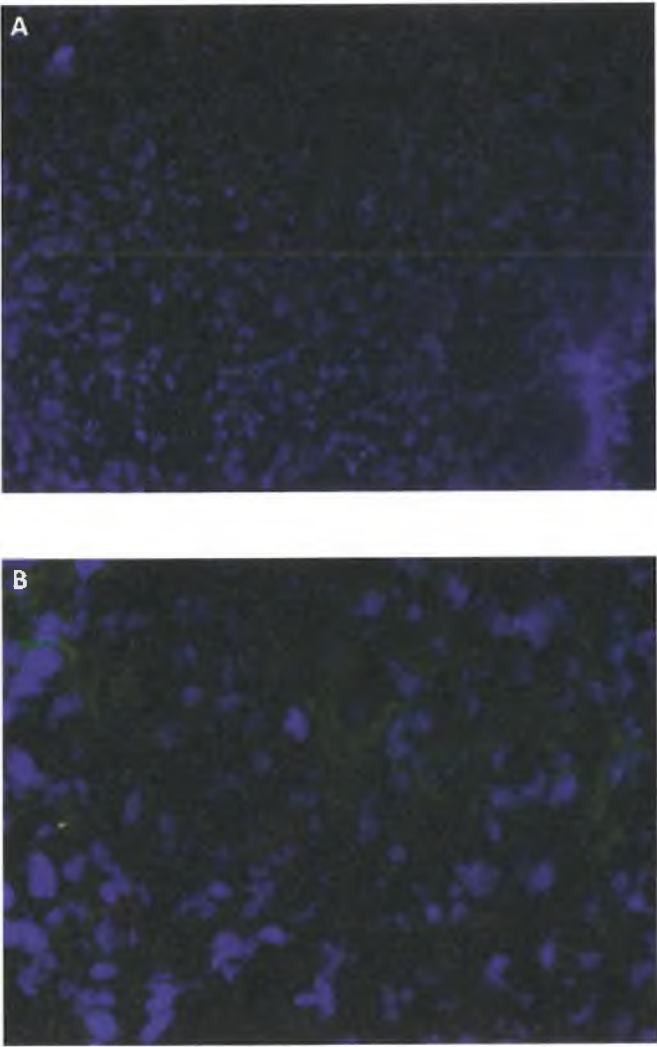
3a; extensive areas of the endogenous hypoxia-related marker CA-9 (red/purple) indicates the presence of potentially radioresistant hypoxic tumor cells. Tumor nuclei are blue (Hoechst 33342), magnification 20 X.

3b; phosphorylated, activated, AKT-expression (pAKT, green) and EGFR-expression (red) relative to tumor nuclei (blue). Mismatch of EGFR and pAKT illustrating the fact that the PI3-K/AKT-signaling pathway can be activated independent of the EGFR (magnification 40 X).

PI3-K/AKT activation as a target for treatment in non-small cell lung cancer

In vitro studies with NSCLC cell lines showed synergistic effects if multiple cell signaling proteins are targeted simultaneously.[65] Persistent activity of the PI3-K/AKT or RAS/ERK-pathway, indicated by elevated levels of phosphorylated AKT (pAKT) or ERK (pERK), despite EGFR-TK-inhibition by gefitinib indicated treatment resistance. Cells with persistent activity of the PI3-K/AKT or RAS/ERK-pathways after EGFR-TK-inhibition were treated in combination with specific inhibitors of PI3-K (Ly294002) or RAS (farnesyl transferase inhibitor SCH66336) respectively. The combination of EGFR inhibition and PI3-K/AKT or RAS/ERK-inhibition clearly showed additive cytotoxicity.[65] Therefore, it is likely that EGFR-TK-inhibitors, such as gefitinib, in combination with specific inhibitors of down stream signaling pathways involved in cell survival, such as the PI3-K/AKT or RAS/ERK-pathway, is a promising strategy to overcome treatment resistance in NSCLC.

In NSCLC cells lines with high levels of pAKT, pharmacological inhibiting of P13-K led to decreased AKT phosphorylation resulting in radiosensitization and an increase in chemotherapy induced apoptosis.[11, 17] Inhibition of the PI3-K/AKT pathway can also be achieved by use of protease inhibitors. Treatment with these compounds resulted in a decrease in pAKT in various cell lines, including NSCLC, leading to increased radiosensitivity. Additionally, overexpression of active PI3-K in cells without activated AKT resulted in radiation resistance that could be inhibited with protease inhibitors. Finally, in xenografted tumors down regulation of pAKT was seen at a dose range comparable to the therapeutic levels used in HIV patients and a synergistic radiosensitisation was observed when nelfinavir was combined with radiotherapy.[49, 66] These studies emphasize the potential for specific targeting the activated PI3-K/AKT pathway to counteract radiation induced cellular defense mechanisms.

Conclusion

It is clear that P13-K/AKT is an important regulator of various cellular functions including proliferation, invasion, apoptosis and upregulation of hypoxia-related proteins. Consequently, this pathway plays a key role in the three major radiotherapy resistance mechanisms, also in non-small cell lung cancer: intrinsic radiosensitivity, tumor proliferation and tumor cell hypoxia. Expression of pAKT is an independent prognostic indicator of clinical outcome of lung cancer in retrospective studies. Blocking of the PI3-K/AKT signaling routes through EGFR-inhibition improves radiosensitivity and can affect tumor growth substantially through various mechanisms including inhibition of neo-angiogenesis via VEGF. Importantly, EGFR-independent activation of the PI3-K/AKT pathway commonly occurs and is an important factor in treatment resistance. Prospective studies are needed to quantify the activated status of the EGFR/P13K/AKT pathway and may be helpful in selecting patients for treatments combining chemotherapy and radiotherapy with targeted therapy.

References

1. Dent P, Yacoub A, Contessa J, et al. Stress and radiation-induced activation of multiple intracellular signaling pathways. Radiat Res 2003; 159(3): 283-300.

2. Sause W, Kolesar P, Taylor S IV, et al. Final results of phase III trial in regionally advanced unresectable non-small cell lung cancer: Radiation Therapy Oncology Group, Eastern Cooperative Oncology Group, and Southwest Oncology Group. Chest 2000; 117(2): 358-64.

3. Cox JD, Pajak TF, Asbell S, et al. Interruptions of high-dose radiation therapy decrease long-term survival of favorable patients with unresectable non-small cell carcinoma of the lung: analysis of 1244 cases from 3 Radiation Therapy Oncology Group (RTOG) trials. Int J Radiat Oncol Biol Phys 1993; 27(3): 493-8.

4. Fowler JF, Chappell R. Non-small cell lung tumors repopulate rapidly during radiation therapy. Int J Radiat Oncol Biol Phys 2000; 46(2): 516-7.

5. Saunders M, Dische S, Barrett A, et al. Continuous hyperfractionated accelerated radiotherapy (CHART) versus conventional radiotherapy in non-small-cell lung cancer: a randomised multicentre trial. CHART Steering Committee. Lancet 1997; 350(9072): 161-5.

6. Dillman RO, Herndon J, Seagren SL, et al. Improved survival in stage III non-small-cell lung cancer: seven-year follow-up of cancer and leukemia group B (CALGB) 8433 trial. J Natl Cancer Inst 1996; 88(17): 1210-5.

7. Rowell NP, O'rourke NP. Concurrent chemoradiotherapy in non-small cell lung cancer. Cochrane Database Syst Rev 2004;(4): CD002140.

8. Kaanders JH, Bussink J, van der Kogel AJ. Clinical studies of hypoxia modification in radiotherapy. Semin Radiat Oncol 2004; 14(3): 233-40.

9. von PJ, von RR, Gatzemeier U, et al. Tirapazamine plus cisplatin versus cisplatin in advanced non-small-cell lung cancer: A report of the international CATAPULT I study group. Cisplatin and Tirapazamine in Subjects with Advanced Previously Untreated Non-Small-Cell Lung Tumors. J Clin Oncol 2000; 18(6):1351-9.

10. Cantley LC. The phosphoinositide 3-kinase pathway. Science 2002; 296(5573): 1655-7.

11. Brognard J, Clark AS, Ni Y, et al. Akt/protein kinase B is constitutively active in non-small cell lung cancer cells and promotes cellular survival and resistance to chemotherapy and radiation. Cancer Res 2000; 61(10):3986-97.

12. Vivanco I, Sawyers CL. The phosphatidylinositol 3-Kinase AKT pathway in human cancer. Nat Rev Cancer 2002; 2(7):489-501.

13. Vanhaesebroeck B, Alessi DR. The PI3K-PDK1 connection: more than just a road to PKB. Biochem J 2000; 346 Pt 3: 561-76.

14. Wang R, Brattain MG. AKT can be activated in the nucleus. Cell Signal 2006; 18(10):1722-31.

15. Klapper LN, Glathe S, Vaisman N, et al. The ErbB-2/HER2 oncoprotein of human carcinomas may function solely as a shared coreceptor for multiple stroma-derived growth factors. Proc Natl Acad Sci USA 1999; 96(9):4995-5000.

16. Qiu W, Schonleben F, Li X, et al. PIK3CA mutations in head and neck squamous cell carcinoma. Clin Cancer Res 2006; 12(5):1441-6.

17. Gupta AK, Soto DE, Feldman MD, et al. Signaling pathways in NSCLC as a predictor of outcome and response to therapy. Lung 2004; 182(3):151-62.

18. Gupta AK, McKenna WG, Weber CN, et al. Local recurrence in head and neck cancer: relationship to radiation resistance and signal transduction. Clin Cancer Res 2002; 8(3):885-92.

19. Bianco R, Shin I, Ritter CA, et al. Loss of PTEN/MMAC1/TEP in EGF receptor-expressing tumor cells counteracts the antitumor action of EGFR tyrosine kinase inhibitors. Oncogene 2003; 22(18):2812-22.

20. Shen WH, Balajee AS, Wang J, et al. Essential role for nuclear PTEN in maintaining chromosomal integrity. Cell 2007; 128(1):157-70.

21. Baker SJ. PTEN enters the nuclear age. Cell 2007; 128(1):25-8.

22. O'Driscoll M, Jeggo PA. The role of double-strand break repair - insights from human genetics. Nat Rev Genet 2006; 7(1):45-54.

23. Lieber MR, Ma Y, Pannicke U, et al. Mechanism and regulation of human non-homologous DNA end-joining. Nat Rev Mol Cell Biol 2003; 4(9):712-20.

24. Toulany M, Kasten-Pisula U, Brammer I, et al. Blockage of epidermal growth factor receptor-phosphatidylinositol 3-kinase-AKT signaling increases radiosensitivity of K-RAS mutated human tumor cells in vitro by affecting DNA repair. Clin Cancer Res 2006; 12(13):4119-26.

25. Szumiel I. Epidermal growth factor receptor and DNA double strand break repair: the cell's self-defence. Cell Signal 2006; 18(10):1537-48.

26. Das AK, Chen BP, Story MD, et al. Somatic mutations in the tyrosine kinase domain of epidermal growth factor receptor (EGFR) abrogate EGFR-mediated radioprotection in non-small cell lung carcinoma. Cancer Res 2007; 67(11):5267-74.

27. Das AK, Sato M, Story MD, et al. Non-small-cell lung cancers with kinase domain mutations in the epidermal growth factor receptor are sensitive to ionizing radiation. Cancer Res 2006; 66(19):9601-8.

28. Toulany M, Dittmann K, Kruger M, et al. Radioresistance of K-Ras mutated human tumor cells is mediated through EGFR-dependent activation of PI3K-AKT pathway. Radiother Oncol 2005; 76(2):143-50.

29. Toulany M, Dittmann K, Baumann M, et al. Radiosensitization of Ras-mutated human tumor cells in vitro by the specific EGF receptor antagonist BIBX1382BS. Radiother Oncol 2005; 74(2):117-29.

30. Dittmann K, Mayer C, Rodemann HP. Inhibition of radiation-induced EGFR nuclear import by C225 (Cetuximab) suppresses DNA-PK activity. Radiother Oncol 2005; 76(2):157-61.

31. Huang SM, Harari PM. Modulation of radiation response after epidermal growth factor receptor blockade in squamous cell carcinomas: inhibition of damage repair, cell cycle kinetics, and tumor angiogenesis. Clin Cancer Res 2000; 6(6):2166-74.

32. Kim IA, Bae SS, Fernandes A, et al. Selective inhibition of Ras, phosphoinositide 3 kinase, and Akt isoforms increases the radiosensitivity of human carcinoma cell lines. Cancer Res 2005; 65(17):7902-10.

33. Webster L, Hodgkiss RJ, Wilson GD. Cell cycle distribution of hypoxia and progression of hypoxic tumour cells in vivo. Br J Cancer 1998; 77(2):227-34.

34. Diehl JA, Cheng M, Roussel MF, et al. Glycogen synthase kinase-3beta regulates cyclin D1 proteolysis and subcellular localization. Genes Dev 1998; 12(22):3499-511.

35. Di GE, Barbarino M, Bruzzese F, et al. Critical role of both p27KIP1 and p21CIP1/WAF1 in the antiproliferative effect of ZD1839 ('Iressa'), an epidermal growth factor receptor tyrosine kinase inhibitor, in head and neck squamous carcinoma cells. J Cell Physiol 2003; 195(1):139-50.

36. Schmidt-Ullrich RK, Mikkelsen RB, Dent P, et al. Radiation-induced proliferation of the human A431 squamous carcinoma cells is dependent on EGFR tyrosine phosphorylation. Oncogene 1997; 15(10):1191-7.

37. Contessa JN, Hampton J, Lammering G, et al. Ionizing radiation activates Erb-B receptor dependent Akt and p70 S6 kinase signaling in carcinoma cells. Oncogene 2002; 21(25):4032-41.

38. Raben D, Helfrich B, Chan DC, et al. The effects of cetuximab alone and in combination with radiation and/or chemotherapy in lung cancer. Clin Cancer Res 2005; 11(2 Pt 1):795-805.

39. Krause M, Ostermann G, Petersen C, et al. Decreased repopulation as well as increased reoxygenation contribute to the improvement in local control after targeting of the EGFR by C225 during fractionated irradiation. Radiother Oncol 2005; 76(2):162-7.

40. Harris AL. Hypoxia-a key regulatory factor in tumour growth. Nat Rev Cancer 2002 ;2(1):38-47.

41. Semenza GL. HIF-1: mediator of physiological and pathophysiological responses to hypoxia. J Appl Physiol 2000; 88(4):1474-80.

42. Rademakers SE, Span PN, Kaanders JHAM, et al. Molecular aspects of tumour hypoxia. Molecular Oncology; 2(1):41-53.

43. Zhong H, Chiles K, Feldser D, et al. Modulation of hypoxia-inducible factor 1alpha expression by the epidermal growth factor/phosphatidylinositol 3-kinase/PTEN/AKT/FRAP pathway in human prostate cancer cells: implications for tumor angiogenesis and therapeutics. Cancer Res 2000; 60(6):1541-5.

44. Blancher C, Moore JW, Robertson N, et al. Effects of ras and von Hippel-Lindau (VHL) gene mutations on hypoxia-inducible factor (HIF)-1alpha, HIF-2alpha, and vascular endothelial growth factor expression and their regulation by the phosphatidylinositol 3'-kinase/Akt signaling pathway. Cancer Res 2001; 61(19):7349-55.

45. Pore N, Gupta AK, Cerniglia GJ, et al. Nelfinavir down-regulates hypoxia-inducible factor 1alpha and VEGF expression and increases tumor oxygenation: implications for radiotherapy. Cancer Res 2006; 66(18):9252-9.

46. Bussink J, Kaanders JH, van der Kogel AJ. Tumor hypoxia at the micro-regional level: clinical relevance and predictive value of exogenous and endogenous hypoxic cell markers. Radiother Oncol 2003; 67(1):3-15.

47. Fukumura D, Xu L, Chen Y, et al. Hypoxia and acidosis independently up-regulate vascular endothelial growth factor transcription in brain tumors in vivo. Cancer Res 2001; 61(16):6020-4.

48. Bussink J, van der Kogel AJ, Kaanders JH. Activation of the PI3-K/AKT pathway and implications for radioresistance mechanisms in head and neck cancer. Lancet Oncol 2008; 9(3):288-96.

49. Pore N, Jiang Z, Gupta A, et al. EGFR tyrosine kinase inhibitors decrease VEGF expression by both hypoxia-inducible factor (HIF)-1-independent and HIF-1-dependent mechanisms. Cancer Res 2006; 66(6):3197-204.

50. Morelli MP, Cascone T, Troiani T, et al. Anti-tumor activity of the combination of cetuximab, an anti-EGFR blocking monoclonal antibody and ZD6474, an inhibitor of VEGFR and EGFR tyrosine kinases. J Cell Physiol 2006; 208(2):344-53.

51. Meert AP, Martin B, Delmotte P, et al. The role of EGF-R expression on patient survival in lung cancer: a systematic review with meta-analysis. Eur Respir J 2002; 20(4):975-81.

52. Herbst RS. Review of epidermal growth factor receptor biology. Int J Radiat Oncol Biol Phys 2004; 59(2 Suppl):21-6.

53. Raymond E, Faivre S, Armand JP. Epidermal growth factor receptor tyrosine kinase as a target for anticancer therapy. Drugs 2000; 60 Suppl 1:15-23.

54. Rusch V, Klimstra D, Venkatraman E, et al. Overexpression of the epidermal growth factor receptor and its ligand transforming growth factor alpha is frequent in resectable non-small cell lung cancer but does not predict tumor progression. Clin Cancer Res 1997; 3(4):515-22.

55. Chinnaiyan P, Huang S, Vallabhaneni G, et al. Mechanisms of enhanced radiation response following epidermal growth factor receptor signaling inhibition by erlotinib (Tarceva). Cancer Res 2005; 65(8):3328-35.

56. Tanaka T, Munshi A, Brooks C, et al. Gefitinib radiosensitizes non-small cell lung cancer cells by suppressing cellular DNA repair capacity. Clin Cancer Res 2008; 14(4):1266-73.

57. Kim DW, Choy H. Potential role for epidermal growth factor receptor inhibitors in combined-modality therapy for non-small-cell lung cancer. Int J Radiat Oncol Biol Phys 2004; 59(2 Suppl):11-20.

58. Morgensztern D, Govindan R. Is there a role for cetuximab in non small cell lung cancer? Clin Cancer Res 2007; 13(15 Pt 2):s4602-s4605.

59. Raben D, Helfrich B, Bunn PA, Jr. Targeted therapies for non-small-cell lung cancer: biology, rationale, and preclinical results from a radiation oncology perspective. Int J Radiat Oncol Biol Phys 2004; 59(2 Suppl):27-38.

60. Jensen AD, Munter MW, Bischoff H, et al. Treatment of non-small cell lung cancer with intensity-modulated radiation therapy in combination with cetuximab: the NEAR protocol (NCT00115518). BMC Cancer 2006; 6:122.

61. Engelman JA, Zejnullahu K, Mitsudomi T, et al. MET amplification leads to gefitinib resistance in lung cancer by activating ERBB3 signaling. Science 2007; 316(5827):1039-43.

62. Kong A, Leboucher P, Leek R, et al. Prognostic value of an activation state marker for epidermal growth factor receptor in tissue microarrays of head and neck cancer. Cancer Res 2006; 66(5):2834-43.

63. Lee SH, Kim HS, Park WS, et al. Non-small cell lung cancers frequently express phosphorylated Akt; an immunohistochemical study. APMIS 2002; 110(7-8):587-92.

64. Hirami Y, Aoe M, Tsukuda K, et al. Relation of epidermal growth factor receptor, phosphorylated-Akt, and hypoxia-inducible factor-1alpha in non-small cell lung cancers. Cancer Lett 2004; 214(2):157-64.

65. Janmaat ML, Rodriguez JA, Gallegos-Ruiz M, et al. Enhanced cytotoxicity induced by gefitinib and specific inhibitors of the Ras or phosphatidyl inositol-3 kinase pathways in non-small cell lung cancer cells. Int J Cancer 2006; 118(1):209-14.

66. Gupta AK, Cerniglia GJ, Mick R, et al. HIV protease inhibitors block Akt signaling and radiosensitize tumor cells both in vitro and in vivo. Cancer Res 2005; 65(18):8256-65.

Chapter 3

Differences in metabolism between adeno- and squamous cell non-small cell lung carcinomas: spatial distribution and prognostic value of GLUT1 and MCT4

Tineke W.H. Meijer

Olga C.J. Schuurbiers

Johannes H.A.M. Kaanders

Monika G. Looijen-Salamon

Lioe-Fee de Geus-Oei

Ad F.T.M. Verhagen

Jasper Lok

Henricus F.M. van der Heijden

Saskia E. Rademakers

Paul N. Span

Johan Bussink

Abstract

Background

Hypoxia leads to changes in tumor cell metabolism such as increased glycolysis. In this study, we examined the spatial distribution of the glycolysis and hypoxia related markers glucose transporter 1 (GLUT1) and monocarboxylate transporter 4 (MCT4) expression in relation to the vasculature in stage I, II and resectable stage IIIA NSCLC. Furthermore, associations of these markers with survival were investigated.

Methods

GLUT1 and MCT4 expression were determined in 90 NSCLC fresh frozen biopsies using immunohistochemical techniques and a computerized image analysis system. Markers were analyzed for adenocarcinomas (n=41) and squamous cell carcinomas (n=34) separately. Eighty-four patients were retrospectively evaluated for relapse and survival.

Results

Squamous cell carcinomas demonstrated higher GLUT1 expression, relative to adenocarcinomas. Also, in squamous cell carcinomas, GLUT1 and MCT4 expression increased with increasing distance from the vasculature, whereas in adenocarcinomas upregulation of MCT4 was already found at closer distance from vessels. In adenocarcinomas, high GLUT1 expression correlated with a poor differentiation grade and positive lymph nodes at diagnosis. High GLUT1 plus high MCT4 expression was associated with a poor disease-specific survival in only adenocarcinomas (p=0.032).

Conclusion

Analysis of GLUT1 and MCT4 expression on the histological level suggested a different metabolism for adenocarcinomas and squamous cell carcinomas. Likely, adenocarcinomas rely mainly on aerobic glycolysis for ATP production, whereas the behavior of squamous cell carcinomas is more physiologically, i.e. mitochondrial oxidation with anaerobic glycolysis under hypoxic conditions. High GLUT1 plus high MCT4 expression indicated an aggressive tumor behavior in adenocarcinomas. This subgroup of tumors may benefit from new treatment approaches, such as MCT4 inhibitors. Since this study has an exploratory character, our results warrant further investigation and need independent validation.

Introduction

Non-small cell lung cancer (NSCLC) is the most important cause of cancer related death.[1] Surgery is possible in patients with stage I, II and limited stage III. Despite resectability of the tumor, approximately 50% of these patients will suffer relapse.[2, 3]

The tumor-node-metastasis (TNM) classification is the most important tool to estimate prognosis and for decision-making regarding treatment. However, since this classification does not provide information about biological behavior of tumors, differences in relapse occur within stage groups.[4] The tumor metabolism influences response to therapy, [5] and could be exploited to predict outcome.[6] Therefore, interest in differences in metabolism between subgroups of tumors and metabolic markers to predict prognosis in NSCLC is growing. These markers could be used to select patients who may benefit from new, biology-based treatment approaches.[5, 7]

A difference between normal and tumor cells, is their metabolic route of energy production. Tumor cells predominantly rely on glycolysis with production of lactate instead of mitochondrial oxidation, even in the presence of oxygen (Warburg effect or 'aerobic glycolysis').[8-10] To support the necessary high rate of glycolysis, tumor cells need an increased transport of glucose into cells. This is facilitated by upregulation of glucose transporters (GLUTs). Glucose transporter 1 (GLUT1) overexpression has been documented in most malignancies.[11] Hypoxia-inducible-factor-1 (HIF-1), which is stabilized under hypoxic conditions, is responsible for GLUT1 upregulation.[9, 12] The increased level of lactate and acid produced by the enhanced glycolysis will decrease intracellular pH, which is potentially cytotoxic. To counteract this cytoplasmic acidification, cells can upregulate monocarboxylate transporter 4 (MCT4), which transports lactate/H^+ out of the cell.[9, 10] MCT4 is also upregulated in response to hypoxia through HIF-1-mediated gene transcription.[13]

Tumor hypoxia predicts poor prognosis in various tumors independent of treatment modality.[12, 14] The Warburg effect increases the malignant potential of tumor cells.[15] Lactate accumulation in malignancies predicts for metastasis formation during follow-up.[16] So, hypoxia and glycolysis related markers, such as GLUT1 and MCT4, which may indicate lactate accumulation, could have an additional value as prognosticators next to the TNM classification in NSCLC.

The aim of this study was to examine the spatial distribution of GLUT1 and MCT4 expression in relation to the vasculature in curatively resected stage I, II and limited stage III NSCLC to unravel differences in metabolism between histological subtypes. Furthermore, associations with treatment outcome were investigated to determine the prognostic value of these markers.

Materials and methods

Patients

One-hundred twenty-seven patients who underwent a curative resection for stage I, II and resectable stage IIIA, cN0-1 NSCLC between January 2002 and December 2008 at the Radboud University Nijmegen Medical Centre, of whom 129 fresh frozen biopsies were available, were included in this study. The study was performed according to institutional ethical rules and regulations.

Of these 127 patients, 5 underwent experimental neo-adjuvant chemotherapy and were excluded. Furthermore, 27 biopsies were not suitable for evaluation due to sampling error (absence of tumor tissue, inflammatory tissue or necrosis), and 7 biopsies were not available. This resulted in 90 tumor biopsies from 88 patients for further analysis.

In three patients, stage IIIB or IV was established during surgery. These patients were excluded from outcome analysis. Further, one patient was lost to follow-up. Also, two patients had two synchronous primary NSCLC. For follow-up analysis, the most advanced tumors were evaluated. Finally, a cohort of 84 tumors of 84 patients was available in which the prognostic potential of GLUT1 and MCT4 was investigated. Patient characteristics are listed in Table I. Seventy patients underwent a (bi)lobectomy, 11 patients a pneumectomy and 3 patients were treated with a wedge resection due to co-morbidity. Twenty patients received adjuvant treatment, either chemotherapy (11 patients) or radiotherapy (9 patients).

Immunohistochemical staining

Biopsies taken from NSCLC resections were frozen in liquid nitrogen and stored at -80°C. Sections of 5 μm, mounted on poly-L-lysine coated slides were stored at -80°C until staining for GLUT1, MCT4 and blood vessels.

Before starting the immunohistochemical staining, sections were fixed for 10 minutes in acetone (4°C) and rehydrated in phosphate buffered saline (PBS) 0.1 mol/L (pH 7.4) (Klinipath, Duiven, The Netherlands). Subsequently, sections were pre-incubated in primary antibody diluent (PAD; GeneTex Inc., San Antonio, USA) for 5 minutes at room temperature. Between all consecutive steps of the staining procedure, slides were rinsed thrice in PBS.

Simultaneous staining for GLUT1 plus vessels or MCT4 plus vessels was performed on two consecutive tumor sections by incubating the sections with rabbit anti-GLUT1 (Neomarkers; Fremont, CA, USA) and rabbit anti-MCT4 (Santa Cruz Biotechnology; Santa Cruz, CA, USA) respectively, diluted 1:100 in PAD, overnight at 4°C. The second incubation took 30 minutes at 37°C with goat anti-rabbitCy3 (Jackson Immuno Research Laboratories Inc.; West Grove, PA, USA), diluted 1:600 in PBS, for both GLUT1 and MCT4 sections. Afterwards, GLUT1 and MCT4 sections were stained for vessels by incubation with mouse antibody to endothelial PAL-E (Euro Diagnostica; Arnhem, The Netherlands) (diluted 1:10 in PAD) for 45 minutes at 37°C. This was followed by adding the secondary antibody chicken anti-mouseAlexa647 (diluted 1:100 in PBS) (Molecular Probes; Leiden, The Netherlands) for 45 minutes at 37°C.

After the staining procedure, sections were mounted in fluorostab (ProGen Biotechnik GmbH, Heidelberg, Germany).

To allow optimal discrimination between tumor and non-tumor tissue, a third consecutive section was stained by haematoxyline and eosin (H&E).

Image acquisition

Slides were scanned using a high-resolution 12-bit CCD camera (Coolsnap HQ, Roper Scientific Inc., Trenton, NJ, USA) on a fluorescence microscope (Axioskop, Zeiss, Göttingen, Germany). Each slide was scanned for two signals (GLUT1 plus vessels or MCT4 plus vessels) at 100x magnification. Image processing was performed using IPLab software (Scanalytics Inc., Fairfax, VA, USA) on a Macintosh computer as described before.[17] This resulted in grey scale images, which were converted to binary images for further analysis. For segmentation, thresholds for the fluorescence signals were interactively set at intensities where the steepest gradient occurred between background and foreground intensity levels.[18-21]

Image analysis

A pathologist specialized in pulmonary pathology indicated the tumor area on the H&E stained sections. Guided by these sections, the tumor area was marked on the GLUT1 and MCT4 stained sections. With this procedure, non-tumor tissue, necrotic areas and artifacts were excluded from the analysis.

Marker fractions were defined as the tumor area positive for the marker, divided by the total tumor area and were calculated by a computerized automated method.[17] To examine the relationship between vessels and GLUT1 and MCT4 expression, a domain was constructed around each vascular structure. The boundaries of these domains were defined in such a way that they were at equal distance from adjacent vessels.[18] Next, each domain was subdivided in arbitrary zones at a distance of 0-50 µm, 51-100 µm, 101-150 µm and 151-200 µm from the nearest vessel. Subsequently, marker fractions were calculated in each of these zones. Tumors without GLUT1 (n=6) or MCT4 expression (n=3) were excluded from this zone analysis.

Vascular density was calculated as the number of vascular structures per square millimeter.

Clinical follow-up

Patients were retrospectively evaluated for disease-specific survival (DSS). This endpoint was calculated from the date of surgery to the date of NSCLC related death. Median follow-up time for survivors was 39 months (range 19-106). In one case, follow-up was censored, due to uncertainty about NSCLC related cause of death. Follow-up was also censored at the time of diagnosis of a second metachronous primary lung carcinoma (n=6).

Table I. Correlation of the clinicopathological status with GLUT1 and MCT4 expression and vascular density in 84 NSCLC patients.

Characteristics	Overall (n (%))	GLUT1 (n (%))		MCT4 (n (%))		Vascular density (n (%))	
		Low	High	Low	High	Low	High
Age (years)							
< 65	42 (50)	19 (45)	23 (55)	20 (48)	22 (52)	21 (50)	21 (50)
≥ 65	42 (50)	23 (55)	19 (45)	22 (52)	20 (48)	21 (50)	21 (50)
Sex							
Male	51 (61)	28 (55)	23 (45)	26 (51)	25 (49)	24 (47)	27 (53)
Female	33 (39)	14 (42)	19 (58)	16 (49)	17 (51)	18 (55)	15 (45)
Histology							
Large cell carcinoma	4 (5)	0 (0)	4 (100) *	1 (25)	3 (75)	3 (75)	1 (25) *
Adenocarcinoma	41 (49)	33 (81)	8 (19)	21 (51)	20 (49)	9 (22)	32 (78)
Squamous cell carcinoma	34 (40)	5 (15)	29 (85)	17 (50)	17 (50)	27 (79)	7 (21)
Other	5 (6)	4 (80)	1 (20)	3 (60)	2 (40)	3 (60)	2 (40)
Tumor size (mm)							
< 30	42 (50)	24 (57)	18 (43)	23 (55)	19 (45)	18 (43)	24 (57)
≥ 30	42 (50)	18 (43)	24 (57)	19 (45)	23 (55)	24 (57)	18 (43)
Differentiation							
Well	9 (11)	8 (89)	1 (11) *	5 (56)	4 (44)	3 (33)	6 (67)
Moderate	38 (45)	20 (53)	18 (47)	16 (42)	22 (58)	18 (47)	20 (53)
Poor	37 (44)	14 (38)	23 (62)	21 (57)	16 (43)	21 (57)	16 (43)
pT							
T1	29 (35)	17 (59)	12 (41)	19 (66)	10 (34) *	12 (41)	17 (59)
T2	42 (50)	17 (40)	25 (60)	19 (45)	23 (55)	25 (60)	17 (40)
T3	8 (9)	5 (63)	3 (37)	3 (37)	5 (63)	2 (25)	6 (75)
T4	5 (6)	3 (60)	2 (40)	1 (20)	4 (80)	3 (60)	2 (40)
pN #							
N0	53 (64)	27 (51)	26 (49)	29 (55)	24 (45)	24 (45)	29 (55)
N1	21 (26)	10 (48)	11 (52)	8 (38)	13 (62)	10 (48)	11 (52)
N2	8 (10)	4 (50)	4 (50)	4 (50)	4 (50)	7 (88)	1 (12)
pTNM 7th edition							
Stage I	46 (55)	25 (54)	21 (46)	28 (61)	18 (39) *	20 (43)	26 (57)
Stage II	24 (28)	9 (37)	15 (63)	9 (37)	15 (63)	12 (50)	12 (50)
Stage IIIA	14 (17)	8 (57)	6 (43)	5 (36)	9 (64)	10 (71)	4 (29)
Surgical margins #							
Free	73 (89)	36 (49)	37 (51)	37 (51)	36 (49)	37 (51)	36 (49)
Not free	9 (11)	5 (56)	4 (44)	4 (44)	5 (56)	4 (44)	5 (56)

Abbreviations: GLUT1=glucose transporter 1, MCT4=monocarboxylate transporter 4, NSCLC=non-small cell lung cancer
In this table, the study population is dichotomized by low and high marker expression with cut-off set at median value of the whole group of NSCLC (13.6% for GLUT1, 16.6% for MCT4 and 102.1 for vascular density).

Analysis performed for 82 patients. Two cases were excluded from the analysis since an incomplete mediastinal staging was performed due to the following reasons:
- Only a wedge resection was performed based on comorbidity
- According to the TNM 6th edition, stage IV was diagnosed as a result of a tumor nodule in a different ipsilaterale lobe. According to the TNM 7th edition however, this patient was classified as stage IIIA.
* p-value significant at the 0.05 level

Statistical analysis

Statistical analyses were done using SPSS 16.0 statistical software (SPSS Inc., Chicago, IL, USA). The Pearson Chi-Square test and Spearman correlation were used to determine associations between the metabolic markers on a dichotomous scale and clinicopathological parameters. The correlation coefficient (r) between the markers on a continuous scale and clinicopathological parameters was calculated using the Pearson's and Spearman's Rank test where appropriate. Survival curves were generated using the Kaplan-Meier method. A log-rank test with linear trend for factor levels was performed to test for statistically significant differences between the survival curves. The number of events precluded multivariate analyses. A $p<0.05$ was considered statistically significant.

Table II. Fractions of GLUT1 and MCT4 and vascular density within all NSCLC and histological subtypes.

Carcinoma	GLUT1 (%)	MCT4 (%)	Vascular density
All NSCLC	13.6 (0.00-62.0)	16.6 (0.0-62.5)	102.1 (23.5-323.6)
Adenocarcinomas	1.8 (0.0-44.5)	16.3 (0.4-53.7)	145.3 (30.2-323.6)
Squamous cell carcinomas	24.1 (5.5-62.0)	17.4 (0.0-61.2)	74.8 (23.5-164.3)

Abbreviations: GLUT1=glucose transporter 1, MCT4=monocarboxylate transporter 4, NSCLC=non-small cell lung cancer
Values expressed as median (range).
GLUT1 and MCT4 expression as percentage of total tumor surface. Vascular density expressed as the number of vascular structures per square millimeter.

Results

Metabolic marker expression and clinicopathology

GLUT1 and MCT4 staining were confined to the cell membrane. Examples of tumors with different marker fractions and vascular density are shown in Figure 1 and quantitative data of marker fractions in Table II.

For quantitative and survival analyses, the study population was dichotomized by low and high marker expression with cut-off set at median values, except for GLUT1 in adenocarcinomas. In this subgroup, an optimal cut-off value of 0.26% was applied (median 1.8%). This resulted in 15 adenocarcinomas with low versus 26 adenocarcinomas with high GLUT1 expression.

Figure 1. Immunofluorescent images of NSCLC showing different fractions of GLUT1 and MCT4 and vascular density.
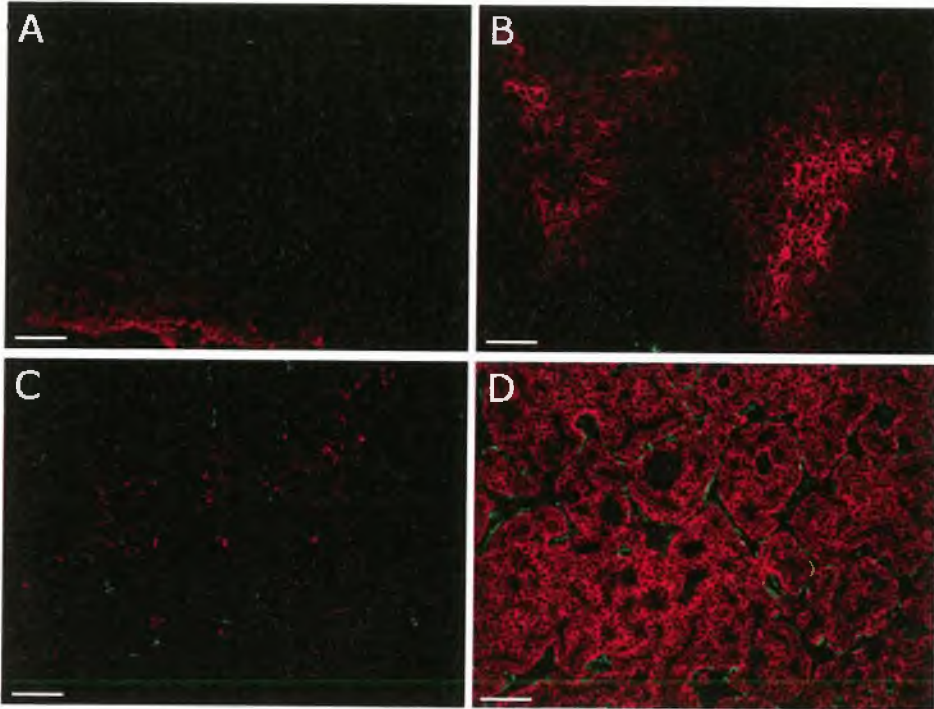
(A, C, D) Adenocarcinoma, (B) squamous cell carcinoma. *Red*, GLUT1 or MCT4; *green*, vessels; magnification 100x; scale bars represent 100 μm.
(A)   Low GLUT1 expression (1.8%) and high vascular density (170/mm^2).
(B)   High GLUT1 expression (30.3%). Vascular density is low (68/ mm^2).
(C)   Low MCT4 expression (2.7%) and low vascular density (84/ mm^2).
(D)   High MCT4 expression (53.7%). Vascular density is high (207/ mm^2).

GLUT1 expression and clinicopathology

GLUT1 expression correlated significantly with histological subtype, being higher in squamous cell carcinomas (Table I-II, Figure 2A).

In adenocarcinomas, median GLUT1 fraction varied from 0.1% in tumors with a good differentiation grade to 2.5% and 13.3% in moderate and poorly differentiated carcinomas respectively (Figure 2B). Furthermore, GLUT1 fraction was significantly higher in adenocarcinomas with lymph node metastases at diagnosis, compared to node negative tumors (Figure 2C). These correlations were not found in squamous cell carcinomas (Figure 2B-C).

Figure 2. GLUT1 expression and the clinicopathological status.
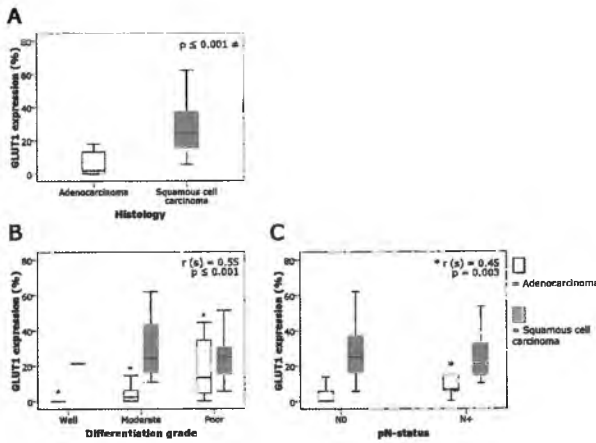
(A) GLUT1 expression in squamous cell carcinomas compared to adenocarcinomas.
≠ Kruskal-Wallis test.
(B, C) Correlation of GLUT1 expression with differentiation grade (B) and pN-status (C), according to histological subtype.
Boxes represent lower quartile, median value and upper quartile, and whiskers represent minimum and maximum value.
Outliers are not shown.

MCT4 expression and clinicopathology
High MCT4 expression correlated with pT-status (p=0.022) and pTNM-stage (p=0.033) (Table I). This significance was lost when pT-status and pTNM-stage were compared with MCT4 expression on a continuous scale.

Vascular density and clinicopathology
Vascular density was significantly higher in adenocarcinomas compared to squamous cell carcinomas (p≤0.001) (Table I-II).

GLUT1 and MCT4 expression and vascular distance
The zone analysis showed an increase in GLUT1 and MCT4 expression with increasing distance from the nearest vessel. This diffusion-limited or chronic hypoxia pattern of expression [12, 22] was more clearly observed in squamous cell carcinomas, in which median GLUT1 fractions increased 4-4.5 fold and median MCT4 fractions 3-3.5 fold at >100 μm from the vessels (Figure 3).
In every zone, median GLUT1 fractions were 4-6 times higher in squamous cell carcinomas compared to adenocarcinomas. Strikingly, MCT4 fractions were comparable in these histological subtypes, except for the first zone. In this zone, stronger upregulation of MCT4 was found in adenocarcinomas.

48

From Figure 3, the ratio of median GLUT1 fraction:median MCT4 fraction was calculated within the different zones around the vessels. Within each of the zones, this ratio differed in adenocarcinomas and squamous cell carcinomas, being <1 in adenocarcinomas and >1 in squamous cell carcinomas.

Figure 3. GLUT1 and MCT4 expression at increasing distances from the vasculature in adenocarcinomas and squamous cell carcinomas.

C and E: GLUT1 expression within an adenocarcinoma

D and F: MCT4 expression within an adenocarcinoma
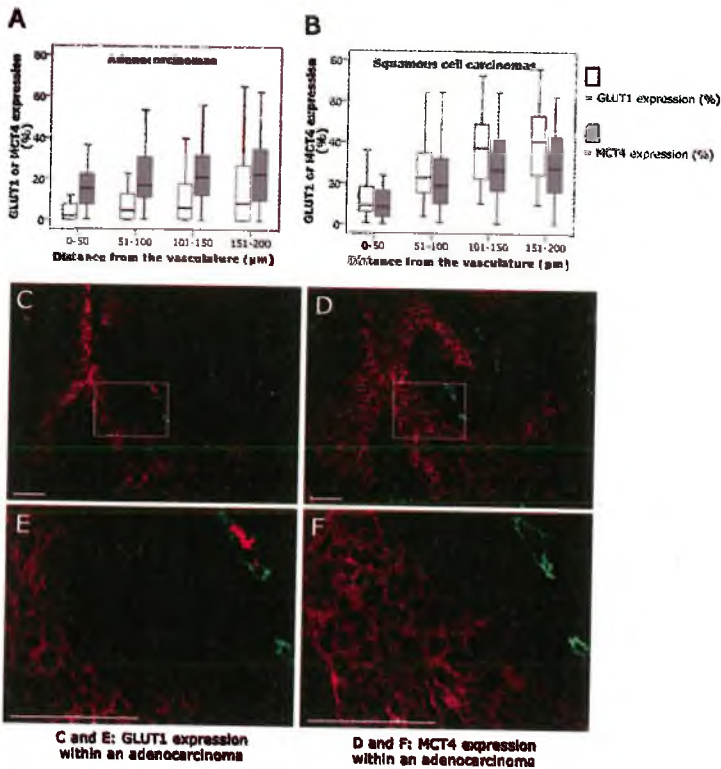
(A, B) Boxplots showing GLUT1 and MCT4 expression at various distances from the blood vessels in adenocarcinomas (A) and squamous cell carcinomas (B). See text for details.

Boxes represent lower quartile, median value and upper quartile, and whiskers represent minimum and maximum value. Outliers are not shown.

(C–F) Immunofluorescent images showing the pattern of distribution of GLUT1 and MCT4 expression within an adenocarcinoma.

(D) Shows higher MCT4 expression compared to GLUT1 expression (C) at closer distance from the vessels.

(E, F) Enlargement of a part of C and D respectively as indicated by the squares.

Red, GLUT1 or MCT4; green, vessels. (C and D) Magnification 100×, (E and F) magnification 400×. Scale bars represent 100 μm. The red artifacts within the vessels (C and E) were excluded from the analysis.

Metabolic marker expression and outcome

Disease-specific survival and clinicopathology
During follow-up, 20 of 84 patients encountered NSCLC related death. Eleven of 41 patients with an adenocarcinoma and 4 of 34 patients with a squamous cell carcinoma died as a result of their disease (p=0.289).
Of the clinicopathological variables, pT-status (p=0.045), positive lymph nodes (p=0.009) or a more advanced pathological stage at diagnosis (p=0.001), and positive surgical margins (p=0.001) were significantly associated with a poor DSS.
The number of events in the squamous cell carcinoma subgroup was too small to allow survival analysis.

Prognostic value of GLUT1 and MCT4
GLUT1 did not reveal an association with DSS in all NSCLC. However, in adenocarcinomas, both high GLUT1 and high MCT4 expression demonstrated a trend towards a worse DSS (p=0.062 and p=0.191 respectively) (Figure 4A-B).

Prognostic value of the combination of GLUT1 plus MCT4
Combined expression patterns in adenocarcinomas showed stronger associations with survival, compared with GLUT1 and MCT4 expression alone. Seven out of 16 patients with high GLUT1 plus high MCT4 expression died as a result of their disease, leading to a 5-year DSS of 30%, versus 4 patients of the group with low expression for one or both markers (n=25), resulting in a 5-year DSS of 70% (p=0.032) (Figure 4C).

Discussion

We investigated the spatial distribution and prognostic impact of GLUT1 and MCT4 in NSCLC. The observed differences in marker expression in adeno- and squamous cell carcinomas suggest a different metabolism between these histological subtypes.

GLUT1 expression and clinicopathology
GLUT1 was found to be extensively expressed in squamous cell carcinomas relative to adenocarcinomas. In adenocarcinomas, higher GLUT1 expression correlated with a poor differentiation grade, as well as with lymph node metastases at diagnosis. These observations are in line with other studies.[4, 23-28]

GLUT1 and MCT4 expression and vascular distance
The diffusion-limited or chronic hypoxia pattern[12, 22] of GLUT1 and MCT4 expression was more clearly observed in squamous cell carcinomas compared to adenocarcinomas. Strikingly, MCT4 expression was already relatively high in the first cell layers around the

vessels in adenocarcinomas. Therefore, GLUT1 and MCT4 upregulation seems to be stronger related to hypoxia in squamous cell carcinomas.

Besides the hypoxia-dependent activation of the HIF-1 pathway, HIF-1 can be activated in a hypoxia-independent way through the PI3K/Akt/mTOR pathway and also due to mutations in the von Hippel-Lindau protein, leading to aerobic glycolysis.[10, 12, 29] In adenocarcinomas MCT4 may be induced in this way under normoxic conditions.

Figure 4. Disease-specific survival according to GLUT1 and/or MCT4 expression in adenocarcinomas.
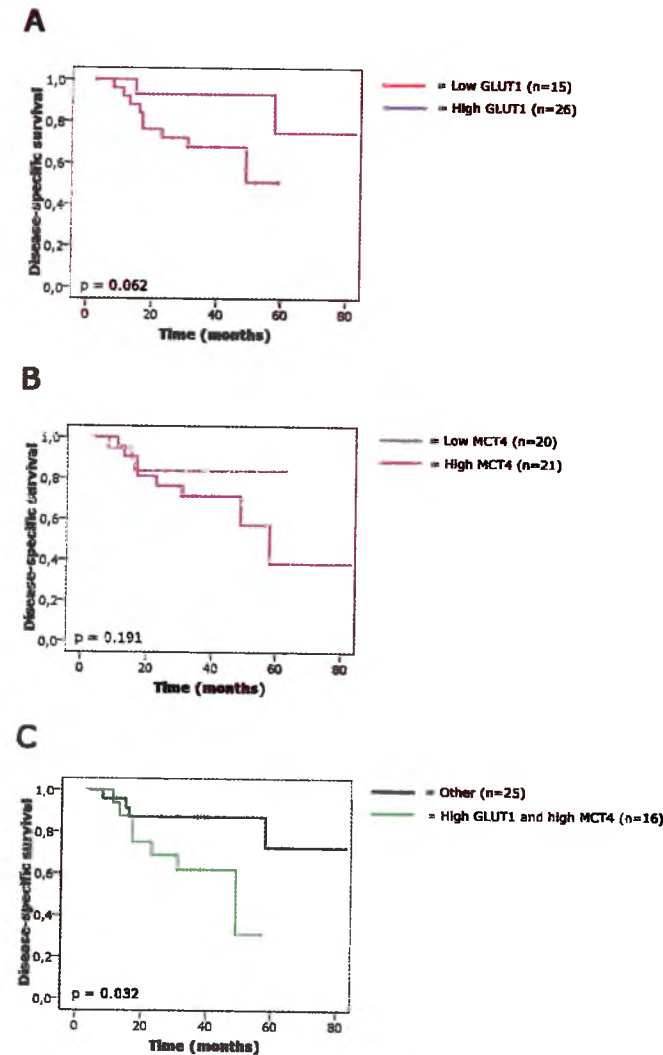
Cut-off value of GLUT1 is set just below the median at 0.26% (median 1.8%), the cut-off value of MCT4 is 16.3% (median level).

Metabolism of adenocarcinomas and squamous cell carcinomas

Glycolysis generates 2 mol of ATP and 2 mol of lactate per mol of glucose consumed [30]. This suggests that glycolytic tumor cells need a lower amount of glucose importers relative to lactate exporters. However, mitochondrial oxidation converts 2 mol of pyruvate into 36 mol of ATP without production of lactate.[30] So, tumor cells that use oxidative phosphorylation need a higher amount of glucose transporters relative to lactate transporters.

The observed differences in marker expression suggest a different metabolism between adeno- and squamous cell NSCLC. Given the observation that GLUT1 and MCT4 expression seem to be less related to hypoxia in adenocarcinomas, and the ratio of GLUT1:MCT4 is <1, this suggests that adenocarcinomas rely mainly on aerobic glycolysis. In contrast, squamous cell carcinomas are probably more hypoxic as a result of low vascular density, exhibit GLUT1 and MCT4 expression in a ratio >1 and the pattern of expression is diffusion-limited. This suggests that squamous cell carcinomas utilize mitochondrial oxidation as an energy source under normoxic conditions with anaerobic glycolysis under hypoxic conditions.

It remains unclear how adenocarcinomas are able to produce enough ATP with those low amounts of GLUT1, since glycolysis is a less efficient energy pathway. Other transporters are possibly involved in glucose uptake, for example GLUT3.[29] It was demonstrated that the combination of both GLUT1 and GLUT3 expression and a poor differentiation grade determined the extent of fluorodeoxyglucose (FDG) accumulation in NSCLC.[4] However, GLUT3 expression by itself does not correlate with the amount of FDG uptake.[4, 31, 32] The utilization of lactate for energetic purposes could be another explanation. Aerobic tumor cells express monocarboxylate transporter 1 (MCT1) on the cell membranes, which allows tumor cells to take up lactate, and use it as a substrate for mitochondrial oxidation, with the production of 36 mol of ATP per 2 mol of lactate consumed.[33]

Another issue that remains to be elucidated is the reason for the high GLUT1 amount in squamous cell carcinomas. If these carcinomas exhibit mitochondrial oxidation, which is energy efficient, with anaerobic glycolysis in hypoxic regions, a lower expression rate would be expected to suffice the demand of glucose.

A limitation of this exploratory study is the question whether the transporter expression level gives sufficient information on the functional activation status of transporters. It was demonstrated that GLUT1 expression and FDG accumulation in NSCLC correlate significantly, [25, 32, 34] reflecting functionally active glucose transporters. Also, MCT4 expression correlated with lactate concentration in lung cancer cell lines *in vitro*.[35] The affinity of MCT4 for lactate is variable and can be increased by exposure to low pH values.[36] However, tumor lactate and glucose concentrations did not correlate with lactate dehydrogenase A, which converts pyruvate to lactate, and GLUT1 expression respectively in tumor xenografts derived from head and neck squamous cell carcinoma lines.[16] Therefore, the functional metabolic consequences of differences in transporter expression between adeno- and squamous cell NSCLC warrant further investigation of for instance direct lactate concentration.[37, 38]

Previous studies investigating the prognostic potential of GLUT1 in NSCLC have found contradicting results.[3, 23, 28] For adenocarcinomas, high GLUT1 expression has been correlated with a poor survival.[7, 23] Our study showed a trend towards a worse DSS for adenocarcinomas with high GLUT1 expression.

Combination of high GLUT1 plus high MCT4 expression correlated significantly with a poor DSS in adenocarcinomas. This stronger effect of the combined expression pattern might be explained by the following mechanism. Glycolysis results in the acid end product CO_2 and lactate, which are transported out of the cell by MCT4. This leads to extracellular acidification and a high extracellular lactate level. Acid and lactate can upregulate matrix-degrading metalloproteinases in stromal fibroblasts and tumor cells, which are involved in invasion, intravasation and metastasis.[9, 10, 39] High lactate levels have been correlated with a poor prognosis in breast, lung and liver carcinomas.[10] Lactate accumulation in malignancies correlates with radioresistance.[16, 37] Furthermore, the Warburg effect increases the malignant potential of tumor cells.[15] MCT4 inhibition may decrease tumor cell invasion and extracellular matrix breakdown.[15, 36, 40, 41]

Although we demonstrated comparable MCT4 fractions in adeno- and squamous cell carcinomas, we found high MCT4 expression close to vessels in only adenocarcinomas. This may result in high acid and lactate levels and consequently metalloproteinases in the proximity of the vasculature, which could promote intravasation and metastases in adenocarcinomas.

Conclusion

We attempted to unravel differences in metabolism between adeno- and squamous cell NSCLC. Adenocarcinomas may use aerobic glycolysis as an energy source, whereas the metabolism of squamous cell carcinomas seems to rely on mitochondrial oxidation with anaerobic glycolysis under hypoxic conditions. Our findings suggest that an aerobic glycolytic metabolism is an additive responsible factor for aggressive behavior in NSCLC. This subgroup of tumors may benefit from new treatment approaches, such as MCT4 inhibitors. Since this is an exploratory study, our results warrant further investigation and need independent validation. The consequences of tumor cell metabolism for the microenvironment and vice versa should be analyzed in adeno- and squamous cell NSCLC with a focus on the activation level of transporters and enzymes.

References

1. Jemal A, Siegel R, Xu J, Ward E. Cancer statistics. CA Cancer J Clin 2010;60:277-300.

2. Kelsey CR, Light KL, Marks LB. Patterns of failure after resection of non-small-cell lung cancer: implications for postoperative radiation therapy volumes. Int J Radiat Oncol Biol Phys 2006;65:1097-105.

3. Nguyen XC, Lee WW, Chung JH, Park SY, Sung SW, Kim YK, et al. FDG uptake, glucose transporter type 1, and Ki-67 expressions in non-small-cell lung cancer: correlations and prognostic values. Eur J Radiol 2007;62: 214-9.

4. de Geus-Oei LF, van Krieken JH, Aliredjo RP, Krabbe PF, Frielink C, Verhagen AF, et al. Biological correlates of FDG uptake in non-small cell lung cancer. Lung Cancer 2007;55:79-87.

5. Schuurbiers OC, Kaanders JH, van der Heijden HF, Dekhuijzen RP, Oyen WJ, Bussink J. The PI3-K/AKT-pathway and radiation resistance mechanisms in non-small cell lung cancer. J Thorac Oncol 2009;4:761-7.

6. Bussink J, Kaanders JH, van der Graaf WT, Oyen WJ. PET-CT for radiotherapy treatment planning and response monitoring in solid tumors. Nat Rev Clin Oncol 2011;8:233-42.

7. Minami K, Saito Y, Imamura H, Okamura A. Prognostic significance of p53, Ki-67, VEGF and Glut-1 in resected stage I adenocarcinoma of the lung. Lung Cancer 2002;38:51-7.

8. Busk M, Horsman MR, Jakobsen S, Bussink J, van der Kogel A, Overgaard J. Cellular uptake of PET tracers of glucose metabolism and hypoxia and their linkage. Eur J Nucl Med Mol Imaging 2008;35:2294-303.

9. Ganapathy V, Thangaraju M, Prasad PD. Nutrient transporters in cancer: relevance to Warburg hypothesis and beyond. Pharmacol Ther 2009;121:29-40.

10. Gillies RJ, Robey I, Gatenby RA. Causes and consequences of increased glucose metabolism of cancers. J Nucl Med 2008;49:24S-42S.

11. Macheda ML, Rogers S, Best JD. Molecular and cellular regulation of glucose transporter (GLUT) proteins in cancer. J Cell Physiol 2005;202:654-62.

12. Rademakers SE, Span PN, Kaanders JH, Sweep FC, van der Kogel AJ, Bussink J. Molecular aspects of tumour hypoxia. Mol Oncol 2008;2:41-53.

13. Ullah MS, Davies AJ, Halestrap AP. The plasma membrane lactate transporter MCT4, but not MCT1, is up-regulated by hypoxia through a HIF-1alpha-dependent mechanism. J Biol Chem 2006;281:9030-7.

14. Moon EJ, Brizel DM, Chi JT, Dewhirst MW. The potential role of intrinsic hypoxia markers as prognostic variables in cancer. Antioxid Redox Signal 2007;9:1237-94.

15. Schneiderhan W, Scheler M, Holzmann KH, Marx M, Gschwend JE, Bucholz M, et al. CD147 silencing inhibits lactate transport and reduces malignant potential of pancreatic cancer cells in in vivo and in vitro models. Gut 2009;58:1391-8.

54

16. Sattler UG, Meyer SS, Quennet V, Hoerner C, Knoerzer H, Fabian C, et al. Glycolytic metabolism and tumour response to fractionated irradiation. Radiother Oncol 2010;94:102-9.

17. Rijken PF, Bernsen HJ, Peters JP, Hodgkiss RJ, Raleigh JA, van der Kogel AJ. Spatial relationship between hypoxia and the (perfused) vascular network in a human glioma xenograft: a quantitative multi-parameter analysis. Int J Radiat Oncol Biol Phys 2000;48:571-82.

18. Bussink J, Kaanders JH, Rijken PF, Martindale CA, van der Kogel AJ. Multiparameter analysis of vasculature, perfusion and proliferation in human tumour xenografts. Br J Cancer 1998;77:57-64.

19. Rademakers SE, Lok J, van der Kogel AJ, Bussink J, Kaanders JH. Metabolic markers in relation to hypoxia; staining patterns and colocalization of pimonidazole, HIF-1alpha, CAIX, LDH-5, GLUT-1, MCT1 and MCT4. BMC Cancer 2011;11:167.

20. Rademakers SE, Rijken PF, Peeters WJ, Nijkamp MM, Barber PR, van der Laak J, et al. Parametric mapping of immunohistochemically stained tissue sections; a method to quantify the colocalization of tumor markers. Cell Oncol 2011;34:119-29.

21. Rijken PF, Bernsen HJ, van der Kogel AJ. Application of an image analysis system to the quantitation of tumor perfusion and vascularity in human glioma xenografts. Microvasc Res 1995;50:141-53.

22. Thomlinson RH, Gray LH. The histological structure of some human lung cancers and the possible implications for radiotherapy. Br J Cancer 1955;9:539-49.

23. Andersen S, Eilertsen M, Donnem T, Al-Shibli K, Al-Saad S, Busund LT, et al. Diverging prognostic impacts of hypoxic markers according to NSCLC histology. Lung Cancer 2011;72:294-302.

24. Brown RS, Leung JY, Kison PV, Zasadny KR, Flint A, Wahl RL. Glucose transporters and FDG uptake in untreated primary human non-small cell lung cancer. J Nucl Med 1999;40:556-65.

25. Higashi K, Ueda Y, Sakurai A, Wang XM, Xu L, Murakami M, et al. Correlation of Glut-1 glucose transporter expression with. Eur J Nucl Med 2000;27:1778-85.

26. Ito T, Noguchi Y, Satoh S, Hayashi H, Inayama Y, Kitamura H. Expression of facilitative glucose transporter isoforms in lung carcinomas: its relation to histologic type, differentiation grade, and tumor stage. Mod Pathol 1998;11:437-43.

27. Mamede M, Higashi T, Kitaichi M, Ishizu K, Ishimori T, Nakamoto Y, et al. [18F]FDG uptake and PCNA, Glut-1, and Hexokinase-II expressions in cancers and inflammatory lesions of the lung. Neoplasia 2005;7:369-79.

28. Younes M, Brown RW, Stephenson M, Gondo M, Cagle PT. Overexpression of Glut1 and Glut3 in Stage I nonsmall cell lung carcinoma is associated with poor survival. Cancer 1997;80:1046-51.

29. Semenza GL. Regulation of cancer cell metabolism by hypoxia-inducible factor 1. Semin Cancer Biol 2009;19:12-6.

30. Semenza GL. Tumor metabolism: cancer cells give and take lactate. J Clin Invest 2008; 118: 3835-3837.

31. Marom EM, Aloia TA, Moore MB, Hara M, Herndon JE II, Harpole DH Jr., et al. Correlation of FDG-PET imaging with Glut-1 and Glut-3 expression in early-stage non-small cell lung cancer. Lung Cancer 2001;33:99-107.

32. van Baardwijk A, Dooms C, van Suylen RJ, Verbeken E, Hochstenbag M, Dehing-Oberije C, et al. The maximum uptake of (18)F-deoxyglucose on positron emission tomography scan correlates with survival, hypoxia inducible factor-1alpha and GLUT-1 in non-small cell lung cancer. Eur J Cancer 2007;43:1392-8.

33. Sonveaux P, Vegran F, Schroeder T, Wergin MC, Verrax J, Rabbani ZN, et al. Targeting lactate-fueled respiration selectively kills hypoxic tumor cells in mice. J Clin Invest 2008;118:3930-42.

34. Jadvar H, Alavi A, Gambhir SS. 18F-FDG uptake in lung, breast, and colon cancers: molecular biology correlates and disease characterization. J Nucl Med 2009;50:1820-7.

35. Izumi H, Takahashi M, Uramoto H, Nakayama Y, Oyama T, Wang KY, et al. Monocarboxylate transporters 1 and 4 are involved in the invasion activity of human lung cancer cells. Cancer Sci;102:1007-13.

36. Kennedy KM, Dewhirst MW. Tumor metabolism of lactate: the influence and therapeutic potential for MCT and CD147 regulation. Future Oncol 2010;6:127-48.

37. Quennet V, Yaromina A, Zips D, Rosner A, Walenta S, Baumann M, et al. Tumor lactate content predicts for response to fractionated irradiation of human squamous cell carcinomas in nude mice. Radiother Oncol 2006;81:130-5.

38. Mueller-Klieser W, Walenta S. Geographical mapping of metabolites in biological tissue with quantitative bioluminescence and single photon imaging. Histochem J 1993;25:407-20.

39. Lu X, Kang Y. Hypoxia and hypoxia-inducible factors: master regulators of metastasis. Clin Cancer Res;16:5928-35.

40. Gallagher SM, Castorino JJ, Philp NJ. Interaction of monocarboxylate transporter 4 with beta1-integrin and its role in cell migration. Am J Physiol Cell Physiol 2009;296:C414-21.

41. Gallagher SM, Castorino JJ, Wang D, Philp NJ. Monocarboxylate transporter 4 regulates maturation and trafficking of CD147 to the plasma membrane in the metastatic breast cancer cell line MDA-MB-231. Cancer Res 2007;67:4182-9.

Chapter 4

Histology-specific glucose metabolism and the tumor microenvironment affect [18]FDG-PET interpretation and prognosis in NSCLC*

Submitted

Olga CJ Schuurbiers

Tineke WH Meijer

Johannes HAM Kaanders

Monika G Looijen-Salamon

Lioe-Fee de Geus-Oei

Miep A van der Drift

Erik HFM van der Heijden

Wim J Oyen

Eric P Visser

Paul N Span

Johan Bussink

Abstract

Introduction
Histological and biological features of non-small cell lung carcinomas (NSCLCs) are important determinants for clinical outcome. In the present study, differences in glucose metabolism between adeno- and squamous cell NSCLCs were quantified using the hypoxia and glycolysis-related markers GLUT1, CAIX, MCT1, MCT4, vascular density, as well as [18]FDG-PET imaging in curatively resected NSCLC patients. The relevance of these metabolic markers for disease-free survival (DFS) was analyzed.

Methods
Patients who underwent a curative resection for stage I, II and resectable stage IIIA, cN0-1 NSCLC of whom fresh frozen lung resection biopsies and/or pre-treatment [18]FDG-PET-scans were available, were included in this study. In 111 patients, pre-treatment [18]FDG-uptake was quantified by calculating SUVmax and TLGmax. Metabolic marker expression, measured by immunofluorescent staining (protein) and qPCR (mRNA), and vascular density were determined in 90 fresh frozen resection specimens. Patients were retrospectively evaluated for DFS.

Results
mRNA and protein expression of metabolic markers, with the exception of MCT4, and [18]FDG-uptake were higher in squamous cell carcinomas than in adenocarcinomas, whereas adenocarcinomas were better vascularized. Adenocarcinomas had a worse DFS compared to squamous cell carcinomas (p=0.016) based on the potential to metastasize. High glucose consumption, as assessed by GLUT1 mRNA, SUVmax or TLGmax, was associated with a worse DFS only in adenocarcinomas.

Conclusion
Our findings suggest that adenocarcinomas exhibit glycolysis under normoxic conditions, whereas squamous cell carcinomas are exposed to diffusion-limited hypoxia resulting in a very high anaerobic glycolytic rate. Although squamous cell carcinomas have a higher [18]FDG-uptake, in general regarded as a poor prognostic factor, adenocarcinomas had a higher metastatic potential and a worse DFS. Therefore, the meaning of [18]FDG accumulation might differ between NSCLC histologies with respect to understanding tumor glucose metabolism, prediction of prognosis, and exploiting [18]FDG-PET in treatment strategies.

Introduction

Biological behavior of cancer cells is not merely determined by the tumor cells' genotype, but is largely temporally and spatially modified by the tumor microenvironment. For example, hypoxia, which is the result of an insufficient and abnormal tumor microvasculature, plays a major role in cancer biology. Hypoxia is associated with more aggressive tumor behavior, impaired response to radio- and chemotherapy, and worse clinical outcome.[1-3] Metabolism of malignant tumors is often affected by hypoxia, as tumor cells switch to anaerobic glycolysis with production of lactate and acid under hypoxic conditions (Pasteur effect). However, in cancer cells, a high rate of glycolysis is also observed in the presence of oxygen (Warburg effect). This is associated with selective growth advantage and tumor cell survival.[4,5] The higher rate of glycolysis with the consequential higher glucose consumption of tumor cells is one of the reasons why 18-fluoro-2-deoxyglucose positron emission tomography (^{18}FDG-PET) is useful as an imaging biomarker in solid tumors.[4]

The hypoxia-inducible factor-1 (HIF-1) pathway plays a pivotal role in cellular adaptation mechanisms to hypoxic conditions. The HIF-1 pathway controls expression of many endogenous hypoxia- and glycolysis-related transporters and enzymes, such as glucose transporter 1 (GLUT1), responsible for cellular glucose uptake, carbonic anhydrase IX (CAIX), which prevents intracellular acidification, and monocarboxylate transporter 1 and 4 (MCT1, MCT4) for the regulation of intracellular lactate level.[2,3,5-10].

Former analysis of GLUT1 and MCT4 protein expression suggested differences in metabolism between adeno- and squamous cell carcinomas.[11] The results of that study implied that adenocarcinomas rely mainly on aerobic glycolysis for ATP production and squamous cell carcinomas behave more 'physiologically' with oxidative phosphorylation in aerobic conditions and anaerobic glycolysis under hypoxic circumstances.[11] This finding may have an important impact on the interpretation of ^{18}FDG-PET scans of these two NSCLC histologies.

Several histological subtypes are categorzied within the same disease entity 'NSCLC'. However, growing evidence shows that biological behavior and treatment-related outcome differ between histological subgroups of NSCLC.[11,12] In the present study, we analyzed the tumor microenvironment and glucose metabolism in adeno- versus squamous cell lung carcinomas by analyzing mRNA and protein levels of GLUT1, CAIX, MCT1 and MCT4, as well as ^{18}FDG uptake in curatively resected NSCLC patients. Moreover, we determined the consequences of differences in tumor glucose metabolism for survival.

Materials and methods

Patients

Patients who underwent a curative resection for stage I, II and resectable stage IIIA, cN0-1 NSCLC at the Radboud University Nijmegen Medical Centre between January 2002 and December 2008, of whom fresh frozen lung resection biopsies and/or pre-treatment [18]FDG-PET-scans were available, were included in this study. One-hundred twenty-nine NSCLCs in 127 patients were identified. Patients who received experimental neo-adjuvant treatment were excluded (n=5). In 5 patients both the PET-scan and fresh frozen tissue were not available. As shown in figure 1, 119 NSCLCs in 117 patients remained. In 111 patients, a pre-treatment diagnostic [18]FDG-PET-scan was available for analysis. Patient and clinicopathological characteristics are shown in Table I.

In the group of 119 NSCLCs, 27 fresh frozen samples were not suitable for evaluation due to sampling error (absence of tumor tissue, presence of inflammatory tissue or necrosis) and two biopsies could not be retrieved. This resulted in 90 tumors of 88 patients available for immunofluorescent staining and qPCR analysis. GLUT1, CAIX and MCT4 qPCR analysis was not succesfull in four cases, MCT1 qPCR analysis failed in five tumors (Figure 1).[11] In these tumors, immunofluorescent staining of GLUT1, CAIX, MCT1 and MCT4, qPCR analysis of these markers and [18]FDG-uptake were correlated with clinicopathological characteristics.

For treatment outcome analysis, three patients with incomplete anatomical resections based on unexpected stage IIIB/IV (TNM 7th edition) were excluded and one patient was lost to follow-up. Of the two patients with two synchronous primary NSCLCs only the most advanced tumors were considered for survival analysis. Figure 1 summarizes numbers of available patients for follow-up analyses.

Immunofluorescent staining for GLUT1, CAIX, MCT1, MCT4 and vessels

Biopsies taken from lung cancer resection specimens were snap frozen in liquid nitrogen and stored at -80°C until further processing. Sections of 5 μm, mounted on poly-L-lysine coated slides, were stored at -80°C until immunofluorescent staining. Immunofluorescent staining methods of metabolic markers, visualizing protein expression, and vasculature were performed as described before.[11,13]

Fluorescence microscope image acquisition and analysis

Immunofluorescent image acquisition and analysis was described before.[11] In short, slides were scanned at 100x magnification using a high-resolution 12-bit CCD camera (Coolsnap HQ, Roper Scientific Inc., Trenton, NJ, USA) on a fluorescence microscope (Axioskop, Zeiss, Göttingen, Germany). This resulted in gray scale images, which were converted to binary images for further analysis. The tumor area was marked on the stained sections. Marker fractions were defined as the tumor area positive for the marker (binary images), divided by the total tumor area.

RT-PCR

Total RNA was isolated with the RNeasy RNA isolation kit (Qiagen, Hilden, Germany), and reversed transcribed using the Reverse Transcription System from Promega Benelux B.V. (Leiden, the Netherlands). qPCR was performed with specific primers for GLUT1, CAIX, MCT1 and GLUT1 on a CFX96 real-time PCR detection system (Bio-Rad Laboratories Inc, Richmond, CA) using SYBR Green, and levels are expressed as ratios of HPRT.[14]

Figure 1. Flowchart of in- and exlusion criteria for correlation and follow-up analyses.
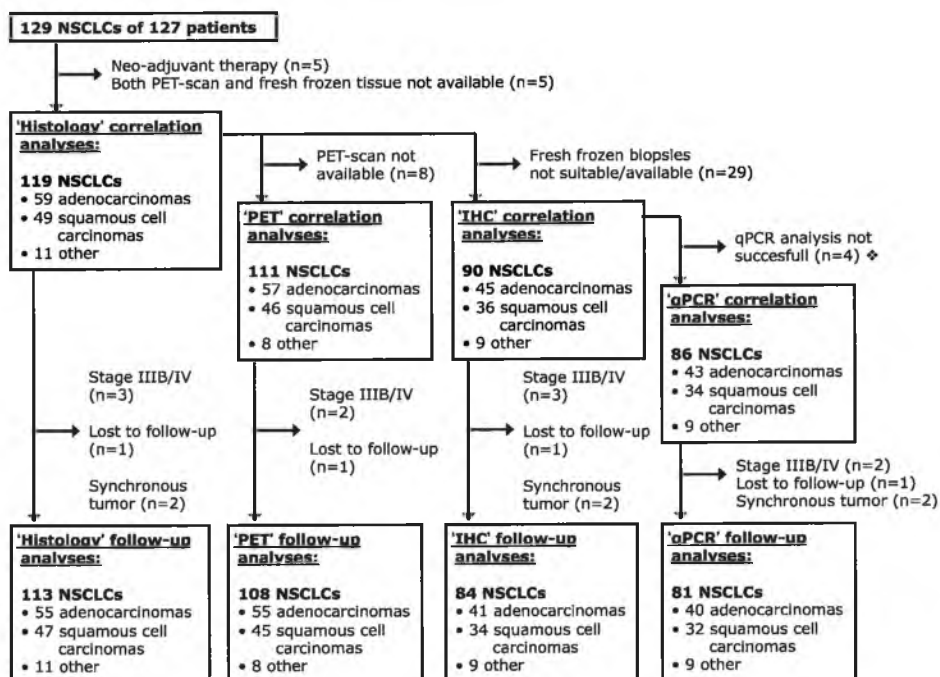
Abbreviations: IHC, immunohistochemistry; PET, positron emission tomography; qPCR, quantitative polymerase chain reaction. v MCT1 qPCR analysis failed in five tumors

[18]FDG-PET

Prior to ^{18}F-fluorodeoxyglucose ([18]FDG) injection, patients fasted for ≥six hours. PET-scans were performed 60 minutes after intravenous injection of ~250 MBq [18]FDG (Covidien, Petten, The Netherlands) and 10 mg furosemide. PET-scans were acquired on an ECAT-EXACT full ring PET-scanner (Siemens/CTI, Knoxville, TN) until September 2005, using three-dimensional emission of 10 min/bed position and germanium-68 2 min/bed position trasmission scans for attenuation correction. PET scans were itteratively reconstructed using two iterations and eight subsets. From September 2005 onwards, PET scans were acquired

on a PET/CT scanner (Biograph Duo, Siemens Medical Solutions USA, Inc.) using three-dimensional emissions of 4 min/bed position. A low-dose CT scan for localization and attenuation-correction purposes was acquired. Scanning parameters included 40 mA·s (50 mA·s for patient weight >100 kg and 60 mA·s for >120 kg), 130 kV, 5 mm slice collimation, 0.8 s rotation time, and pitch of 1.5, reconstructed to 3 mm slices for smooth coronal representation. Both PET scanners were cross-calibrated.

Regions of interest were drawn using a 40% fixed threshold isocontour value. Subsequently, tumor volumes and the maximum standardized uptake value (SUVmax) were calculated. Maximum total lesion glycolysis (TLGmax) was calculated by multiplying tumor volume (cm^3) and SUVmax.[15,16]

Clinical follow-up

Patients were retrospectively evaluated for disease-free survival (DFS), which was calculated from the date of surgery to the date of lung cancer related relapse. Follow-up was according to national guidelines and consisted of clinical and radiological (at least chest X-ray) routine follow-up every 3 months in the first year and every 6 months from the second year or earlier if patients were symptomatic. Follow-up was censored at the time of diagnosis of a second metachronous primary lung cancer (n=7).

Statistical analysis

Statistical analyses were performed using SPSS 18.0 statistical software (SPSS Inc., Chicago, IL, USA). The correlation coefficient (r) between the hypoxia and glycolysis-related markers on a continuous scale and the clinicopathological parameters was calculated using the Pearson's and Spearman's rank test where appropriate. Differences between histological subtypes were measured by means of the Mann-Whitney U test or the Independent-Samples T Test where appropriate. Survival analyses were done with the Cox Regression and Kaplan-Meier method. A log-rank test with linear trend for factor levels was performed to test for statistically significant differences between the survival curves. A p<0.05 was regarded statistically significant.

Results

Metabolic marker expression in NSCLC

GLUT1, CAIX, MCT1 and MCT4 protein expression was confined to the cell membrane. Examples of tumors after immunofluorescent staining for these markers and vasculature are shown in Figure 2. mRNA results of GLUT1, CAIX, MCT1 and MCT4 are shown in Table II. GLUT1, CAIX, MCT1 and MCT4 protein expression correlated significantly with qPCR mRNA data in all NSCLC patients (r (s)=0.44, 0.40, 0.62 and 0.36 respectively; p≤0.001).

Table I. Patient and clinicopathological characteristics of NSCLCs with available [18]FDG-PET

Characteristics	Overall (n (%))	
Age (years)		
Median (range)	66	(46-82)
Sex		
Male	67	(60)
Female	44	(40)
Histology		
Large cell carcinoma	3	(3)
Adenocarcinoma	57	(51)
Squamous cell carcinoma	46	(41)
Other	5	(5)
Tumor size (mm)		
Median (range)	30	(5-122)
Differentiation $		
Well	9	(8)
Moderate	47	(44)
Poor	52	(48)
pT		
T1	38	(34)
T2	54	(49)
T3	12	(11)
T4	7	(6)
pN #		
N0	68	(63)
N1	28	(26)
N2	12	(11)
pTNM 7th edition		
Stage I	59	(53)
Stage II	31	(28)
Stage IIIA	19	(17)
Stage IIIB	1	(1)
Stage IV	1	(1)
Surgical margins #		
R0	98	(91)
R1	9	(8)
R2	1	(1)
Type of resection		
(Bi)lobectomy	91	(82)
Pneumectomy	16	(14)
Wedge resection	4	(4)
Adjuvant treatment *		
Radiotherapy	10	(9)
Chemotherapy	16	(15)
No	84	(76)

Abbreviations: [18]FDG-PET = 18-fluoro-2-deoxyglucose positron emission tomography

$ Differentiation grade is unknown in three patients.

\#   In three cases, pN-status and surgical resection margins are unkown, because an incomplete anatomical resection was performed based on comorbidity (n=2) or because of stage IV peroperatively (n=1).

*   One case is missing.

Tumor microenvironment and glucose metabolism of adeno- versus squamous cell carcinomas

Despite the fact that adeno- and squamous cell carcinomas are categorized within the same disease entity of NSCLCs, we found remarkable differences between these histological types. Protein and mRNA expression of GLUT1, CAIX and MCT1 were significantly higher insquamous cell carcinomas relative to adenocarcinomas (Figure 3A-C and Table II). CAIX protein expression was present in 83% of the squamous cell carcinomas, whereas only in 47% of the adenocarcinomas (p<0.001). MCT1 protein expression was detectable in 42% of squamous cell carcinomas compared to only 7% of adenocarcinomas (p<0.001). MCT4 expression did not differ between adeno- and squamous cell NSCLC (Figure 3D).

Other prominent differences were a significantly higher vascular density in adenocarcinomas (p<0.001) (Figure 3E), and a trend towards larger tumor diameter (p=0.087) and higher SUVmax (p=0.10) in squamous cell carcinomas. When integrating SUVmax with metabolic tumor volume, thereby calculating TLGmax, a significant higher value was found for squamous cell carcinomas (p=0.003) (Figure 3F-H).

In summary, squamous cell carcinomas tend to be larger, have a significantly lower vascular density and a higher expression of hypoxia and glycolysis related markers on both mRNA and protein level, compared to adenocarcinomas. Furthermore, squamous cell carcinomas are better visualized by [18]FDG-PET.

Disease-free survival in adeno- versus squamous cell carcinomas according to metabolic markers and [18]FDG-PET

In our cohort of NSCLC patients, DFS was longer for patients with squamous cell carcinomas relative to adenocarcinomas based on the potential of adenocarcinomas to metastasize (HR=0.37 (95% CI 0.16-0.86), p=0.022) (Figure 4A). Of the adenocarcinomas, 6% developed a local relapse, 7% a regional relapse, and 36% distant metastases during follow-up, whereas 6% of the squamous cell carcinomas encountered a local relapse, 6% a regional relapse, and only 17% developed distant metastases.

DFS analyses of mRNA and PET data were performed for adeno- and squamous cell carcinomas separately. For these analyses, the study population was dichotomized into low and high based on median mRNA and PET values of the adeno- and squamous cell carcinomas separately. Due to the small number of events (n=7 for the PET group and n=4 for the mRNA group) and consequently low statistical power, no further subgroup analysis was performed within the squamous cell carcinomas subgroup.

For high GLUT1 mRNA (Figure 4B) and high SUVmax we observed a trend towards a worse DFS in adenocarcinomas (p=0.051 and p=0.056 respectively). High TLGmax identified patients with a significant worse DFS in this histology (cut-off value set at median (18.3); HR 3.03, 95% CI 1.21-7.60, p=0.018) (Figure 4C). Despite the fact that squamous cell carcinomas have a high [18]FDG-uptake and high GLUT1 mRNA expression, in general regarded as a poor prognostic factor, this histology had a better DFS than the adenocarcinomas. Furthermore, a subset of adenocarcinomas with high TLGmax or high GLUT1 mRNA expression (comparable

Figure 2. Immunofluorescent images of squamous cell NSCLCs showing GLUT1 (A), CAIX (B), MCT1 (C) and MCT4 (D) protein expression.
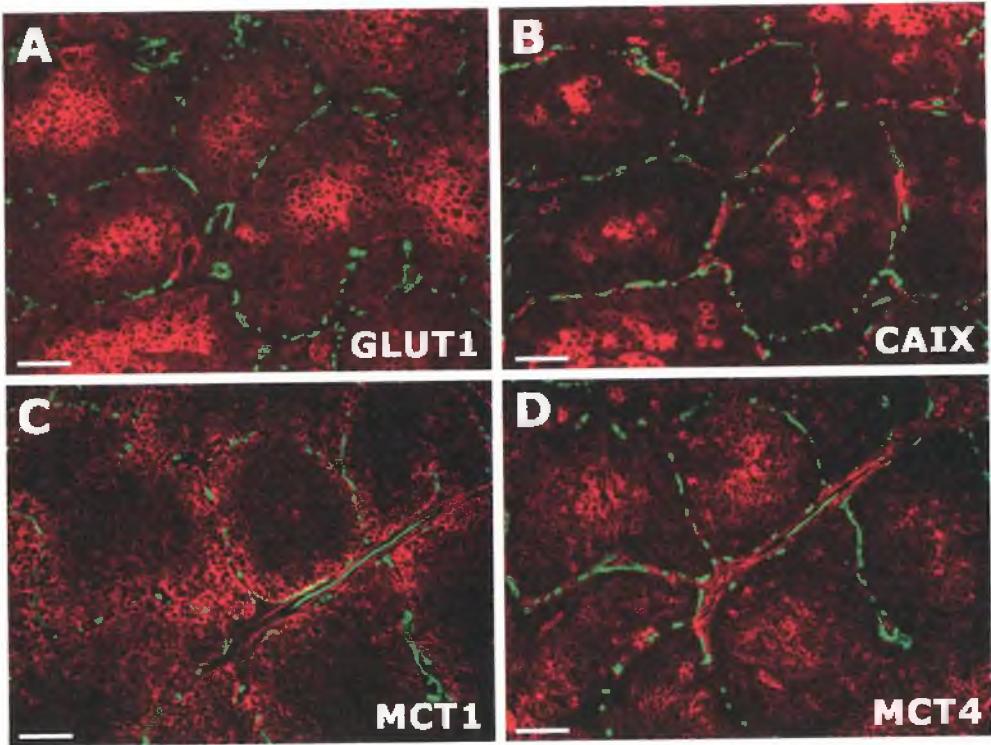
GLUT1, CAIX and MCT4 expression show a diffusion-limited pattern, whereas MCT1 is upregulated at the proximity of vessels.
Red, GLUT1, MCT4, CAIX or MCT1; *green,* vessels; magnification 100x; scale bars represent 100 μm.

Table II. Expression of GLUT1, MCT4, CAIX and MCT1 mRNA within all NSCLC and histological subgroups

	GLUT1 HPRT	CAIX HPRT	MCT1 HPRT *	MCT4 HPRT
All NSCLC (n=86)	2.59 (0.0-99.73)	0.03 (0.00-1.59)	0.15 (0.00-2.27)	0.09 (0.01-1.67)
AC (n=43)	1.89 (0.0-99.73)	0.03 (0.00-1.34)	0.07 (0.01-1.20)	0.12 (0.01-0.84)
SCC (n=34)	3.50 (0.13-49.52)	0.06 (0.00-1.59)	0.21 (0.00-2.27)	0.08 (0.01-0.71)
P-value AC vs SCC	0.005	0.057	<0.001	0.372

Abbreviations: GLUT1 = glucose transporter 1, CAIX = carbonic anhydrase IX, MCT1 = monocarboxylate transporter 1, MCT4 = monocarboxylate transporter 4, LCC = Large cell Carcinoma, AC = Adenocarcinoma, SCC = Squamous cell carcinoma. Values expressed as median (range). * MCT1 PCR analysis was succesfull in 85 NSCLCs and in 33 squamous cell carcinomas.

to the GLUT1 mRNA and TLGmax values in squamous cell carcinomas) had a worse DFS compared to squamous cell carcinomas (p≤0.001 and p=0.005 respectively) (Figure 4B-C). DFS of squamous cell carcinomas versus adenocarcinomas with low TLGmax or low GLUT1 mRNA did not differ (p=0.45 and p=0.73 respectively (Figure 4B-C).

Figure 3. Tumor microenvironment and tumor glucose metabolism of adeno- versus squamous cell carcinomas.
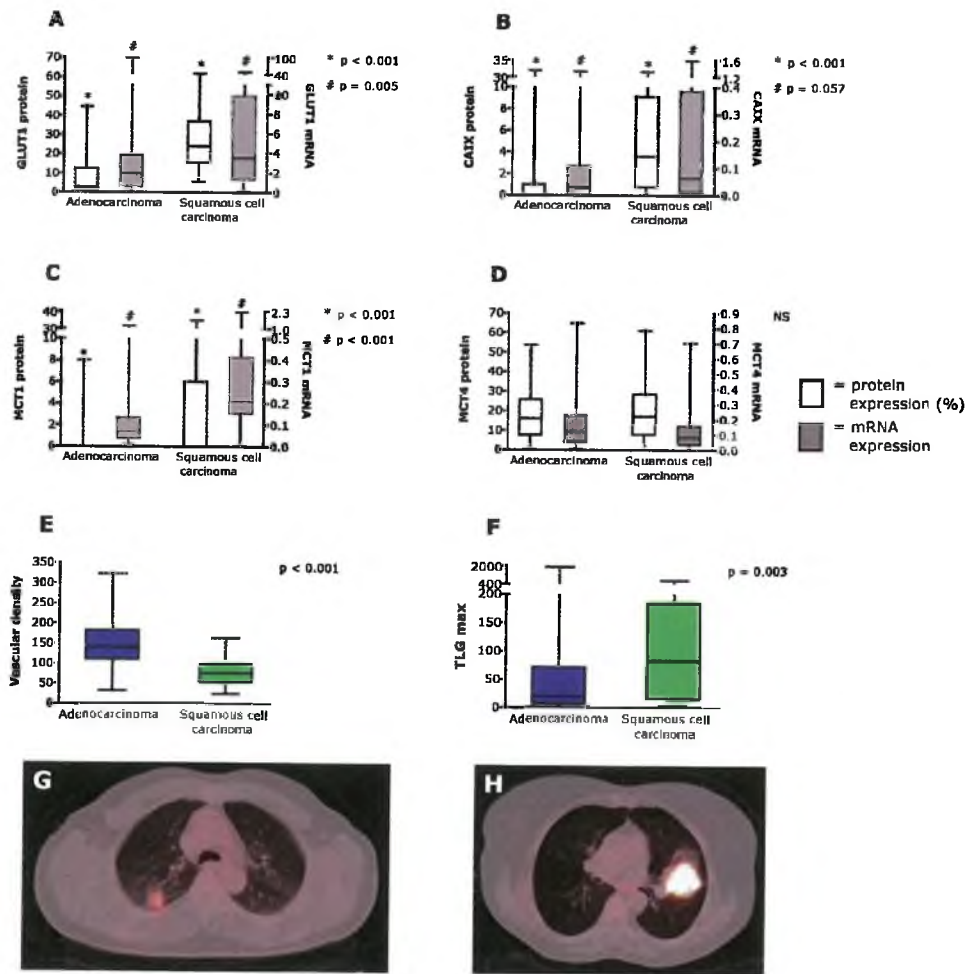
A-D: Squamous cell carcinomas demonstrate higher expression of the hypoxia- and glycolysis related markers on both protein and mRNA level, with the exception of MCT4, compared to adenocarcinomas.

Boxes represent lower quartile, median value and upper quartile, and whiskers represent minimum and maximum value.

E: Vascular density (number of vessels/mm^2) is significantly higher in adenocarcinomas.

F-H: Squamous cell carcinomas are better visualized on ^{18}FDG-PET as measured by TLGmax (SUVmax x metabolic tumor volume [cm^3]) (F). Figure G demonstrates a pT1aN0M0 adenocarcinoma with a tumor size of 2 cm. TLGmax is 14. Figure H shows a pT2aN0M0 squamous cell carcinoma. Tumor size is 4.5 cm and TLGmax is 421.

Figure 4. Disease-free survival according to histological subtype and glucose consumption in adenocarcinomas.
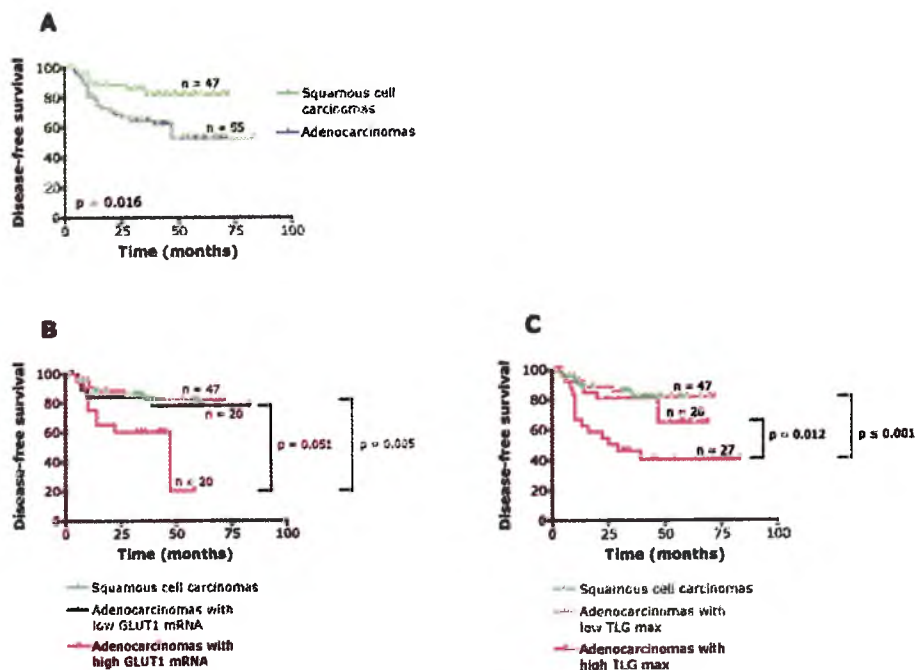
Cut-off value of GLUT1 mRNA and TLGmax is set at median (1.86 and 18.3 respectively).

Discussion

In this study, we analyzed the tumor microenvironment and tumor glucose metabolism of adeno- versus squamous cell lung carcinomas using expression of hypoxia and glycolysis-related markers, vascular density and [18]FDG-uptake in curatively resected stage I-IIIA NSCLC.

Tumor microenvironment and glucose metabolism of adeno- versus squamous cell lung carcinomas

Expression of the hypoxia- and glycolysis-related markers GLUT1, CAIX and MCT1 on both mRNA and protein level, and [18]FDG-uptake were stronger in squamous cell carcinomas compared to adenocarcinomas. Other studies also showed a higher expression of GLUT1 and CAIX protein, and higher [18]FDG-uptake in squamous cell carcinomas.[17-24] Intermediates of glycolysis can be utilized in the pentose phosphate pathway to synthetize precursors of nucleotides and amino acids, which are macromolecules required for tumor cell growth and proliferation.[25,26] Proliferation rate, as assessed by Ki67 and MCM7 expression, is higher in

NSCLCs with higher SUVmax [24,27], in CAIX-positive areas of NSCLCs [20], in less vascularized carcinomas [28] and in squamous cell lung carcinomas.[24,29]

The lower vascular density in squamous cell carcinomas suggests that tumor blood perfusion is less optimal in these tumors, which could lead to areas of diffusion-limited hypoxia and subsequent upregulation of the metabolic markers. Earlier we demonstrated the diffusion-limited pattern of GLUT1 and MCT4 protein expression in squamous cell NSCLCs.[11] Diffusion-limited hypoxia is an important cause of tumor necrosis, which is a known feature of squamous cell carcinomas.[30,31] Fan et al. also showed that the microvessel density is higher in adenocarcinomas.[32] Flow extraction product on dynamic contrast-enhanced computed tomography (DCE-CT), which represents both blood flow and vascular permeability, is also significantly higher in adenocarcinomas than in squamous cell carcinomas, which was however not confirmed by others.[23,27]

In summary, regarding the tumor microenvironment and glucose metabolism of NSCLCs, our results indicate that squamous cell carcinomas might be exposed to diffusion-limited hypoxia, resulting in an anaerobic glycolytic tumor metabolism. This metabolism may contribute to a high proliferation rate through the pentose phosphate pathway resulting in a large tumor size. In adenocarcinomas, expression of the hypoxia- and glycolysis related markers and [18]FDG-uptake was lower, accompanied with high vascular density. This suggests that adenocarcinomas produce pyruvate and lactate under normoxic conditions.[11]

Survival of adeno- versus squamous cell NSCLCs in relation to metabolic markers and [18]FDG-PET

A retrospective multivariate analysis of prognostic factors analyzed 12.428 stage I-IV NSCLC patients. In this multivariate analysis, squamous cell carcinoma histology was identified as an independent favorable prognostic factor, which is in agreement with our results.[33]

Within the adenocarcinoma subgroup of our cohort, high glucose dependency, measured by GLUT1 mRNA, was associated with a worse DFS. Several studies have also shown the prognostic potential of GLUT1 expression in adenocarcinomas.[11,34,35] Furthermore, high degree of glucose use based on [18]FDG-PET correlated with positive lymph nodes and more advanced stage at diagnosis (data not shown), and a significant worse DFS in this histology. The prognostic significance of [18]FDG-PET measurements has been shown in NSCLC patients treated with surgery, chemo- or radiotherapy.[36,37] However, despite the fact that the squamous cell carcinomas have a high [18]FDG-uptake, in general regarded as a poor prognostic factor, this histology had a significant better prognosis in our cohort than a subset of adenocarcinomas with a comparable high [18]FDG-uptake. DFS did not differ between squamous cell carcinomas and adenocarcinomas with low [18]FDG-uptake. Therefore, the meaning of [18]FDG accumulation might differ among NSCLC histologies with respect to understanding tumor glucose metabolism and prediction of prognosis.

A limitation of our study is that PET-scans were acquired on two different scanners. Although both machines were cross calibrated it might have had an influence on SUV measurements. Nowadays PET-imaging is standardized according to NEDPAS or EARL

guidelines, which were not available yet in the time period of our study. Furthermore, calculation of TLG based on a single treshold of 40% of the maximum SUV, might be inaccurate in smaller tumors due to the partial volume effect.[38,39]

The question remains why the squamous cell carcinomas with their high rate of glucose metabolism have a favorable prognosis compared to the adenocarciomas. Adenocarcinomas are known to have a high metastatic potential, whereas progressive localized disease is more often found for squamous cell histology.[30] The high rate of glucose metabolism in squamous cell carcinomas may support the high proliferation rate resulting in local growth.[10] Other (microenvironmental) factors and cellular processes than proliferation, such as epithelial-mesenchymal transition (EMT), cell motility and invasion, are required for the formation of distant metastases.[40] Adenocarcinomas may use their energy metabolism to support these latter processes instead of proliferation. For example, high MCT4 expression and resulting lactate levels at the proximity of vessels in adenocarcinomas may create a tumor microenvironment favorable for tumor cell migration.[10,11] Expression of FoxQ1, which has a key role in regulating EMT, and vimentin, a mesenchymal marker, was significantly higher in adenocarcinomas than in squamous cell carcinomas, which was however not confirmed by others.[41-43] Signalling through the MET pathway promotes EMT and the development of an invasive phenotype.[40,44] c-MET and phospho-MET proteins are higher expressed in adenocarcinomas than in squamous cell carcinomas.[44] Future studies are warranted to further explore the metastatic potential of adeno- versus squamous cell NSCLCs and its relation to tumor glucose metabolism.

Exploiting differences in biological behavior between adeno- and squamous cell NSCLCs in treatment strategies

Emerging evidence shows that histology is predictive for treatment efficacy and clinical outcome.[12] For example, a consistent link between histology and treatment outcome was established for epidermal growth factor receptor (EGFR) tyrosine kinase inhibitors (TKIs) and pemetrexed.[12,45-48] Differences in metabolism between histologies may also be exploited in treatment strategies. Apart from hypoxia,[3] high rate of glucose metabolism is also involved in resistance to radiotherapy.[10] Squamous cell histology is an adverse prognostic factor for radiotherapy efficacy, which might be explained by the high level of hypoxia and anaerobic glycolysis.[49] Therefore, hypoxia-modifying treatment or glycolysis inhibitors in combination with radiotherapy, and a radiation boost directed towards regions with high [18]FDG-uptake may be used to enhance radiotherapy efficacy especially in squamous cell carcinomas.[10,50-53]

As adenocarcinomas with a high glucose consumption have a worse survival, a subset of this histological subtype may also benefit from glycolysis targeting in combination with chemo- or radiotherapy.[11] To assess treatment-by-histology interactions large studies are needed, which may aid in maximizing survival in NSCLC patients by refinement of therapy allied to histology.[12]

Conclusion

In the present study, we analyzed differences in the tumor microenvironment and glucose metabolism of adeno- versus squamous cell NSCLCs, and the consequences of these differences for prognosis. Squamous cell carcinomas have a higher glycotic rate on both the mRNA and protein level, are better visualized on [18]FDG-PET, and have a worse vascularization compared to adenocarcinomas. This suggests that squamous cell carcinomas demonstrate glycolysis mainly under hypoxic conditions. Despite the fact that adenocarcinomas have a lower [18]FDG-uptake, generally believed to be a favorable prognostic factor, relative to squamous cell carcinomas, adenocarcinomas are better able to metastasize and have a worse DFS. These findings suggest that [18]FDG-PET should be interpreted in relation to histology in the clinic. This may improve the prognostic potential of [18]FDG-PET and may aid in exploiting [18]FDG-PET in treatment strategies allied to histology.

References

1. Moon EJ, Brizel DM, Chi JT, Dewhirst MW. The potential role of intrinsic hypoxia markers as prognostic variables in cancer. Antioxid Redox Signal. 2007;9:1237-1294.

2. Rademakers SE, Span PN, Kaanders JH, Sweep FC, van der Kogel AJ, Bussink J. Molecular aspects of tumour hypoxia. Mol Oncol. 2008;2:41-53.

3   Wilson WR, Hay MP. Targeting hypoxia in cancer therapy. Nat Rev Cancer. 2011;11:393-410.

4. Busk M, Horsman MR, Jakobsen S, Bussink J, van der KA, Overgaard J. Cellular uptake of PET tracers of glucose metabolism and hypoxia and their linkage. Eur J Nucl Med Mol Imaging. 2008;35:2294-2303.

5. Ganapathy V, Thangaraju M, Prasad PD. Nutrient transporters in cancer: relevance to Warburg hypothesis and beyond. Pharmacol Ther. 2009;121:29-40.

6. Macheda ML, Rogers S, Best JD. Molecular and cellular regulation of glucose transporter (GLUT) proteins in cancer. J Cell Physiol. 2005;202:654-662.

7. Ullah MS, Davies AJ, Halestrap AP. The plasma membrane lactate transporter MCT4, but not MCT1, is up-regulated by hypoxia through a HIF-1alpha-dependent mechanism. J Biol Chem. 2006;281:9030-9037.

8. Milosevic MF. Hypoxia, anaerobic metabolism and interstitial hypertension. In: Siemann DW, ed. Tumormicroenvironment. 1st ed. John Wiley and Sons, Ltd; 2011:183-206.

9. Semenza GL. Regulation of oxygen homeostasis by hypoxia-inducible factor 1. Physiology Bethesda. 2009;24:97-106.

10. Meijer TW, Kaanders J.H.A.M., Span PN, Bussink J. Targeting hypoxia, HIF-1 and tumor glucose metabolism to improve radiotherapy efficacy. Clin Cancer Res. 2012;In press.

11. Meijer TW, Schuurbiers OC, Kaanders JH et al. Differences in metabolism between adeno- and squamous cell non-small cell lung carcinomas: Spatial distribution and prognostic value of GLUT1 and MCT4. Lung Cancer. 2012;76:316-323.

12. Hirsch FR, Spreafico A, Novello S, Wood MD, Simms L, Papotti M. The prognostic and predictive role of histology in advanced non-small cell lung cancer: a literature review. J Thorac Oncol. 2008;3:1468-1481.

13. Rademakers SE, Lok J, van der Kogel AJ, Bussink J, Kaanders JH. Metabolic markers in relation to hypoxia; staining patterns and colocalization of pimonidazole, HIF-1alpha, CAIX, LDH-5, GLUT-1, MCT1 and MCT4. BMC Cancer. 2011;11:167.

14. de Kok JB, Roelofs RW, Giesendorf BA et al. Normalization of gene expression measurements in tumor tissues: comparison of 13 endogenous control genes. Lab Invest. 2005;85:154-159.

15. Hoekstra CJ, Paglianiti I, Hoekstra OS et al. Monitoring response to therapy in cancer using [18F]-2-fluoro-2-deoxy-D-glucose and positron emission tomography: an overview of different analytical methods. Eur J Nucl Med. 2000;27:731-743.

16.   Usmanij EA, de Geus-Oei LF, Troost EG et al. 18F-FDG PET early response evaluation of locally advanced non-small cell lung cancer treated with concomitant chemoradiotherapy. J Nucl Med. 2013;54:1528-1534.

17.   Brown RS, Leung JY, Kison PV, Zasadny KR, Flint A, Wahl RL. Glucose transporters and FDG uptake in untreated primary human non-small cell lung cancer. J Nucl Med. 1999;40:556-565.

18.   de Geus-Oei LF, van Krieken JH, Aliredjo RP et al. Biological correlates of FDG uptake in non-small cell lung cancer. Lung Cancer. 2007;55:79-87.

19.   Ilie M, Mazure NM, Hofman V et al. High levels of carbonic anhydrase IX in tumour tissue and plasma are biomarkers of poor prognostic in patients with non-small cell lung cancer. Br J Cancer. 2010;102:1627-1635.

20.   Kim SJ, Rabbani ZN, Vollmer RT et al. Carbonic anhydrase IX in early-stage non-small cell lung cancer. Clin Cancer Res. 2004;10:7925-7933.

21.   Kim SJ, Rabbani ZN, Dewhirst MW et al. Expression of HIF-1alpha, CA IX, VEGF, and MMP-9 in surgically resected non-small cell lung cancer. Lung Cancer. 2005;49:325-335.

22.   Mamede M, Higashi T, Kitaichi M et al. [18F]FDG uptake and PCNA, Glut-1, and Hexokinase-II expressions in cancers and inflammatory lesions of the lung. Neoplasia. 2005;7:369-379.

23.   Mandeville HC, Ng QS, Daley FM et al. Operable Non-Small Cell Lung Cancer: Correlation of Volumetric Helical Dynamic Contrast-enhanced CT Parameters with Immunohistochemical Markers of Tumor Hypoxia. Radiology. 2012;264:581-589.

24.   Vesselle H, Salskov A, Turcotte E et al. Relationship between non-small cell lung cancer FDG uptake at PET, tumor histology, and Ki-67 proliferation index. J Thorac Oncol. 2008;3:971-978.

25.   Hanahan D, Weinberg RA. Hallmarks of cancer: the next generation. Cell. 2011;144:646-674.

26.   Vander Heiden MG, Cantley LC, Thompson CB. Understanding the Warburg effect: the metabolic requirements of cell proliferation. Science. 2009;324:1029-1033.

27.   Sauter AW, Winterstein S, Spira D et al. Multifunctional profiling of non-small cell lung cancer using 18F-FDG PET/CT and volume perfusion CT. J Nucl Med. 2012;53:521-529.

28.   Cherk MH, Foo SS, Poon AM et al. Lack of correlation of hypoxic cell fraction and angiogenesis with glucose metabolic rate in non-small cell lung cancer assessed by 18F-Fluoromisonidazole and 18F-FDG PET. J Nucl Med. 2006;47:1921-1926.

29.   Liu YZ, Jiang YY, Hao JJ et al. Prognostic significance of MCM7 expression in the bronchial brushings of patients with non-small cell lung cancer (NSCLC). Lung Cancer. 2012;77:176-182.

30.   Cagle PT. Carcinoma of the lung. In: Churg A.M., Meyers L.L., Tazelaar HD, Whright JL, eds. Thurlbeck's Pathology of the Lung. New York: Thieme Medical Publishers, Inc; 2005:413-79.

31.   Swinson DE, Jones JL, Cox G, Richardson D, Harris AL, O'Byrne KJ. Hypoxia-inducible factor-1 alpha in non small cell lung cancer: relation to growth factor, protease and apoptosis pathways. Int J Cancer. 2004;111:43-50.

32. Fan C, Yu J, Liu Y, Xu H, Wang E. Increased NDRG1 expression is associated with advanced T s tages and poor vascularization in non-small cell lung cancer. Pathol Oncol Res. 2012;18:549-556.

33. Sculier JP, Chansky K, Crowley JJ, Van MJ, Goldstraw P. The impact of additional prognostic f actors on survival and their relationship with the anatomical extent of disease expressed by the 6th Edition of the TNM Classification of Malignant Tumors and the proposals for the 7th Edition. J Thorac Oncol. 2008;3:457-466.

34. Andersen S, Eilertsen M, Donnem T et al. Diverging prognostic impacts of hypoxic markers according to NSCLC histology. Lung Cancer. 2011;72:294-302.

35. Minami K, Saito Y, Imamura H, Okamura A. Prognostic significance of p53, Ki-67, VEGF and Glut-1 in resected stage I adenocarcinoma of the lung. Lung Cancer. 2002;38:51-57.

36. de Geus-Oei LF, van der Heijden HF, Corstens FH, Oyen WJ. Predictive and prognostic value of FDG-PET in nonsmall-cell lung cancer: a systematic review. Cancer. 2007;110:1654-1664.

37. Liao S, Penney BC, Wroblewski K et al. Prognostic value of metabolic tumor burden on 18F-FDG PET in nonsurgical patients with non-small cell lung cancer. Eur J Nucl Med Mol Imaging. 2012;39:27-38.

38. Boellaard R, Oyen WJ, Hoekstra CJ et al. The Netherlands protocol for standardisation and quantification of FDG whole body PET studies in multi-centre trials. Eur J Nucl Med Mol Imaging. 2008;35:2320-2333.

39. Boellaard R, O'Doherty MJ, Weber WA et al. FDG PET and PET/CT: EANM procedure guidelines for tumour PET imaging: version 1.0. Eur J Nucl Med Mol Imaging. 2010;37:181-200.

40. Lu X, Kang Y. Hypoxia and hypoxia-inducible factors: master regulators of metastasis. Clin Cancer Res. 2010;16:5928-5935.

41. Feng J, Zhang X, Zhu H, Wang X, Ni S, Huang J. FoxQ1 overexpression influences poor prognosis in non-small cell lung cancer, associates with the phenomenon of EMT. PLoS One. 2012;7:e39937.

42. Kim SH, Kim JM, Shin MH et al. Correlation of epithelial-mesenchymal transition markers with clinicopathologic parameters in adenocarcinomas and squamous cell carcinoma of the lung. Histol Histopathol. 2012;27:581-591.

43. Prudkin L, Liu DD, Ozburn NC et al. Epithelial-to-mesenchymal transition in the development and progression of adenocarcinoma and squamous cell carcinoma of the lung. Mod Pathol. 2009;22:668-678.

44. Tsuta K, Kozu Y, Mimae T et al. c-MET/phospho-MET protein expression and MET gene copy number in non-small cell lung carcinomas. J Thorac Oncol. 2012;7:331-339.

45. Rollins KD, Lindley C. Pemetrexed: a multitargeted antifolate. Clin Ther. 2005;27:1343-1382.

46. Hanna N, Shepherd FA, Fossella FV et al. Randomized phase III trial of pemetrexed versus docetaxel in patients with non-small-cell lung cancer previously treated with chemotherapy. J Clin Oncol. 2004;22:1589-1597.

47. Scagliotti GV, Parikh P, von PJ et al. Phase III study comparing cisplatin plus gemcitabine with cisplatin plus pemetrexed in chemotherapy-naive patients with advanced-stage non-small-cell lung cancer. J Clin Oncol. 2008;26:3543-3551.

48. Al-Saleh K, Quinton C, Ellis PM. Role of pemetrexed in advanced non-small-cell lung cancer: meta-analysis of randomized controlled trials, with histology subgroup analysis. Curr Oncol. 2012;19:e9-e15.

49. Milano MT, Zhang H, Usuki KY, Singh DP, Chen Y. Definitive radiotherapy for stage I nonsmall cell lung cancer: A population-based study of survival. Cancer. 2012;118;5572-5579.

50. Bussink J, Kaanders JH, van der Graaf WT, Oyen WJ. PET-CT for radiotherapy treatment planning and response monitoring in solid tumors. Nat Rev Clin Oncol. 2011;8:233-242.

51. Janssens GO, Rademakers SE, Terhaard CH et al. Accelerated radiotherapy with carbogen and nicotinamide for laryngeal cancer: results of a phase III randomized trial. J Clin Oncol. 2012;30:1777-1783.

52. Meijer G, Steenhuijsen J, Bal M, De JK, Schuring D, Theuws J. Dose painting by contours versus dose painting by numbers for stage II/III lung cancer: practical implications of using a broad or sharp brush. Radiother Oncol. 2011;100:396-401.

53. Elmpt van W, De Ruysscher D, Salm van der A et al. The PET-boost randomised phase II dose-escalation trial in non-small cell lung cancer. Radiother Oncol. 2012;104:67-71.

Chapter 5

The role of F-18-FDG-PET in the differentiation between lung metastases and synchronous second primary lung tumors

Bernadette G. Dijkman

Olga C.J. Schuurbiers

Dennis Vriens

Monika Looijen-Salamon

Johan Bussink, MD

Johanna N.H. Timmer-Bonte

Miranda M. Snoeren

Wim J.G. Oyen

Henricus F.M. van der Heijden

Lioe-Fee de Geus-Oei

Abstract

Introduction

In lung cancer patients with multiple lesions, the differentiation between metastases and second primary tumors has significant therapeutic and prognostic implications. The aim of this retrospective study was to investigate the potential of ^{18}F-FDG-PET to discriminate metastatic disease from second primary lung tumors.

Methods

Out of 1396 patients evaluated by the thoracic oncology group between January 2004 and April 2009 at the Radboud University Nijmegen Medical Centre, patients with a synchronous second primary lung cancer were selected. Patients with metastatic disease involving the lungs served as the control group. Maximum standardized uptake values (SUVs) measured with ^{18}F-FDG-PET were determined for two tumors in each patient. The relative difference between the SUVs of these tumors (ΔSUV) was determined and compared between the second primary group and metastatic disease group. Receiver-operating characteristic (ROC) curve analysis was performed to determine the sensitivity and specificity of the ΔSUV for an optimal cut-off value.

Results

A total of 37 patients (21 metastatic disease, 16 second primary cancer) were included for analysis. The ΔSUV was significantly higher in patients with second primary cancer than in those with metastatic disease (58% vs. 28%, respectively, $P<0.001$). The area under the ROC curve was 0.81 and the odds ratio for the optimal cut-off was 18.4.

Conclusions

SUVs from ^{18}F-FDG-PET images can be helpful in differentiating metastatic disease from second primary tumors in patients with synchronous pulmonary lesions. Further studies are warranted to confirm the consistency of these results.

Introduction

Lung cancer is the leading cause of cancer-related mortality.[1] Although the incidence of lung cancer is decreasing,[1] the number of patients presenting with a second primary cancer has dramatically increased in the last decades.[2, 3] A simultaneous second primary lung carcinoma occurs in 1-8% of lung cancer patients.[4, 5] The occurrence of multiple primary cancers may be attributed to shared etiologic factors.[3, 6] Specifically, seventy percent of second primary cancers presenting in lung cancer patients are tobacco-related, the most common locations including the upper aerodigestive tract, the uroepithelium and the colorectum.[7]

Second primary cancers can be divided into synchronous cancers, occurring simultaneously with the index tumor, and metachronous cancers, presenting more than six months after the index tumor.[8]

For lung cancer patients ^{18}F-fluorodeoxyglucose positron emission tomography (FDG-PET) is recommended according to the American College of Chest Physicians (ACCP) guidelines as standard work-up in potentially curable lung cancer based on conventional imaging. The rate of detection of unanticipated metastasis by FDG-PET has been reported as 1 to 18% in patients with clinical stage I or II disease.[9] When an FDG-PET-scan is made for lung cancer staging, both metastases as well as synchronous primary tumors can be visualized. While multiple lung nodules of varying sizes are usually classified as metastases, it is a much greater challenge to distinguish a lung metastasis from a second primary lung carcinoma when only one additional pulmonary lesion is detected.[10]

Discriminating metastatic disease from second primary lung cancer is of great clinical interest because it has large therapeutic and prognostic implications. Metastatic lung cancer is considered incurable and is treated with palliative intent.[1] The survival of lung cancer patients presenting with multiple primary cancers has found to be similar compared to patients with solitary primary lung cancer,[7, 11] and an aggressive surgical approach has proven to be safe and justified in patients with synchronous multiple primary lung cancers and node-negative disease.[12] Therefore, multiple primary cancers should be staged separately and - in case of early stage - treated with curative intent, including surgery when the tumors are resectable.

Obviously, when two tumors are histologically different they are easily recognized as separate primary tumors. However, when tumors share common histological features, it remains uncertain whether they should be classified as metastases or separate primary tumors. Immunohistochemistry and TP53 gene mutation analyses may be used to ascertain the clonality of synchronous tumors. The latter has been promoted as a gold standard for differentiation of second primary tumors from metastatic disease.[13-15]

FDG uptake reflects metabolic activity of tumor lesions, which depends on a variety of tumor characteristics, such as degree of proliferation, hypoxia, and tumor aggressiveness. FDG uptake can be quantified by calculating standardized uptake values (SUVs) on PET images. SUVs have been reported to correlate with histological subtypes and tumor stage,[16-

[18] and have been shown to increase with poorer tumor differentiation,[16, 19] a higher proportion of actively proliferating cells,[19] and increased aggressiveness of the tumor.[20]

Since tumors with a shared clonal origin often behave similarly and have common histological features, we hypothesized that the SUVs of clonally related tumors (i.e. metastases) would be more similar than those of tumors with a different clonal origin. Consequently, we hypothesized that the SUVs of metastases approach the SUV of the primary tumor they originate from, and that the SUVs of two primary tumors differ to a greater extent.

This retrospective study evaluated the potential of SUVs measured with FDG-PET for the characterization of synchronous pulmonary lesions.

Materials and methods

Patients

A total of 1396 patients (536 female, 860 male) who had been evaluated by the multidisciplinary thoracic oncology group between January 2004 and April 2009 at the Radboud University Nijmegen Medical Centre were retrospectively screened. First, patients were included to the 'second primary group' when they presented with two primary tumors, including any index tumor and a synchronous pulmonary tumor, defined as a tumor diagnosed within six months of diagnosis of the index tumor.[8] Second, patients with lung cancer metastasized to the same lobe (stage IIIB) or to different lobes or other organs (stage IV), and patients with a primary cancer elsewhere in the body metastasized to the lungs (stage IV) were consecutively searched for and included to form the control group (or 'metastatic disease group'), until a similar sample size as of the second primary group was reached. Patients with any cancer-related treatment prior to FDG-PET were excluded from the study. In all patients, a diagnostic contrast-enhanced chest computed tomography (CT) scan was performed including CT-scan of liver and adrenal glands prior to or directly following the FDG-PET. An overview of the inclusion and exclusion criteria is presented in the flowchart of Fig. 1.

A tumor was considered a second primary tumor when histopathological or immunohistochemical features differed from those of the index tumor. In cases of tumors with identical histological and immunohistochemical features, TP53 mutation analysis had to be performed demonstrating different clonal origins of the tumors. Patients without conclusive diagnosis of second primary cancer due to impossibility of gaining adequate tissue samples were excluded. Metastatic disease was concluded based on identical histopathological findings of multiple lesions. Additionally, tumors were considered metastases when multiple (more than two) tumors in a pattern typical for metastatic spread of the identified primary tumor had been localized on imaging modalities.

When FDG uptake is measured in small tumors, bias can be introduced by the partial volume effect resulting in underestimation of the tumor SUV.[21] To prevent bias by partial volume effects, patients with a tumor smaller than 15 mm were excluded from analysis.

Data on patient and tumor characteristics were extracted from patient charts and histopathology reports.

^{18}F-FDG PET Data Acquisition and Reconstruction

All patients underwent whole body FDG-PET as part of their routine preoperative staging procedure. Prior to FDG-injection, patients fasted for at least six hours. Intake of sugar-free liquids was permitted. Immediately prior to the procedure, patients were hydrated with 500 ml of water and 60 minutes after intravenous injection of approximately 250 MBq FDG (Covidien, Petten, The Netherlands) and 10 mg furosemide, images of the area between the proximal femora and the base of the skull were acquired.

Scans were acquired with a hybrid PET/CT scanner (Biograph Duo, Siemens Medical Solutions USA, Inc.) containing a 2-slice CT scanner. A low-dose CT scan for localization and attenuation-correction purposes was acquired in the caudocranial direction. Scanning parameters included 40 mA·s (50 mA·s for patient weight >100 kg and 60 mA·s for >120 kg), 130 kV, 5-mm slice collimation, 0.8-s rotation time, and pitch of 1.5, reconstructed to 3-mm slices for smooth coronal representation. CT scans were acquired during timed unforced expiration breath-hold. No intravenous contrast was applied. For PET, a 3-dimensional whole body emission scan was acquired during free breathing, the acquisition time per bed position was 4 minutes for emission only. All images were iteratively reconstructed using 2 iterations and 8 subsets and a 5-mm 3D Gaussian filter, resulting in an effective spatial resolution of 5 mm FWHM.

Standardized Uptake Values (SUVs)

The maximum standardized uptake value (SUV_{max}, the activity from the maximum-valued pixel within the tumor volume of interest (VOI); hereafter referred to as SUV) normalized to injected activity and patient body weight was calculated at approximately 60 minutes after tracer injection for each primary lesion and the chosen metastatic lesion with use of the following equation: SUV = maximum activity concentration in the VOI [kBq/ml] / (injected dose [MBq/ml] / patient body weight [kg]). In patients with multiple metastatic lesions, the lesion with the largest diameter was chosen to prevent partial volume effects. Subsequently, the relative difference between the SUV of the index tumor and the SUV of the synchronous tumor (the second primary tumor or metastatic lesion) was assessed (ΔSUV) and expressed in percentages of the highest SUV. Examples of deduction of the ΔSUV from the SUVs of two tumors are given in Figure 2 and 3. Image-analyses were performed on the Inveon Research Workplace version 2.2 (IRW, Siemens/CT, Knoxville, Tennessee, USA).

Area Under the Receiver Operating Characteristics (ROC) curve and Cut-Off Value

After constructing a Receiver Operating Characteristics (ROC) curve of the ΔSUV, the area under the curve (AUC) was assessed, and the sensitivity, specificity, positive predictive value (PPV), negative predictive value (NPV), and odds ratio (OR) were determined for an optimal cut-off of the ΔSUV.

Chest CT

In all patients, a diagnostic contrast-enhanced chest CT scan was performed. For each patient, CT tumor characteristics were assessed by two radiologists. Morphologic features of pulmonary nodules suspect for a primary cancer were speculation, cavitation, irregular margins, pleural or bronchial traction. Tumors were considered metastases if the following features were present: round lesions, sharp borders, homogenous. In case of more than two pulmonary nodules the same nodules used for the FDG-PET evaluation were chosen.

Statistical Analyses

Since the ΔSUV was not normally distributed in both groups (Shapiro-Wilk test, P<0.05), an independent-samples one-tailed Mann-Whitney U-test was used to compare the mean ΔSUV between the second primary tumor and metastatic disease group. Mean age and number of pack years were compared using a two-sided t-test. A chi-square test was used to compare the proportions of smokers between the groups. The level of significance was set at 0.05 for all analyses.

Results

Patient Characteristics

A total of 54 eligible patients with synchronous malignancies (32 metastatic disease and 22 second primary cancer, respectively) were included. After exclusion of patients of whom the digital PET data were unavailable (n=3), and after exclusion of patients with lesions < 15 mm (n=14), 37 patients remained for analysis. Of those patients, 21 were diagnosed with metastatic disease and 16 with two primary tumors (Figure 1).

Mean age of the patients (23 male, 14 female) was 68 years (range 47-85 years). Other patient characteristics, including smoking status, are presented in Table 1. Patient age, sex, and smoking status were not significantly different between patients with metastatic disease and a second primary tumor (p>0.05).

Sites of the index tumor in patients with second primary lung cancer were the lung (n = 7), the colorectum (n = 5), and the head and neck (n = 4). Out of 16 second primary cancer patients, 12 (75%) had two tumors of early stage (stage I-IIIA) and were considered potentially curable.

In the majority of cases (76%), metastatic disease was diagnosed based on the clinical pattern (multiple lesions spread in a manner consistent of metastatic pulmonary cancer). The diagnosis of second primary cancer was primarily (81%) - as can be expected - based on histopathological differences. Only in three cases further immunohistochemistry (two patients) or TP53 mutation (one patient) analysis was required for a definite conclusion.

Figure 1. Flowchart of the included and excluded patients
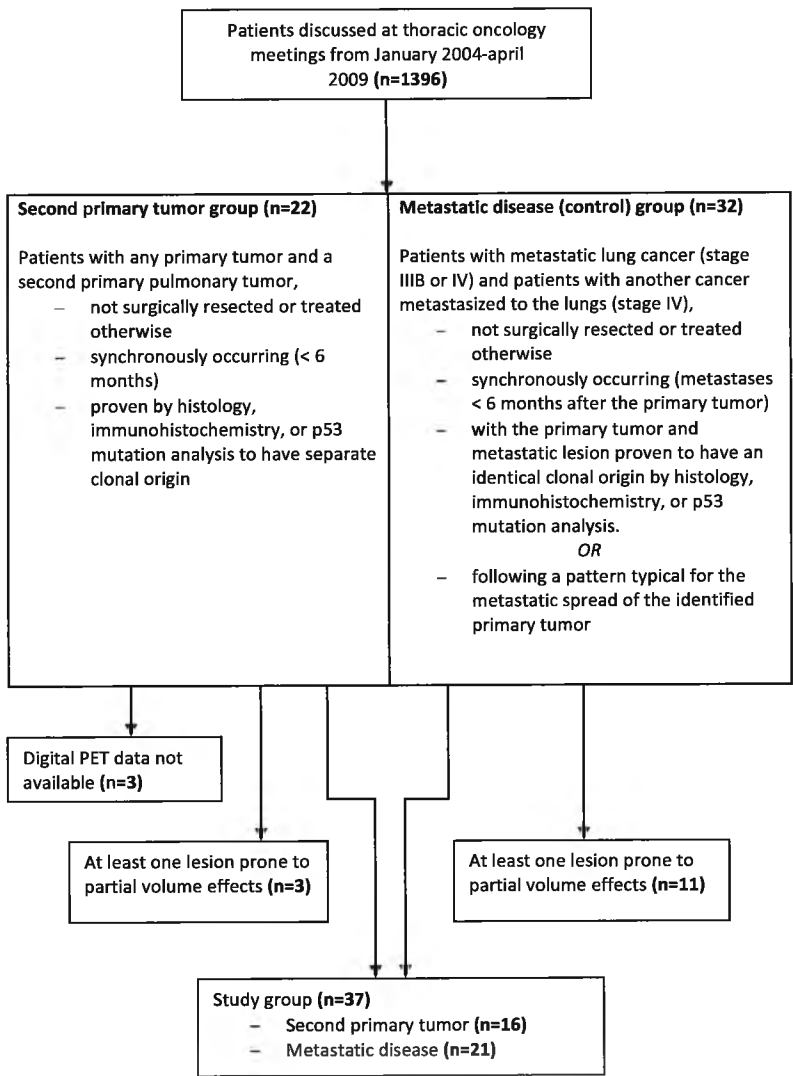
Figure 2. FDG-PET of a patient with two primary lung tumors

FDG-PET demonstrating a moderately differentiated adenocarcinoma (**A**) in the left upper lobe with a SUV of 12.1 and a synchronous second primary with similar histology but a different clonal origin demonstrated by TP53 mutation analysis (**B**) in the right lower lobe with a SUV of 3.5. The relative difference (ΔSUV) between the SUVs of the two primary tumors was $(12.1 - 3.5) / 12.1 * 100\% = 71\%$

Figure 3. FDG-PET of a patient with metastasized lung cancer (stage IV)
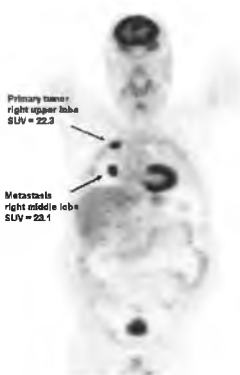
FDG-PET demonstrating a primary well differentiated adenocarcinoma located in the right upper lobe of the lung with a SUV of 22.3 and a metastatic lesion in the right middle lobe of the lung with a SUV of 23.1. The ΔSUV in this patient was $(23.1 - 22.3) / 23.1 * 100\% = 3\%$.

Tumor Characteristics

Tumor characteristics are presented in Table 1. All tumors were carcinomas, except for one tumor in the second primary group which was classified as a mesothelioma. Adenocarcinomas were the most commonly diagnosed tumors in both groups. Differentiation of the tumors was better in the second primary group than in the metastatic disease group, although in both groups tumors were most frequently poorly differentiated.

87

Table 1. Patient and Primary Tumor Characteristics

Patient characteristics		Second primary group (n=16)	Metastatic disease group (n=21)	P-value
Mean age (range)		68 y (49-85 y)	67 y (47-84 y)	0.715
Sex (m:v)		11:5	12:9	0.471
Smoking status	Smoker	7	10	0.713
	Ex-smoker	7	9	
	Non-smoker	2	1	
	Missing	0	1	
Mean no. of pack years		33.6 ± 15.9	35.0 ± 21.2	0.842
Conclusion* based on	Histopathology	13	5	
	P53 mutation analysis	1	0	
	Immunohistochemistry	2	0	
	Clinical features	0	16	
Curability[†]	Potentially curable	12	0	
	Incurable	4	21	

Characteristics of Primary Tumors		Second primary group (n=16)		Metastatic disease group (n=21)
		Index tumor	Synchronous pulmonary tumor	
Site	Lung	7	16	21
	Colorectum	5	0	0
	Head and neck	4	0	0
Histopathology	SCLC	0	0	3
	NSCLC AC	9	9	13
	BAC	0	1	0
	SCC	7	2	1
	LCC	0	2	2
	Undifferentiated	0	0	2
	Other	0	2	0
Differentiation	Very poor	0	0	3
	Poor	6	8	7
	Intermediate	8	2	1
	Well	0	2	1
	Unspecified	2	4	9
Stage[‡]	IA	4	5	0
	IB	2	1	0
	IIA	2	2	0
	IIB	2	3	0
	IIIA	4	2	0
	IIIB	0	1	2
	IV	2	1	19
	Missing	0	1	0

* The conclusion second primary tumor or metastatic disease was based on histopathological or immunohistochemical features, TP53 mutation analysis results, or clinical features. The latter included localization of multiple (more than two) malignancies in a pattern typical for metastatic spread of the identified primary tumor

[†]Patients with two tumors of stage I-IIIA were considered potentially curable, whereas patients with at least one tumor staged IIIB/IV were considered incurable (TNM staging system version 6)

[‡]According to the sixth edition of the TNM classification for lung cancer developed by the International Association for the Study of Lung Cancer (IASLC)[42] Abbreviations: SCLC, small cell lung carcinoma; NSCLC, non-small cell lung carcinoma; AC, adenocarcinoma; BAC, bronchioloalveolar carcinoma; SCC, squamous cell carcinoma; LCC, large cell carcinoma.

Relative Differences Between Standardized Uptake Values (ΔSUVs)

The mean intra-individual ΔSUV between lesions was significantly higher in patients with a second primary tumor (58%, 95% CI 46-70%) as compared to those with metastatic disease (28%, 95% CI 19-37%) (P<0.001). Figure 4 shows boxplots of the ΔSUV for both groups. Although the ranges of the groups show overlap, the majority (75%) of patients with metastatic disease has a ΔSUV below 39%, whereas the ΔSUV exceeds 46% for the majority of the second primary group (Figure 4). The individual patient data on SUV$_{max}$ and ΔSUV for the metastasis and second primary group are outlined in tables 2 and 3.

Area Under the ROC (AUC) and Cut-Off Value

The AUC for ΔSUV was 0.81 (95% CI 0.67-0.96, P=0.001) to predict a second primary tumor (Figure 5), which represents moderately high discriminative ability of the ΔSUV.[22] The left upper corner of the ROC curve was chosen as the optimal cut-off, which corresponds with a ΔSUV of 41%. This cut-off was associated with a sensitivity, specificity, PPV, NPV, and OR of 81%, 81%, 76%, 85% and 18.4, respectively.

Figure 4: Box and whisker plots of the ΔSUV for both groups
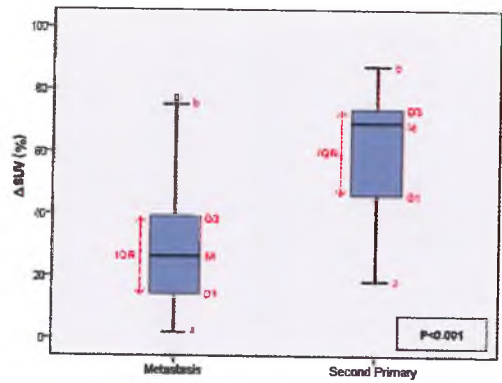
Values	Metastatic disease group (n=21)	Second primary group (n=16)
Lowest value within Q1 - 1.5·IQR (a)	2	18
25% percentile (Q1)	14	46
Median (50% percentile) (M)	26	69
75% percentile (Q3)	39	73
Interquartile range (IQR)	25	27
Highest value within Q3 + 1.5·IQR (b)	76.5	87
Outlier (o)	77	

Box and whisker plots showing the distribution of the ΔSUV for both groups. Abbreviations: Q1, first quartile; M, median; Q3, third quartile; IQR, interquartile range.

Chest CT

Individual data of CT characteristics are outlined in Table 4. Of 21 patients in the metastasis group, 19 (90%) had at least one tumor containing morphological features of a metastasis. In the second primary group, a definite diagnosis based on CT morphological features could be made in only eight patients (50%). Of these, three patients had a tumor being suspicious for a metastasis, and five patients had two tumors both suspected of being a second primary tumor.

Table 2. Individual Results of Metastasis Group

Patient no.	Location tumor 1	SUV_{max} tumor 1	Location tumor 2	SUV_{max} tumor 2	ΔSUV*	ΔSUV%[†]
1	Lung, left hilum	7.90	Left 5th rib	7.30	0.60	8
2	Lung, RUL	6.30	Lung, RUL	4.30	2.00	32
3	Lung, RUL	16.2	Liver	14.3	1.90	12
4	Lung, LLL	8.00	Larynx	9.30	1.30	14
5	Lung, right hilum	18.2	Lung, left	24.6	6.40	26
6	Lung, RML	34.8	Th 12	26.6	10.2	29
7	Lung, RLL	27.6	Lung, LUL	13.4	14.2	51
8	Lung, RLL	2.50	Lung, RLL	2.20	0.30	12
9	Lung, LLL	10.5	Left iliac bone	10.7	0.20	2
10	Lung, RUL	5.90	Lung, right hilum	3.60	2.30	29
11	Lung, LUL	16.5	Right 6th rib	4.10	12.4	75
12	Lung, RUL	22.3	Lung, RML	23.1	0.80	3
13	Lung, RUL	6.20	Th 11	4.90	1.30	21
14	Lung, right	12.4	Lung, LUL	7.10	5.30	43
15	Lung, RUL	9.60	Right adrenal gland	5.70	3.90	41
16	Lung, RUL	13.2	Right iliac crest	3.00	10.2	77
17	Lung, RLL	7.20	Right 5th rib	5.30	1.90	26
18	Lung, RML	12.5	Lung, RLL	16.4	3.90	24
19	Lung, RUL	13.5	Right PSIS	11.4	2.10	16
20	Lung, RLL	5.40	L1	6.40	1.00	16
21	Lung, RML	5.90	Lung, RML	4.10	1.80	31
Mean ± SD					**4.00 ± 4.22**	**28 ± 21**

* ΔSUV: the absolute difference between the SUV_{max} of tumor 1 and SUV_{max} of tumor 2

[†] ΔSUV%: the relative difference between the SUV_{max} of tumor 1 and the SUV_{max} of tumor 2, expressed in percentages of the highest SUV_{max}

Abbreviations: SUV_{max}, maximum standardized uptake value; RUL, right upper lobe; RLL, right lower lobe; LUL, left upper lobe; LLL, left lower lobe; Th, thoracic vertebra; L, lumbar vertebra; PSIS, posterior superior iliac spine; SD, standard deviation of the mean

## Table 3. Individual Results of Second Primary Group

Patient no.	Location tumor 1	SUV$_{max}$ tumor 1	Location tumor 2	SUV$_{max}$ tumor 2	ΔSUV*	ΔSUV%[†]
1	Lung, RUL	4.50	Cecum	7.70	3.20	42
2	Lung, RLL	8.00	Lung, LLL	3.00	5.00	63
3	Lung, RML	20.7	Lung, RLL	5.00	15.7	76
4	Lung, RUL	10.3	Lung, LUL	8.40	1.90	18
5	Rectum	16.3	Lung, RUL	4.83	11.47	70
6	Colon	9.90	Lung, LLL	2.40	7.50	76
7	Lung, LUL	8.70	Lung, LLL	7.10	1.60	18
8	Soft palate	2.70	Lung, LUL	17.6	14.9	85
9	Lung, LUL	13.4	Lung, RML	6.70	6.70	50
10	Right oro/hypopharynx	18.0	Lung, LLL	5.20	12.8	71
11	Colon	19.4	Lung, LUL	5.70	13.7	71
12	Left oropharynx	23.4	Lung, RUL	7.60	15.8	68
13	Larynx	3.90	Lung, RLL	4.80	0.90	19
14	Lung, LUL	12.12	Lung, RLL	3.54	8.58	71
15	Colon	5.40	Lung, RUL	11.1	5.70	51
16	Left distal main bronchus	13.5	Lung, RUL	1.70	11.8	87
Mean ± SD					8.58 ± 5,24	58 ± 23

* ΔSUV: the absolute difference between the SUV$_{max}$ of tumor 1 and SUV$_{max}$ of tumor 2

[†] ΔSUV%: the relative difference between the SUV$_{max}$ of tumor 1 and the SUV$_{max}$ of tumor 2, expressed in percentages of the highest SUV$_{max}$

Abbreviations: SUV$_{max}$, maximum standardized uptake value; RUL, right upper lobe; RLL, right lower lobe; LUL, left upper lobe; LLL, left lower lobe; SD, standard deviation of the mean

Figure 5: Receiver Operating Characteristics curve of the ΔSUV
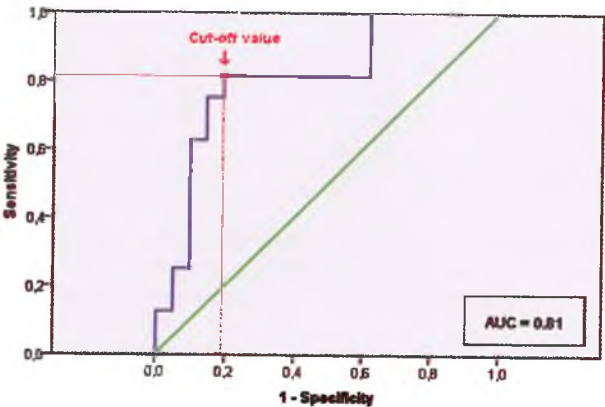
Receiver Operating Characteristics (ROC) curve and corresponding area under the curve (AUC) statistics for the ΔSUV. For the optimal cut-off of ΔSUV=41%, both the sensitivity and specificity are 81%.

91

Table 4 Individual data of CT characteristics

Metastasis group	Patient no.	Tumor 1	Tumor 2	ΔSUV%
	1	Metastasis*	Metastasis	8
	2	Metastasis	Unsure[†]	32
	3	Metastasis	Unsure	12
	4	Metastasis	Unsure	14
	5	Metastasis	Unsure	26
	6	Metastasis	Metastasis	29
	7	Metastasis	Unsure	51
	8	Primary[‡]	Unsure	12
	9	Metastasis	Unsure	2
	10	Metastasis	Metastasis	29
	11	Metastasis	Metastasis	75
	12	Unsure	Unsure	3
	13	Metastasis	Unsure	21
	14	Primary	Metastasis	43
	15	Metastasis	Unsure	41
	16	Metastasis	Unsure	77
	17	Metastasis	Unsure	26
	18	Metastasis	Unsure	24
	19	Metastasis	Unsure	16
	20	Metastasis	Unsure	16
	21	Metastasis	Metastasis	31
Second primary group	Patient no.	Tumor 1	Tumor 2	ΔSUV%
	1	Primary	Unsure	42
	2	Primary	Unsure	63
	3	Metastasis	Unsure	76
	4	Primary	Primary	18
	5	Unsure	Primary	70
	6	Unsure	Primary	76
	7	Primary	Primary	18
	8	Unsure	Primary	85
	9	Primary	Primary	50
	10	Unsure	Metastasis	71
	11	Unsure	Unsure	71
	12	Unsure	Metastasis	68
	13	Unsure	Primary	19
	14	Primary	Primary	71
	15	Unsure	Primary	51
	16	Primary	Primary	87

* Tumors were considered metastases if the following features were present: round lesions, sharp borders, homogenous.

[†] Based on CT characteristics, no definite diagnosis of a primary tumor or metastasis could be made

[‡] Tumors were considered primary tumors if the following features were present: speculation, cavitation, irregular margins, pleural or bronchial traction

Abbreviations: ΔSUV%: the relative difference between the SUV_{max} of tumor 1 and the SUV_{max} of tumor 2, expressed in percentages of the highest SUV_{max}

Discussion

To our knowledge, this is the first study investigating the role of quantitative FDG-PET in discriminating metastases from second primary tumors in cases of synchronously presenting lesions. A significantly larger relative difference in standardized uptake values (ΔSUV) between two tumors was found in patients presenting with two primary tumors as compared to patients with metastatic disease involving the lungs. The moderately high accuracy, as measured with the area under the curve, as well as the good sensitivity and specificity of the ΔSUV support the use of FDG-PET as a modality for discriminating second primary lung tumors from metastases. The odds ratio for the optimal cut-off of 41% was 18.4, indicating that the odds of a second primary tumor was 18.4 times higher in patients with a ΔSUV > 41% than in those with a ΔSUV < 41%. Most patients with second primary cancer (75%) had two early stage tumors (I-IIIA), meaning they were potentially curable.

A definite diagnosis of metastatic disease or second primary tumor based on CT-scan characteristics could be made in 90% of patients with metastases and in only 8 patients (50%) with second primary cancer. Furthermore, in only 5 of 8 patients the diagnosis was right.

Previously, multiple case reports and studies have been published presenting cases of unexpected synchronous primary lung tumors detected by FDG-PET.[23-26] On the contrary, only few reports exist in which FDG-PET contributes in determining the clonal origin of synchronous tumors.[27, 28] The current available literature further supports our hypothesis that SUVs can differentiate tumors of common origin and with common biological behavior (i.e. metastases) from those of separate clonal origin (i.e. multiple primary tumors). That is, FDG uptake has been reported to relate to several tumor characteristics, including histological subtype[16-19, 29] and tumor aggressiveness.[16, 19, 20]

FDG-PET imaging is already extensively being used in patients with lung cancer for several purposes, including the diagnosis of recurrent disease, staging, prognostic stratification, and radiotherapy planning.[30-33] Also, it has been shown an accurate modality to differentiate benign from malignant solitary pulmonary lesions.[30, 34] Furthermore, FDG-PET can be used to monitor the response of non-small cell lung cancer to chemotherapy,[35] radiotherapy, and potentially to targeting of cell signaling pathways.[36] The presented results implicate that the use of FDG-PET might be expanded to the identification of early stage second primary tumors in patients with synchronous pulmonary lesions.

Currently, elaborate and invasive diagnostic procedures are required for the diagnosis of second primary cancer. FDG-PET may be a cost-effective modality as it may identify second primary lung tumors at an early and curable stage (stage I-IIIA) in a non-invasive way. Large differences in SUVs between lung tumors in a single patient should urge physicians to consider a second primary lung cancer rather than metastatic disease, resulting in fewer patients wrongfully being withheld a curative treatment. Since our study also included patients with second primary cancer of the colorectum and head and neck, FDG-PET might

also be useful in patients with synchronous cancers of other organs in whom a diagnosis of metastasis or second primary cancer has yet to be made.

The studied population was carefully defined by stringent inclusion criteria. By including only those patients of whom sufficient data for a definite diagnose of second primary cancer were available, the validity of this study was strengthened. Additionally, conditions between the studied patient groups were equalized as much as possible by choosing one reconstruction method for all PET-images, since this is known to affect the SUV.[37]

Several limitations to this study should be noted. First, this study has a small sample size. Because of the retrospective nature of the study, TP53 mutation analysis was missing in many patients with histologically identical lesions and suspicion of a second primary tumor. After exclusion of patients with missing digital PET data and lesions prone to partial volume effects, only one patient in whom TP53 analysis was performed was left for inclusion.

Second, diagnosis was made without histological confirmation in most cases of metastatic disease. In these patients, histopathology of the metastatic lesion was lacking, because the clinical presence of multiple lesions in a pattern typical for metastatic spread was considered sufficient for diagnosis of metastatic disease. When this study would have been prospectively conducted, however, tissue for immunohistochemical and mutation analyses could have been sampled for all tumors, thereby assuring validity of diagnoses of both studied patient groups.

Full kinetic analysis of the metabolic rate of FDG has several advantages over the use of SUVs.[38] However, dynamic scans are required for kinetic analysis, which are not readily available in clinical settings.[34] Therefore, the SUV is the most commonly used measure to quantify tumor glucose metabolism on static PET images and its use is further supported by studies showing high reproducibility.[39, 40]

To secure comparability of ΔSUVs between patients, only patients with FDG-PET images reconstructed at the same resolution (two iterations and eight subsets) were included. However, reconstruction with a higher amount of iterations may be preferred to obtain sufficient convergence, which makes the SUV less dependent on surrounding activity.[37] Also, the SUV was normalized to body weight and not to the more preferable body surface area or plasma glucose values.[41] However, these limitations affect the absolute values of SUVs and do not have a large impact on intra-individual differences in SUVs (ΔSUVs), as used in this study.

Conclusions

The results of this study suggest that measurement of the SUV using FDG-PET images can be useful in differentiating metastatic disease from second primary cancer in patients presenting with synchronous pulmonary lesions. This non-invasive technique, which is standard available in pre-surgically staged lung cancer patients, may increase cost-effectiveness due to less cumbersome diagnostic procedures and more efficient

identification of potentially curable second primary cancer patients. However, larger and prospectively conducted studies are warranted to confirm the consistency of these results and to test the accuracy of the ΔSUV at the cut-off value proposed in this study.

References

1. Molina JR, Yang P, Cassivi SD et al. Non-small cell lung cancer: epidemiology, risk factors, treatment, and survivorship. Mayo Clin Proc 2008; 83(5):584-594.

2. Travis LB. The epidemiology of second primary cancers. Cancer Epidemiol Biomarkers Prev 2006; 15(11):2020-2026.

3. Soerjomataram I, Coebergh JW. Epidemiology of multiple primary cancers. Methods Mol Biol 2009; 471:85-105.

4. van Rens MT, Zanen P, Brutel de La Rivière A et al. Survival in synchronous vs. single lung cancer: upstaging better reflects prognosis. Chest 2000; 118(4):952-958.

5. Battafarano RJ, Meyers BF, Guthrie TJ et al. Surgical resection of multifocal non-small cell lung cancer is associated with prolonged survival. Ann Thorac Surg 2002; 74(4):988-993.

6. Ng AK, Travis LB. Subsequent malignant neoplasms in cancer survivors. Cancer J 2008; 14(6):429-434.

7. Aguiló R, Macià F, Porta M et al. Multiple independent primary cancers do not adversely affect survival of the lung cancer patient. Eur J Cardiothorac Surg 2008; 34(5):1075-1080.

8. Douglas WG, Rigual NR, Loree TR et al. Current concepts in the management of a second malignancy of the lung in patients with head and neck cancer. Curr Opin Otolaryngol Head Neck Surg 2003; 11(2):85-88.

9. Silvestri GA, Gould MK, Margolis ML et al. Noninvasive staging of non-small cell lung cancer: ACCP evidenced-based clinical practice guidelines (2nd edition). Chest 2007; 132:178S-201S.

10. Leong PP, Rezai B, Koch WM et al. Distinguishing second primary tumors from lung metastases in patients with head and neck squamous cell carcinoma. J Natl Cancer Inst 1998; 90(13):972-977.

11. Koppe MJ, Zoetmulder FA, van Zandwijk N et al. The prognostic significance of a previous malignancy in operable non-small cell lung cancer. Lung Cancer 2001; 32(1):47-53.

12. Chang YL, Wu CT, Lee YC. Surgical treatment of synchronous multiple primary lung cancers: experience of 92 patients. J Thorac Cardiovasc Surg 2009; 134(3):630-637.

13. Chhieng DC, Cangiarella JF, Zakowski MF et al. Use of thyroid transcription factor 1, PE-10, and cytokeratins 7 and 20 in discriminating between primary lung carcinomas and metastatic lesions in fine-needle aspiration biopsy specimens. Cancer 2001; 93(5):330-336.

14. van Oijen MG, Leppers Vd Straat FG, Tilanus MG et al. The origins of multiple squamous cell carcinomas in the aerodigestive tract. Cancer 2000; 88(4):884-893.

15. van Rens MT, Eijken EJ, Elbers JR et al. p53 mutation analysis for definite diagnosis of multiple primary lung carcinoma. Cancer 2002; 94(1):188-196.

16. de Geus-Oei LF, van Krieken JH, Aliredjo RP et al. Biological correlates of FDG uptake in non-small cell lung cancer. Lung Cancer 2007; 55(1):79-87.

17. Cerfolio RJ, Bryant AS, Ohja B et al. The maximum standardized uptake values on positron emission tomography of a non-small cell lung cancer predict stage, recurrence, and survival. J Thorac Cardiovasc Surg 2005; 130(1):151-159.

18. Jeong HJ, Min JJ, Park JM et al. Determination of the prognostic value of [(18)F]fluorodeoxyglucose uptake by using positron emission tomography in patients with non-small cell lung cancer. Nucl Med Commun 2002; 23(9):865-870.

19. Vesselle H, Salskov A, Turcotte E et al. Relationship between non-small cell lung cancer FDGuptake at PET, tumor histology, and Ki-67 proliferation index. J Thorac Oncol 2008; 3(9):971-978.

20. Higashi K, Ueda Y, Ayabe K et al. FDG PET in the evaluation of the aggressiveness of pulmonary adenocarcinoma: correlation with histopathological features. Nucl Med Commun 2000; 21(8):707-714.

21. Soret M, Bacharach SL, Buvat I. Partial-volume effect in PET tumor imaging. J Nucl Med 2007; 48(6):932-945.

22. Swets JA. Measuring the accuracy of diagnostic systems. Science 2009; 240(4857):1285-1293.

23. Jeon SY, Ahn SH, Kim CH et al. Esophageal and laryngeal cancer incidentally found on [18F]fluorodeoxyglucose positron emission tomography/computed tomography during the staging workup for lung cancer. Clin Lung Cancer 2008; 9(4):230-231.

24. Mittra E, Vasanawala M, Niederkohr R et al. A case of three synchronous primary tumors demonstrated by F-18 FDG PET. Clin Nucl Med 2007; 32(8):666-667.

25. van Westreenen HL, Westerterp M, Jager PL et al. Synchronous primary neoplasms detected on 18F-FDG PET in staging of patients with esophageal cancer. J Nucl Med 2005; 46(8):1321-1325.

26. Adriaensen M, Schijf L, de Haas M et al. Six synchronous primary neoplasms detected by FDG-PET/CT. Eur J Nucl Med Mol Imaging 2008; 35(10):1931.

27. Obando JA, Samii JM, Yasrebi M. A case of two synchronous primary lung tumors demonstrated by FDG positron emission tomography. Clin Nucl Med 2008; 33(11):775-777.

28. Wilkinson MD, Fulham MJ, McCaughan BC et al. Differentiation of synchronous tumors using FDG positron emission tomography. Clin Nucl Med 2003; 28(6):489-491.

29. Aquino SL, Halpern EF, Kuester LB et al. FDG-PET and CT features of non-small cell lung cancer based on tumor type. Int J Mol Med 2007; 19(3):495-499.

30. Gould MK, Maclean CC, Kuschner WG et al. Accuracy of positron emission tomography for diagnosis of pulmonary nodules and mass lesions: a meta-analysis. JAMA 2001; 285(7):914-924.

31. Gould MK, Kuschner WG, Rydzak CE et al. Test performance of positron emission tomography and computed tomography for mediastinal staging in patients with non-small-cell lung cancer: a meta-analysis. Ann Intern Med 2003; 139(11):879-892.

32. de Geus-Oei LF, van der Heijden HF, Corstens FH et al. Predictive and prognostic value of FDG-PET in nonsmall-cell lung cancer: a systematic review. Cancer 2007; 110(8):1654-1664.

33. MacManus M, Nestle U, Rosenzweig KE et al. Use of PET and PET/CT for radiation therapy planning: IAEA expert report 2006-2007. Radiother Oncol 2009; 91(1):85-94.

34. Degirmenci B, Wilson D, Laymon CM et al. Standardized uptake value-based evaluations of solitary pulmonary nodules using F-18 fluorodeoxyglucose-PET/computed tomography. Nucl Med Commun 2008; 29:614-622.

35. de Geus-Oei LF, van der Heijden HF, Visser EP et al. Chemotherapy response evaluation with 18F-FDG PET in patients with non-small cell lung cancer. J Nucl Med 2007; 48(10):1592-1598.

36. Schuurbiers OC, Kaanders JH, van der Heijden HF et al. The PI3-K/AKT-pathway and radiation resistance mechanisms in non-small cell lung cancer. J Thorac Oncol 2009; 4(6):761-767.

37. Jaskowiak CJ, Bianco JA, Perlman SJ et al. Influence of reconstruction iterations on 18F-FDG PET/CT standardized uptake values. J Nucl Med 2005; 46(3):424-428.

38. Lammertsma AA, Hoekstra CJ, Giaccone G et al. How should we analyse FDG PET studies for monitoring tumour response? Eur J Nucl Med Mol Imaging 2006; 33 Suppl 1:16-21.

39. Nakamoto Y, Zasadny KR, Minn H et al. Reproducibility of common semi-quantitative parameters for evaluating lung cancer glucose metabolism with positron emission tomography using 2-deoxy-2-[18F]fluoro-D-glucose. Mol Imaging Biol 2002; 4:171-178.

40. Nahmias C, Wahl LM. Reproducibility of standardized uptake value measurements determined by 18F-FDG PET in malignant tumors. J Nucl Med 2008; 49(11):1804-1808.

41. Kim CK, Gupta NC, Chandramouli B et al. Standardized uptake values of FDG: Body surface area correction is preferable to body weight correction. J Nucl Med 1994; 35:164-167.

42. Sobin LH, Wittekind C. UICC: TNM Classification of Malignant Tumours. 6th ed. New York: Wiley, 2002.

Chapter **6**

EUS-FNA for the detection of left adrenal metastasis in patients with lung cancer

Olga C. J. Schuurbiers

Kurt G. Tournoy

Hans J. Schoppers

Bernadette G. Dijkman

Henri J. L. M. Timmers

Lioe-Fee de Geus-Oei

Johanna M. M. Grefte

Klaus F. Rabe

P. N. Richard Dekhuijzen

Henricus F. M. van der Heijden

Jouke T. Annema

Abstract

Introduction
In patients with lung cancer, enlarged or [18]Fluoro-deoxyglucose positron emission tomography ([18]FDG-PET) positive left adrenal glands are suspected for distant metastases and require tissue confirmation for a definitive assessment. The aim of this study was to assess the sensitivity of endoscopic ultrasound-guided fine-needle aspiration (EUS-FNA) for left adrenal metastases in lung cancer patients with a suspect adrenal gland based on imaging.

Methods
EUS-FNA findings of patients with (suspected) lung cancer and CT enlarged or [18]FDG-PET positive left adrenal glands were retrospectively evaluated. In the absence of metastases at EUS, clinical and radiological follow-up was obtained.

Results
In 85 patients, EUS-FNA demonstrated left adrenal metastases of lung cancer in 53 (62%), benign adrenal tissue in 25 (29%), a metastasis from colon carcinoma in 1 (1%) and a primary adrenocortical carcinoma in 1 (1%) patient. In five patients (5.9%), the aspirates contained non-representative material. EUS outcomes were false negative in two patients. Sensitivity and negative predictive value (NPV) for EUS-FNA of the left adrenal gland were at least 86% (95% CI 74-93%) and 70% (95% CI 50-85%). No complications occurred.

Conclusion
EUS-FNA is a sensitive, safe and minimally invasive technique to provide tissue proof of left adrenal metastases in patients with (suspected) lung cancer and enlarged or [18]FDG-PET positive adrenal glands. Therefore, EUS-FNA qualifies as the staging test of choice for patients with lung cancer with suspected left adrenal metastases.

Introduction

Adrenal glands are a predilection site for metastatic spread in patients with lung cancer. Autopsy series have shown a prevalence of adrenal metastases in 35% to 59% of patients with lung cancer.[1, 2] The incidence of adrenal masses in patients with lung cancer varies from 4.1% to 18%.[3] Up to 4-7% of patients with otherwise operable NSCLC present with a unilateral adrenal mass; 40% of these are malignant and present as a solitary site of metastatic spread.[4, 5] As the majority (approximately two-thirds) of adrenal masses in patients with non-small cell lung cancer (NSCLC) represent benign adenomas [6], tissue verification of suspected malignant involvement is essential.

Computed tomography (CT) or integrated [18]FDG-PET-CT are used in standard diagnostic work-up of lung cancer patients and are helpful in the detection of distant metastases.[6] Due to the limited positive predictive value (PPV) of both CT (62%) and [18]FDG-PET-CT (81%) for the assessment of left adrenal metastases, tissue proof of malignant involvement is needed.[7-9] Chemical shift MRI [10-12] and CT protocols with unenhanced and delayed enhanced techniques [13, 14] seem interesting non invasive alternative approaches, but await further validation.

Traditional techniques to obtain tissue of left adrenal glands include percutaneous CT-guided FNA and open or laparoscopic adrenalectomies. These procedures are either invasive and associated with considerable complications such as pneumothorax and haemorrhage.[15-18] The left adrenal gland can be visualised and real-time sampled from the stomach using endoscopic ultrasound.[19] Transesophageal ultrasound guided fine needle aspiration (EUS-FNA) is a safe and minimally invasive alternative for surgical mediastinal staging that is incorporated in international guidelines.[20, 21] Reports about EUS-FNA for the assessment of left adrenal metastases in patients with lung cancer are limited, mostly single centre case series and rarely take PET findings into account.[19, 22-27] The aim of this multicentre study was to investigate the sensitivity of EUS-FNA in patients with (suspected) lung cancer with a suspect left adrenal gland metastasis based on CT and/or [18]FDG-PET imaging.

Methods

Patients

Patients who underwent EUS-FNA for the diagnosis and staging of lung cancer and in whom the left adrenal gland had been evaluated and aspirated between November 2001 and October 2009 were retrospectively identified. Patients with either enlarged left adrenal glands (short axis of the body > 10 mm), [18]FDG-PET uptake in the left adrenal gland or those in whom the loss of the typical seagull shape was missing were included in the study. Prior to EUS, all patients underwent CT or [18]FDG-PET-CT as part of their routine staging procedure. Data on patient demographics and clinical and radiological follow-up were extracted from patient charts. Patients underwent EUS in the Ghent University Hospital,

Belgium, the Leiden University Medical Centre, the Netherlands or the Radboud University Nijmegen Medical Centre, The Netherlands. These centres are referral centres for the diagnosis and staging of lung cancer by endosonography.

EUS-FNA

EUS-FNA examinations were performed by chest physicians who were specifically trained in EUS for the diagnosis and staging of lung cancer.[7, 28] EUS was performed in a standardized way in an outpatient setting under conscious sedation using midazolam. A linear scanning Pentax EG 3870 UTK/ 34 UX, Olympus/ Olympus GF-UCT 140-AL5 echo-endoscope was used in combination with a Hitachi or Aloka ultrasound scanner. The adrenal gland was routinely evaluated from the stomach in all patients prior to the mediastinal evaluation. With colour Doppler the presence of vessels in the vicinity of the LAG was evaluated. Sonographically suspect left adrenal glands (defined as short axis of the body > 1 cm, presence of hypo-echoic texture in the left adrenal body or absence of normal sea-gull shape) were punctured under real-time ultrasound guidance from the stomach with a 22-gauge needle (Medi-Globe type Sonotip II (GUS-01-27-022), Hancke-Villman needle (Medi-Globe) and Olympus: EZ Shot NA-200H-8022). Fine needle aspirates were in general repeated until - according to rapid on site examination (ROSE) of the obtained aspirates - representative material was obtained (Figure 1).

## Handling of the EUS aspirates and cytological examination

The aspirated material was processed in the following way: one smear was allowed to dry and stained with Diff-Quik for ROSE by a trained cytotechnician or chest physician to assess specimen adequacy. An additional smear was fixed in alcohol 96% and subsequently Papanicolaou-stained in the laboratory. The needle and remainder of the aspirate was rinsed in Unifix (a formaldehyde-based fixative; Klinipath, Duiven, the Netherlands) and processed into a paraffin-embedded cellblock for additional immunocytochemical staining using several organ- and tissue-specific markers.[29] Specific cell markers used in this study were among others cytokeratins 7 and 20, vimentin, thyroid transcription factor 1 (TTF-1), CD56, synaptophysin, chromogranin and p63.

All specimens were examined by a cytopathologist for a definitive diagnosis. Final diagnoses were classified as metastasis of primary lung cancer, metastasis of malignancy of other primary site, benign adrenal tissue, primary adrenocortical carcinoma or non-representative material.

FDG-PET Metabolic Activity Scoring

An FDG-PET scan was readily available for revision in a subgroup of 31 patients. The FDG-PET scans were interpreted by an experienced nuclear physician (LFdGO). The FDG-uptake in the left adrenal gland was visually scored as "not suspect" if the metabolic activity in the left adrenal gland was equal to that of the liver and as "suspect" if the metabolic activity was increased above liver background.

Figure 1. Details of the LAG on CT, integrated [18]FDG-PET-CT and cytological processing methods
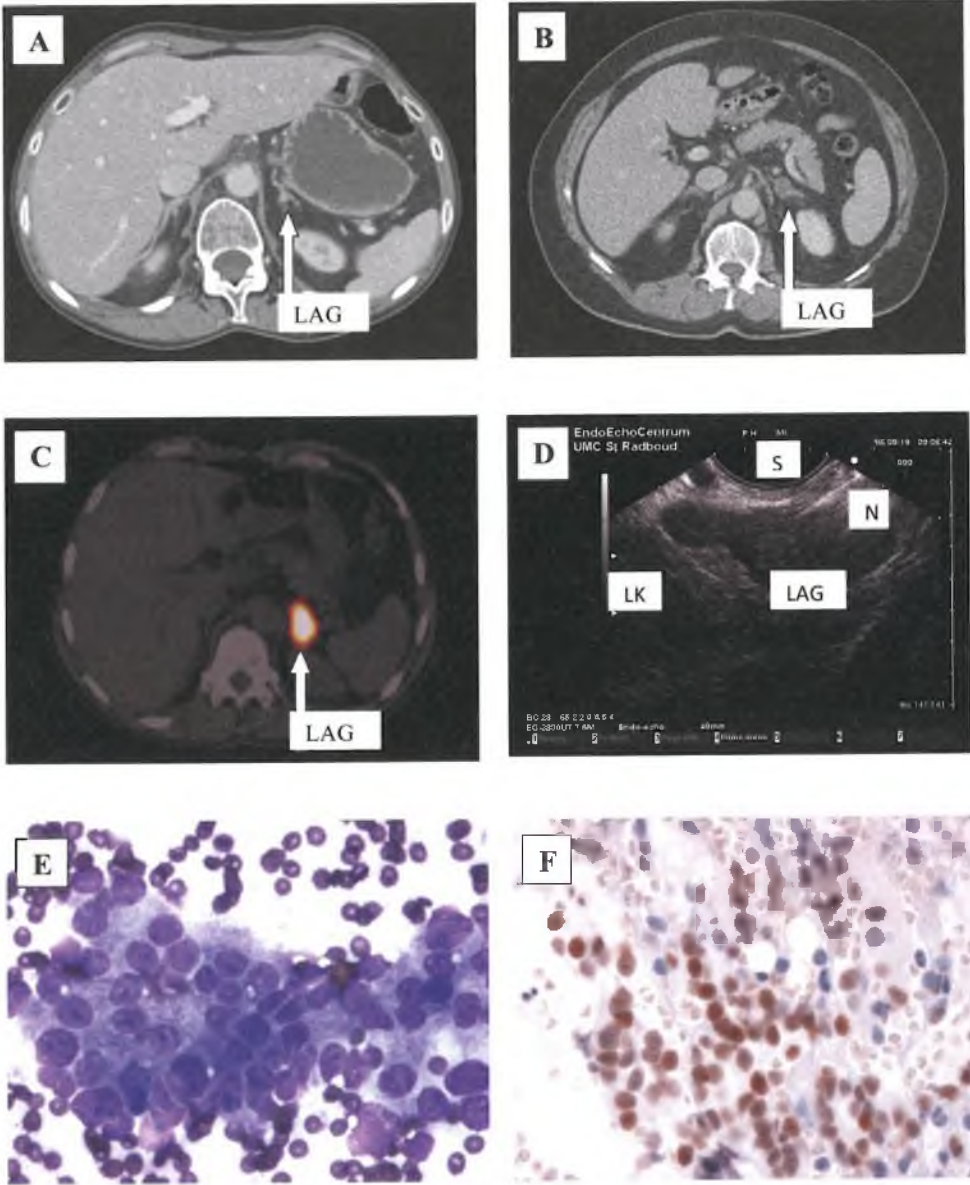
(A) CT image of a normal shaped left adrenal gland (LAG). (B) CT image of an enlarged left adrenal gland (LAG). (C) Integrated [18]PET-CT image of an enlarged PET positive left adrenal gland (LAG). (D) EUS- FNA (Transgastric) of an enlarged left adrenal gland (LAG); N= Needle, LK= Left Kidney S= Stomach. (E) EUS obtained aspirate of the left adrenal gland showing adenocarcinoma cells after staining with the Giemsa method (60-fold enlargement). (F) Fine needle aspirate of the left adrenal gland processed into paraffin cell-block demonstrating positive TTF-1 staining.

Statistical Methods

SPSS software was used for descriptive analyses to summarize patient characteristics and EUS-FNA results. The reference standard for the final diagnosis was a combination of clinical and radiological follow-up. Missing values regarding follow-up were regarded false negative. Continuous variables were described as means, and dichotomous variables were expressed as simple proportions. The chi-square test was used for correlating two categorical variables. A p-value <0.05 was considered statistically significant.

Results

Patients

Eighty-five patients (51 men, 34 women; mean age 64 years, range 36-85) were included. Patient characteristics and EUS indications are summarized in Table 1. EUS-FNA was performed for the staging of known lung cancer in 45 patients, and in 40 patients for the diagnosis and staging of suspected lung cancer.

Table 1: Patient (n=85) and imaging characteristics of LAG

Mean age (range), yr	65	(37-86)
Gender, No. (%)		
Male	51	(60)
Female	34	(40)
Indication for EUS, No. (%)		
Staging of biopsy-proven lung cancer	45	(53)
Diagnosis and staging of suspected lung cancer	40	(47)
CT scan characteristics LAG, No. (%)		
Enlarged [a]	71	(84)
Normal shape and size	11	(13)
Mean adrenal diameter of LAG	33	(5-120)
on CT in mm (mean (range))		
Metabolic activity LAG on PET-scan, No. (%)		
Increased [b]	46	(54)
Not increased	7	(8)
PET scan not available	32	(38)

Abbreviations: EUS, endoscopic ultrasound; LAG, left adrenal gland; PET, positron emission tomography; CT, computed tomography.

[a] loss of normal seagull shape or LAG body short axis > 1cm

[b] increased FDG uptake relative to uptake in the liver

EUS-FNA Results

EUS-FNA provided tissue proof of left adrenal metastases of a primary lung cancer in 53 of 85 patients (62%). Benign adrenal tissue was found in 25 patients (29%), a primary adrenocortical carcinoma in one, a metastasis from colon carcinoma in another patient and not representative material was obtained in five (6.4%) patients (Table 2). The median number of aspirations of the left adrenal gland was 3.0 (range 1-6). No complications occurred. The proportion of left adrenal metastases found by EUS-FNA was comparable between patients with enlarged and [18]FDG-PET-positive left adrenal glands (63% vs. 67%, respectively).

Out of 81 left adrenal glands of which the diameter on EUS or CT was recorded, 33 had a diameter of 30 mm or more (table 3). Of those, 26 (79%) were malignant (OR 2.41 (95% CI 0.90 to 6.42)). On the other hand, 58% (28 out of 48) left adrenal glands with a diameter smaller than 30 mm were found to be malignant.

Table 2: LAG diagnoses after EUS-FNA in relation to CT/ PET findings

Diagnosis	LAG enlarged on CT[a] and/or PET positive[b], No. (%)	LAG enlarged on CT[a], No. (%)	LAG PET positive[b], No. (%)	LAG enlarged on CT[a] and PET positive[b], No. (%)
Metastasis of lung cancer	53 (62.4)	45 (63.4)	31 (67.4)	25 (73.5)
NSCLC	48 (56.5)	42 (59.2)	27 (58.7)	22 (64.7)
Not specified	27 (31.8)	25 (35.2)	11 (23.9)	10 (29.4)
SCC	6 (7.1)	5 (7.0)	5 (15.9)	4 (11.7)
AC	10 (11.8)	8 (11.3)	7 (15.2)	5 (14.7)
LCC	5 (5.9)	4 (5.6)	4 (8.7)	3 (8.8)
SCLC	5 (5.9)	3 (4.2)	4 (8.7)	3 (8.8)
Primary adrenocortical carcinoma	1 (1.2)	1 (1.4)	1 (2.2)	1 (2.9)
Metastasis of colon carcinoma	1 (1.2)	1 (1.4)	0 (0.0)	0 (0.0)
Benign adrenal tissue	25 (29.4)	20 (28.2)	11 (23.9)	6 (17.6)
Non-diagnostic	5 (5.9)	4 (5.6)	3 (6.5)	2 (5.8)
Total	85(100)	71 (100)	46 (100)	34 (100)

Abbreviations: EUS, endoscopic ultrasound; FNA, fine-needle aspiration; LAG, left adrenal gland; CT, computed tomography; PET, positron emission tomography; NSCLC, non-small cell lung carcinoma; SCC, squamous cell carcinoma; AC, adenocarcinoma; LCC, large cell carcinoma; SCLC, small cell lung carcinoma.
[a]Loss of normal seagull shape or LAG body short axis > 1cm
[b]Increased FDG uptake relative to uptake in the liver

Final diagnosis

Follow-up information was available for 23 of 30 patients in whom no left adrenal metastases were found by EUS. Follow-up (12.9 months, range 2.0 - 40 months) was not suspicious for metastatic malignant disease based on clinical grounds (11 patients) and/or on repeat CT of the left adrenal gland (10 patients). in two patients the left adrenal gland increased in size considerable in 3 months after EUS and was considered metastatic. In one

of these patients the adrenal metastasis was confirmed with a surgical biopsy. These false negatives were probably due to a sampling error as the cytology specimen showed benign adrenal cells.

Sensitivity and NPV of EUS-FNA for malignant involvement of the left adrenal gland were 86% (95% CI 74-93%) and 70% (95% CI 50-85%). For this calculation we assumed that all 7 patients in whom follow-up was missing were false negative. If all missing values were true negative sensitivity and NPV would reach 96% and 91%.

Correlation of EUS-FNA results with FDG-uptake

In 32 of 46 patients referred for EUS-FNA of the left adrenal gland based on [18]FDG-PET positive results, malignancy of the left adrenal gland was confirmed. In 11 patients EUS-FNA did not find malignancy (benign adrenal tissue). When EUS-FNA of the left adrenal gland was considered as a gold standard, any [18]FDG uptake had a PPV of 74%.

In the subgroup of patients (n=31) in whom the degree of FDG-uptake by the left adrenal gland was scored by an experienced nuclear physician, correlation of EUS-FNA results with FDG-uptake was significant (Pearson chi-square value 17.9; p=0.001). In [18]FDG-PET negative left adrenal glands, no metastases have been identified by EUS-FNA (Table 4). The vast majority (82%) of left adrenal glands with increased FDG-uptake was found to be malignant.

Table 3: LAG size in relation to cytological outcome

LAG size [a]	Benign (n=22)	Malignant (n=54)	Not diagnostic (n=5)	Total (n=81)
Range	7 - 40	9 - 120	5 - 38	5 – 120
Mean ± SD	22.3 ± 9.4	32.4 ± 21.3	19.4 ± 13.3	28.6 ± 19.1
Median	22.5	27	19.0	25
≥ 30	6	26	1	33
< 30	16	28	4	48

Abbreviations: EUS, endoscopic ultrasound; LAG, left adrenal gland.
[a]LAG body short axis in mm (on EUS or if not available on CT).

Table 4: EUS-FNA findings of LAG related to FDG PET findings

Interpretation of PET	Final diagnoses of EUS-FNA, No. (%)			
	Malignant	Benign	Not-representative	Total
Not suspect[a]	0	5	2	7
Suspect[b]	18	4	2	24
Total	18	9	4	31

Abbreviations: EUS, endoscopic ultrasound; FNA, fine-needle aspiration; LAG, left adrenal gland; PET, positron emission tomography.
[a] The metabolic activity of the left adrenal gland was classified as 'not suspect' if the uptake was equal to or less than the FDG-uptake in the liver
[b]Metabolic activity above liver background

Discussion

In this retrospective multicenter study in patients with lung cancer and suspected left adrenal metastases, EUS-FNA provided tissue proof of metastatic spread in 53 of 85 patients (62%). The sensitivity for EUS-FNA of the left adrenal gland was at least 86%. Additionally, EUS-FNA also excluded the presence of left adrenal metastases in 25 patients (29%) with a NPV of at least 70%. These operating characteristics are very conservative and are probably better as patients with missing follow up were regarded false negative. The PPV of [18]FDG-PET for assessment of left adrenal gland metastases in our subgroup with a FDG-PET available for revision was 82% in case of PET positive left adrenal glands. The data confirm the need for tissue proof of suspected metastatic spread to correctly stage lung cancer patients in order to prevent over staging.

The present study is a multicentre study on EUS-FNA of the left adrenal gland in lung cancer patients that is performed by chest physicians trained in pulmonary oncology and EUS-FNA. EUS-FNA is already an established technique for mediastinal nodal staging.[20, 21] The advantage of EUS is that mediastinal nodal staging and assessment of the left adrenal gland can be performed during the same procedure.

Previously, EUS-FNA for the analysis of the left adrenal gland has been reported in six single centre case series of patients with left adrenal metastases.[22-27] Four studies included heterogeneous populations with a wide variety of EUS indications (not specifically patients with lung cancer).[22, 24, 25, 27] Furthermore, none of these studies particularly took CT-enlargement or PET-positivity of the adrenal masses into account. Among the included patients with known or suspected lung cancer in whom EUS-FNA of the left adrenal gland was performed, 40-68% of EUS-FNA yielded benign adrenal tissue, and adrenal metastases from lung cancer were found in 14-60% of patients.[22-25, 27] In the most recently published study, 59 cases of patients with enlarged or [18]FDG-PET positive (left) adrenal glands were retrospectively selected from a pool of 7500 patients referred for EUS.[26] Left adrenal gland metastasis was confirmed in 22 patients (37%). Altered shape of the left adrenal gland on EUS imaging was a significant predictor for malignancy whereas left adrenal gland size (> 30 mm) on CT and hypo echoic EUS features were not.[26]

In the present study the degree of [18]FDG-uptake was interpreted qualitatively, since it was previously reported that additional SUV analysis does not help to further differentiate between malignant and benign adrenal lesions, due to a distinct overlap in SUVs between benign and malignant lesions.[9] From the present data it can be concluded that it is relatively save to consider any [18]FDG- uptake in the adrenal above physiological accumulation in the liver as "positive or suspicious". Such criterion results in a PPV of 82% and did not misclassify any of the seven PET-negative cases.

Previous PET-CT studies that assessed left adrenal gland metastases using SUVmax cut-off levels also report PPVs of 81%. However, in these studies histological prove was only available in the minority of cases.[7, 9]

Whether normal sized [18]FDG-PET negative patients should be routinely investigated cannot be answered. One report on a patient with a normal left adrenal gland on CT (and no PET performed) showed an enlarged left adrenal gland on EUS examination and EUS-FNA revealed a left adrenal gland metastasis.[30] Also two cases of malignancy in the left adrenal gland were detected in subjects, referred for EUS-FNA as part of mediastinal staging, with normal left adrenal glands on CT.[23]

Various limitations apply to this study. Its retrospective design, the absence of surgical verification of the left adrenal gland on those patients in whom EUS did not find malignant involvement and the missing follow-up in several patients. However, we choose a conservative approach reporting our data classifying missing follow-up as false negative most likely underestimating the value of EUS. The patients included in this study are a subset of a much larger population. A selection bias is present, as the population studied represents a subgroup of lung cancer patients that were referred from other centers for EUS-FNA. It's unknown how many centers base their stage M1b adrenal metastasis on radiologic or nuclear findings only. Left adrenal gland size was only measured by the short axis of the corpus of the left adrenal gland body, loss of the typical "sea-gull shape " was not always specifically mentioned. Whether the short axis of the corpus of the left adrenal gland or the altered shape of the left adrenal gland is predictive of malignancy cannot be answered. In the present study only patients with suspected left adrenal glands- and not right adrenal glands were considered. The right adrenal gland should be approached from the duodenum – this is technically more demanding- and only 10 cases have been described.[26, 27, 31]

An important issue when new approaches are validated for clinical implementation is to report complications. One case of left adrenal hemorrhage after EUS-FNA has been reported.[32] In contrast to the reported complication rate for percutaneous adrenal biopsies of 8.4%[16, 17], and open adrenalectomies of 34%[18], no complications occurred during or shortly after EUS-FNA procedures in this and previous case series on left adrenal gland EUS-FNA.[22-27] In patients with suspected pheochromocytoma - for instance in patients with an enlarged adrenal gland without a known primary tumour with a predilection for metastatic spread to the adrenal gland - metanephrines in plasma or 24-hour urine should be measured to rule out this clinical condition and to prevent a hypertensive crisis. To date, endosonography is implemented for minimally invasive mediastinal staging of lung cancer. An important advantage of EUS above EBUS (endobronchial ultrasound) is the ability to evaluate the left adrenal glands in addition to staging of the mediastinal nodes.

Conclusion

EUS-FNA is a sensitive, safe and minimally invasive technique to provide tissue proof of left adrenal metastases in patients with (suspected) lung cancer and enlarged or PET positive left adrenal glands. Therefore EUS-FNA qualifies as the staging test of choice for patients with lung cancer with suspected left adrenal metastases.

References

1. Engelman RM, McNamara WL. Bronchiogenic carcinoma: a statistical review of two hundred and thirty-four autopsies. J Thorac Surg 1954; 27(3):227-237.

2. Ettinghausen SE, Burt ME. Prospective evaluation of unilateral adrenal masses in patients with operable non-small-cell lung cancer. J Clin Oncol 1991; 9(8):1462-1466.

3. Chapman GS, Kumar D, Redmond J, III et al. Upper abdominal computerized tomography scanning in staging non-small cell lung carcinoma. Cancer 1984; 54(8):1541-1543.

4. Albain KS, Crowley JJ, LeBlanc M et al. Survival determinants in extensive-stage non-small-cell lung cancer: the Southwest Oncology Group experience. J Clin Oncol 1991; 9(9):1618-1626.

5. Burt M, Heelan RT, Coit D et al. Prospective evaluation of unilateral adrenal masses in patients with operable non-small-cell lung cancer. Impact of magnetic resonance imaging. J Thorac Cardiovasc Surg 1994; 107(2):584-588.

6. Quint LE. Staging non-small cell lung cancer. Cancer Imaging 2007; 7:148-159.

7. Brady MJ, Thomas J, Wong TZ et al. Adrenal nodules at FDG PET/CT in patients known to have or suspected of having lung cancer: a proposal for an efficient diagnostic algorithm. Radiology 2009; 250(2):523-530.

8. Gupta NC, Graeber GM, Tamim WJ et al. Clinical utility of PET-FDG imaging in differentiation of benign from malignant adrenal masses in lung cancer. Clin Lung Cancer 2001; 3(1):59-64.

9. Okada M, Shimono T, Komeya Y et al. Adrenal masses: the value of additional fluorodeoxyglucose-positron emission tomography/computed tomography (FDG-PET/CT) in differentiating between benign and malignant lesions. Ann Nucl Med 2009; 23(4):349-354.

10. Inan N, Arslan A, Akansel G et al. Dynamic contrast enhanced MRI in the differential diagnosis of adrenal adenomas and malignant adrenal masses. Eur J Radiol 2008; 65(1):154-162.

11. Maurea S, Imbriaco M, D'Angelillo M et al. Diagnostic accuracy of chemical-shift MR imaging to differentiate between adrenal adenomas and non adenoma adrenal lesions. Radiol Med 2006; 111(5):674-686.

12. Savci G, Yazici Z, Sahin N et al. Value of chemical shift subtraction MRI in characterization of adrenal masses. AJR Am J Roentgenol 2006; 186(1):130-135.

13. Blake MA, Kalra MK, Sweeney AT et al. Distinguishing benign from malignant adrenal masses: multi-detector row CT protocol with 10-minute delay. Radiology 2006; 238(2):578-585.

14. Caoili EM, Korobkin M, Francis IR et al. Adrenal masses: characterization with combined unenhanced and delayed enhanced CT. Radiology 2002; 222(3):629-633.

15. Marangos IP, Kazaryan AM, Rosseland AR et al. Should we use laparoscopic adrenalectomy for metastases? Scandinavian multicenter study. J Surg Oncol 2009; 100(1):43-47.

16. Mody MK, Kazerooni EA, Korobkin M. Percutaneous CT-guided biopsy of adrenal masses: immediate and delayed complications. J Comput Assist Tomogr 1995; 19(3):434-439.

17. Silverman SG, Mueller PR, Pinkney LP et al. Predictive value of image-guided adrenal biopsy: analysis of results of 101 biopsies. Radiology 1993; 187(3):715-718.

18. Strong VE, D'Angelica M, Tang L et al. Laparoscopic adrenalectomy for isolated adrenal metastasis. Ann Surg Oncol 2007; 14(12):3392-3400.

19. Stelow EB, Debol SM, Stanley MW et al. Sampling of the adrenal glands by endoscopic ultrasound-guided fine-needle aspiration. Diagn Cytopathol 2005; 33(1):26-30.

20. De Leyn P, Lardinois D, Van Schil PE et al. ESTS guidelines for preoperative lymph node staging for non-small cell lung cancer. Eur J Cardiothorac Surg 2007; 32(1):1-8.

21. Detterbeck FC, Jantz MA, Wallace M et al. Invasive mediastinal staging of lung cancer: ACCP evidence-based clinical practice guidelines (2nd edition). Chest 2007; 132(3 Suppl):202S-220S.

22. Ang TL, Chua TS, Fock KM et al. EUS-FNA of the left adrenal gland is safe and useful. Ann Acad Med Singapore 2007; 36(11):954-957.

23. Bodtger U, Vilmann P, Clementsen P et al. Clinical Impact of Endoscopic Ultrasound-Fine Needle Aspiration of Left Adrenal Masses in Established or Suspected Lung Cancer. J Thorac Oncol 2009; 4(12):1485-1489.

24. Dewitt J, Alsatie M, LeBlanc J et al. Endoscopic ultrasound-guided fine-needle aspiration of left adrenal gland masses. Endoscopy 2007; 39(1):65-71.

25. Eloubeidi MA, Seewald S, Tamhane A et al. EUS-guided FNA of the left adrenal gland in patients with thoracic or GI malignancies. Gastrointest Endosc 2004; 59(6):627-633.

26. Eloubeidi MA, Black KR, Tamhane A et al. A large single-center experience of EUS-guided FNA of the left and right adrenal glands: diagnostic utility and impact on patient management. Gastrointest Endosc 2010; 71(4):745-753.

27. Jhala NC, Jhala D, Eloubeidi MA et al. Endoscopic ultrasound-guided fine-needle aspiration biopsy of the adrenal glands: analysis of 24 patients. Cancer 2004; 102(5):308-314.

28. Annema JT, Bohoslavsky R, Burgers S et al. Implementation of endoscopic ultrasound for lung cancer staging. Gastrointest Endosc 2009.

29. Bahrami A, Truong LD, Ro JY. Undifferentiated tumor: true identity by immunohistochemistry. Arch Pathol Lab Med 2008; 132(3):326-348.

30. Ringbaek TJ, Krasnik M, Clementsen P et al. Transesophageal endoscopic ultrasound/fine-needle aspiration diagnosis of a malignant adrenal gland in a patient with non-small cell lung cancer and a negative CT scan. Lung Cancer 2005; 48(2):247-249.

31. Eloubeidi MA, Morgan DE, Cerfolio RJ et al. Transduodenal EUS-guided FNA of the right adrenal gland. Gastrointest Endosc 2008; 67(3):522-527.

32. Haseganu LE, Diehl DL. Left adrenal gland hemorrhage as a complication of EUS-FNA. Gastrointest Endosc 2009; 69(6):e51-e52.

Chapter **7**

A brief retrospective report on the feasibility of *EGFR* and *KRAS* mutation analysis in EUS and EBUS guided fine needle cytological aspirates*

Olga CJ Schuurbiers

Monika G. Looijen-Salamon

Marjolijn J.L. Ligtenberg

Henricus FM van der Heijden

Abstract

Introduction
Molecular testing for *EGFR* and *KRAS* mutations is of increasing clinical importance in daily practice. In this study we aimed to investigate the yield and applicability of molecular testing for *KRAS* and *EGFR* mutations in cytological specimens obtained by EUS or EBUS guided fine needle aspiration.

Methods
We selected all patients with an EUS- or EBUS-guided FNA positive for lung adenocarcinoma from the database of our tertiary care center for endosonography. Direct smears were Giemsa and Papanicolaou stained. The remaining material was processed in cell blocks. Both cell blocks and smears were considered suitable for molecular analysis when >40% of the aspirated cells were tumor cells. All eligible samples were investigated for *KRAS* and *EGFR* mutations by PCR followed by direct sequencing.

Results
462 patients underwent EUS or EBUS-FNA using 22G needles. In 35 patients FNA showed lung adenocarcinoma. In 8 patients, molecular analysis could not be performed because of insufficient material after routine and immunocytochemistry (n=3), a low percentage (<40%) of tumor cells (n=3) or an insufficient DNA quality (n=2). The average percentage of tumor cells was 73 ± 23%. Molecular analysis could reliably be performed in 27 patients (77 %). Mutation analysis showed *KRAS* and *EGFR* mutations in tumor samples from 10 (37%) and 2 (7%) patients, respectively. In one patient two *EGFR* mutations (p.Thr790Met and p.Leu858Arg) were detected.

Conclusion
Molecular analysis for *KRAS* and *EGFR* mutations can be performed routinely in cytological specimens from EUS- and EBUS-guided FNA.

Introduction

Determination of the mutation status of the epidermal growth factor receptor (*EGFR*) gene is of importance to adequately select patients with both early and advanced non-small cell lung cancer (NSCLC) for targeted treatment with tyrosine kinase inhibitors (TKI's) or monoclonal antibodies and to predict the prognosis and response to *EGFR* targeted treatment as well as systemic chemotherapy.[1-3] Also the *KRAS* mutational status is of importance since *KRAS* is an important proliferation step downstream of the EGF-receptor and mutations in *KRAS* relate to resistance to EGFR targeted therapy and adjuvant chemotherapy.[4-6] *KRAS* mutations may also be of relevance to other downstream pathways like the PI3K/AKT pathway.[7, 8]

Recent landmark studies investigating the effects of different TKI's in NSCLC all used histological specimens for molecular analysis of the mutation status. However, in clinical practice the diagnosis of lung cancer is often based on cytological specimens since tissue samples are increasingly obtained by ultrasound guided techniques and on transthoracic fine needle aspirations. Recent developments have shown that transesophageal ultrasound guided fine needle aspiration (EUS-FNA) and endobronchial ultrasound guided FNA (EBUS) are minimally invasive diagnostic and staging procedures which have shown to be highly sensitive and accurate.[9-11] They allow safe cytological sampling of mediastinal lymph nodes and centrally located intrapulmonary tumors or metastases in the upper abdomen including the left adrenal gland. EUS-FNA and EBUS have therefore been incorporated in the guidelines of the ESTS and ACCP [12, 13] and a combination of these techniques has been shown to have a better sensitivity and negative predictive value than cervical mediastinoscopy (the now debated gold standard).[14, 15]

However, in contrast to cervical mediastinoscopy EUS-FNA and EBUS will result in cytological specimens, preferably processed on slides for rapid onsite evaluation (ROSE) and vials for cell blocks. Since these samples are often the only available proof of lung cancer, mutation analysis performed on cytological specimens is of increasing interest.[16] Furthermore, differences in mutations in the primary tumor site compared to metastatic disease sites have been shown and may be of importance to daily clinical practice.[17] Therefore, in case of recurrent disease renewed tissue sampling needs to be considered increasing the necessity to use minimal invasive techniques for sampling of tumor material on which molecular analyses can be performed.

Recently two studies reported on *EGFR* analysis in cell-block based cytological specimens from EBUS.[18, 19] In this study we aimed to investigate the yield and applicability of molecular testing for both *KRAS* and *EGFR* mutations in all available cytological specimens, both cell blocks and direct smears, obtained by EUS-FNA or EBUS guided fine needle aspiration in routine daily practice.

Methods

Between January 2006 and January 2010 462 patients were evaluated in our tertiary care university hospital center for endosonography. EUS was available since December 2005 and EBUS from December 2008 onwards. Of these 462 patients 289 were referred for diagnosis or staging of proven or suspected lung cancer.

All patients were investigated in an out-patient procedure using midazolam (2,5-5 mg) for conscious sedation. EUS and EBUS were performed using Pentax EG 3870UTK or EB-1970UK echo-endoscopes in combination with a Hitachi EUB 6500 or 7000HV ultrasound scanner. In all patients FNA was performed using 22G needles (Medi-Globe); on average 2.9±1.1(SD; range 1-5) aspirations per diagnostic site were performed. Direct smears were made for Giemsa and Papanicolaou staining. Giemsa stained smears were processed and analysed onsite for rapid onsite evaluation (ROSE) by a cytotechnician. The remaining material was processed in cell blocks; from which 4 µm slides were cut for Hematoxyline-eosine staining and immunocytochemistry. To minimize the chance of false-negative results, based on our experience in histological NSCLC and colorectal cancer specimens [20], both cell blocks and smears were considered suitable for molecular analysis when DNA could be isolated from regions with >40% tumor cells. For DNA isolation from the cell blocks the relevant regions were manually microdissected from two to three 20 µm sections using flanking hematoxyline-eosine stained slides as a reference and incubated overnight at 56 °C in 200 µl lysis buffer (10 mM Tris pH 8.5, 1 mM EDTA; 0.05% tween20, 5% Chelex-100, 2 µg/µl Proteinase K), followed by 10 min at 95 °C. After centrifugation the supernatant is used for subsequent analyses. For the DNA isolation from the smears, regions with over 40% tumor cells are scraped from the glass slides and incubated overnight at 56 °C in 400 µl lysis buffer (10 mM Tris pH7.5, 2 mM EDTA, 400 mM NaCl, 1% SDS, 2 µg/µl Proteinase K) followed by a salt precipitation with 140 µl 6 M NaCl and ethanol precipitation of the supernatant. The DNA pellet is dissolved in 20 µl TE (10 mM Tris pH 7.5, 1 mM EDTA). Mutation analysis of *EGFR* exons 18, 19, 20 and 21 and *KRAS* codons 12, 13 and 61 was performed using 1 µl DNA solution in PCRs followed by Big-Dye terminator sequencing (BigDye ® Terminators (v 1.1); Applied Biosystems, USA) and analysis on an ABI 3730 DNA Analyzer (Applied Biosystems; primer sequences and PCR conditions are available upon request).

As the molecular analyses performed in this study have been performed as part of routine diagnostic daily practice, there was no need to consulting our ethics committee. Full disclosure of results was given to the patients and results were discussed in our multidisciplinary tumor-board meetings to determine the optimal treatment strategies.

Results

In 112 patients (82 male and 30 female) cytological proof of lung cancer was obtained by EUS (n=77), EBUS (n=30) or combined EUS and EBUS (n=5). The average age was 64.8±9.7

years (range 36-90 years). Giemsa and Papanicolaou and immunocytochemical stainings showed squamous cell carcinoma in 38 cases (34%), adenocarcinoma in 35 cases (31%), large cell or undifferentiated NSCLC in 26 patients (23%) and SCLC in 13 cases (12%) (Table 1).

The average percentage of tumor cells in the 35 specimens containing adenocarcinoma was 73±23%. Molecular analysis could not be performed in 8 patients because of insufficient material after routine cytology and immunocytochemistry(n=3), a low percentage (<40%) of tumor cells (n=3) or an insufficient DNA quality (n=2).

Molecular analysis could reliably be performed in 27 patients (77%). The average percentage of tumor cells in the 27 samples was 79 ± 12%. Analysis was performed on material obtained from cell blocks (n=19), Giemsa-stained (n=3) or Papanicolaou stained smears (n=5).

Mutation analysis showed *KRAS* mutations in tumor samples from 10 patients (37%). Six mutations were detected in cell block preparations and four in material from Papanicolaou stained smears. *EGFR* mutations were found in two patients (7.4%). One patient had an activating exon 19 (p.Leu747_Ala750delinsPro) mutation detected in material from a Papanicolaou stained smear. The second patient, with recurrent, TKI-naïve adenocarcinoma, had two *EGFR* mutations (p.Thr790Met and p.Leu858Arg), detected in a cell block specimen (Table 1 and Figure 1).

Table 1. Patients with EUS- or EBUS-guided cytology proven lung cancer

Patient characteristics (n=112)	
Age (yr)	64.8 ± 9.7 (range, 36-90)
Gender: female:male, n (%)	30:82 (27:73)
Histology (n (%))	
SCC	38 (34)
AC	35 (31)
LC/undifferentiated NSCLC	26 (23)
SCLC	13 (12)
Adenocarcinoma (n=35), n (%)	
Samples available for analysis	27 (77)
Gender (female: male)	11:16 (41:59)
Percentage tumor cells	73% ± 21%
KRAS mutation positive, n (%)	10 (37)
c.35G>T (p.Gly12Val)	5
c.35G>A (p.Gly12Asp)	2
c.34G>T (p.Gly12Cys)	1
c.182A>T (p.Glu61Leu)	1
c.37G>T (p.Gly13Cys)	1
EGFR mutation positive, n (%)	2 (7)
c.2369C>T (p.Thr790Met) and c.2573T>G (p.Leu858Arg)[a]	1
c.2239_2248delinsC (p.Leu747_Ala750delinsPro)	1
KRAS and *EGFR* mutation negative, n (%)	15 (56)

[a]Double mutation in one patient. AC= adenocarcinoma; LC= large cell undifferentiated NSCLC; NSCLC= non-small cell lung cancer; SCLC= small cell lung cancer; SCC= squamous cell carcinoma; EGFR= epidermal growth factor receptor.

Discussion

This study shows that molecular analysis of *EGFR* and *KRAS* mutations on cytological material obtained by EUS or EBUS is feasible and can be performed in daily practice. Molecular analysis could be performed in 77% of the adenocarcinoma samples. Biomarker analysis on cytological material is becoming increasingly available. A far as we know this is the first study to report successful mutation analysis of both the *KRAS* and *EGFR* gene on both cytological smears and cell blocks obtained by EUS or EBUS.

In 27 of 35 patients (77%) with cytologically proven lung adenocarcinomas we were able to perform molecular analysis using PCR and subsequent sequence analysis. This is in agreement with the study by Garcia-Olive and co-workers, where EGFR gene analysis of the EBUS-TBNA sample was feasible in 26 (72.2%) out of the 36 patients with lymph node metastasis and similar methods were used.[21] Nakajima and coworkers were able to perform molecular analysis in histological cores obtained by EBUS in 43 of 46 lung adenocarcinoma patients (94%).[22] In this study the assessment of tumor cells is not described but the short axis of the sampled lymph nodes with EGFR mutations was approximately similar to the our study (16.8±7.0 mm).[23] The percentage of *EGFR* mutations found in the above mentioned Spanish and Japanese studies was 10% and 26%, respectively. Especially the percentage from the latter study is much higher than the percentage *EGFR* mutations (7.4%) found in our cohort. This might reflect a high percentage of cigarette smoking patients in our predominantly male, Caucasian group of patients. Unfortunately exact data on smoking status is not available since the majority of our patients were referred for the diagnostic endosonographic procedure only and treated in the referring hospitals. However, in our own clinic for thoracic oncology approximately 87% of patients are current or former smokers.

The percentage of *KRAS* mutations (37%) in our cohort is in line with other studies reporting *KRAS* mutations ranging from 15-22% and 18-43% in nonsmoking and smoking subjects, respectively.[24, 25] Earlier studies used paraffin embedded material from cell-blocks [26, 27] whereas in the present study tumor cells could also be retrieved from direct cytological smears. This may offer additional opportunities for mutation analysis, especially when histological biopsies and cell blocks do not contain enough tumor cells.

In our feasibility study we concentrated on the molecular analyses of adenocarcinoma, however the technique will also be applicable in other histological groups. Since the predictive value of *EGFR* amplification is still under debate [28, 29] FISH analysis was not routinely performed in our samples, however in the only cytological sample, in which FISH analysis was performed an *EGFR* amplification was detected.

Figure 1.
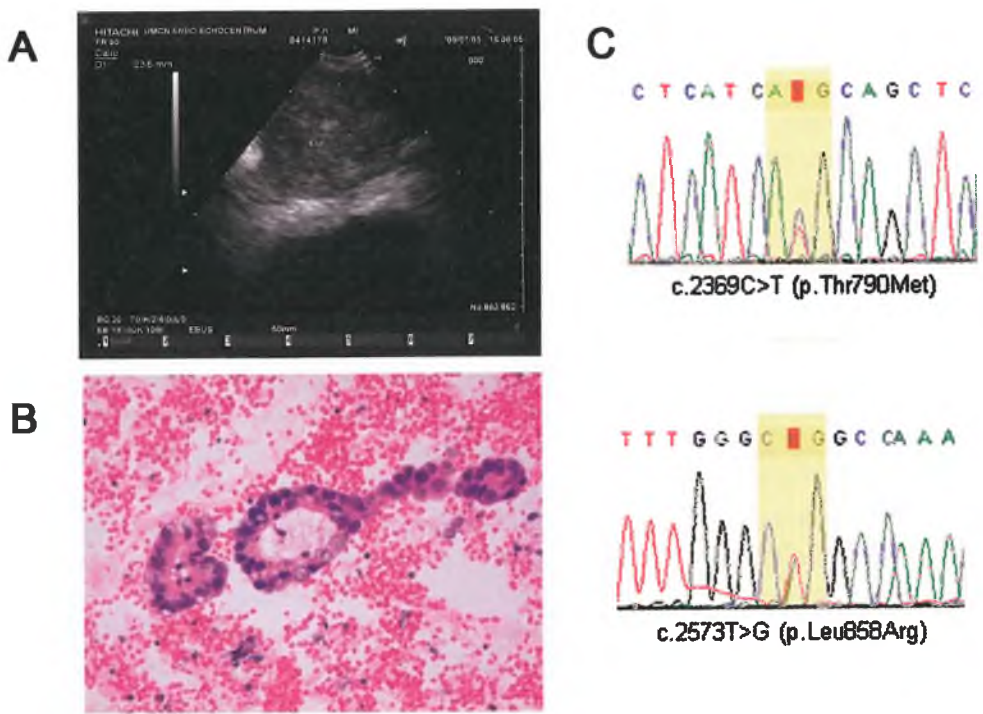
Representative sample of a 77 year old patient referred for analysis of suspected recurrent lung cancer 4 years after a left upper lobe resection for a pT1aN0M0 adenocarcinoma. EBUS guided lymph node sampling revealed recurrent disease with a double *EGFR* mutation:
Panel A: endosonographic EBUS image of the enlarged subcarinal lymph node at position number 7 (diameter 23.5 mm);
Panel B: HE staining of lymph node aspirate (200x) revealing adenocarcinoma;
Panel C: sequence chromatograms of *EGFR* mutations c.2369C>T (p.Thr790Met) (top) and c.2573T>G (p.Leu858Arg) (bottom).

Conclusion

This study shows that molecular analysis for *KRAS* and *EGFR* mutations can be performed routinely on cytological specimens from EUS and EBUS guided FNA. Molecular analysis could be performed in 77% of the lung adenocarcinomas found in these cytological samples. With this paper we hope to increase awareness of these techniques and show that also in daily clinical practice EGFR and KRAS analysis can be performed in a high percentage of patients.

References

1. Rosell R, Moran T, Queralt C et al. Screening for Epidermal Growth Factor Receptor Mutations in Lung Cancer. The New England Journal of Medicine 2009; 361(10):958-967.

2. Shepherd FA, Tsao MS. Epidermal Growth Factor Receptor Biomarkers in Non-Small-Cell Lung Cancer: A Riddle, Wrapped in a Mystery, Inside an Enigma. Journal of Clinical Oncology 2010; 28(6):903-905.

3. Mok TS, Wu YL, Thongprasert S et al. Gefitinib or carboplatin-paclitaxel in pulmonary adenocarcinoma. N Engl J Med 2009; 361(10):947-957.

4. Riely GJ, Marks J, Pao W. KRAS mutations in non-small cell lung cancer. Proc Am Thorac Soc 2009; 6(2):201-205.

5. Takeda M, Okamoto I, Fujita Y et al. De Novo Resistance to Epidermal Growth Factor Receptor-Tyrosine Kinase Inhibitors in EGFR Mutation-Positive Patients with Non-small Cell Lung Cancer. Journal of Thoracic Oncology 2010; 5(3):399-400.

6. Schuurbiers OCJ, Kaanders JH, van der Heijden HF et al. The PI3-K/AKT-pathway and radiation resistance mechanisms in non-small cell lung cancer. J Thorac Oncol 2009; 4(6):761-767.

7. Micames CG, McCrory DC, Pavey DA et al. Endoscopic ultrasound-guided fine-needle aspiration for non-small cell lung cancer staging: A systematic review and metaanalysis. Chest   2007; 131(2):539-548.

8. Varela-Lema L, Fernandez-Villar A, Ruano-Ravina A. Effectiveness and safety of endobronchial ultrasound-transbronchial needle aspiration: a systematic review. Eur Respir J 2009; 33(5):1156-1164.

9. Wallace MB, Pascual JM, Raimondo M et al. Minimally invasive endoscopic staging of suspected lung cancer. JAMA 2008; 299(5):540-546.

10. De Leyn P, Lardinois D, Van Schil PE et al. ESTS guidelines for preoperative lymph node staging for non-small cell lung cancer. Eur J Cardiothorac Surg 2007; 32(1):1-8.

11. Silvestri GA, Gould MK, Margolis ML et al. Noninvasive Staging of Non-small Cell Lung Cancer: ACCP Evidenced-Based Clinical Practice Guidelines (2nd Edition). Chest 2007; 132(3_suppl):178S-201.

12. Szlubowski A, Zielinski M, Soja J et al. A combined approach of endobronchial and endoscopic ultrasound-guided needle aspiration in the radiologically normal mediastinum in non-small-cell lung cancer staging -- a prospective trial. 2010.

13. Travis WD, Rekhtman N, Riley GJ et al. Pathologic Diagnosis of Advanced Lung Cancer Based on Small Biopsies and Cytology: A Paradigm Shift. Journal of Thoracic Oncology 2010; 5(4):411-414.

14. Schmid K, Oehl N, Wrba F et al. EGFR/KRAS/BRAF mutations in primary lung adenocarcinomas and corresponding locoregional lymph node metastases. Clinical Cancer Research 2009; 15(14):4554-4560.

15. Garcia-Olive I, Monso E, Andreo F et al. Endobronchial ultrasound-guided transbronchial needle aspiration for identifying EGFR mutations. Eur Respir J 2010; 35(2):391-395.

16. Nakajima T, Yasufuku K, Suzuki M et al. Assessment of epidermal growth factor receptor mutation by endobronchial ultrasound-guided transbronchial needle aspiration. Chest 2007; 132(2):597-602.

17. Tol J, Dijkstra JR, Vink-Borger ME et al. High sensitivity of both sequencing and real-time PCR analysis of KRAS mutations in colorectal cancer tissue. J Cell Mol Med 2009; epub; DOI 10.1111/j.1582-4934.2009.00788.x.

18. Yamamoto H, Toyooka S, Mitsudomi T. Impact of EGFR mutation analysis in non-small cell lung cancer. Lung Cancer 2009; 63(3):315-321.

19. Dahabreh IJ, Linardou H, Siannis F et al. Somatic EGFR mutation and gene copy gain as predictive biomarkers for response to tyrosine kinase inhibitors in non-small cell lung cancer. Clin Cancer Res 2010; 16(1):291-303.

Chapter **8**

Summary and general discussion

Summary

Lung cancer is one of the most lethal forms of cancer. Most patients have advanced disease at presentation resulting in 5-year survival rates of only 16%. The most important prognostic indicator still is the TNM classification. However this classification does not provide information about biological behavior of tumors and differences in relapse rates within stage groups. Histology has an important role in tumor behavior and treatment outcome of subgroups of non-small cell lung carcinoma (NSCLC) patients. In this thesis, the tumor microenvironment, in specific hypoxia- and glycolysis related markers, in relation to imaging with ^{18}FDG-PET were examined with special interest in histology specific features. In the field of pulmonary medicine endosonography has proven its role in mediastinal staging of lung cancer patients. The value of endoscopic ultrasound guided fine needle aspiration (EUS-FNA) for the detection of left adrenal gland (LAG) metastases, a predilection site, was examined. Furthermore the role of endosonography in molecular analysis of EUS-FNA or endobronchial ultrasound guided transbronchial needle aspirations (EBUS-TBNA) specimens was studied.

Radiation resistance mechanisms in non-small cell lung cancer

The phosphatidylinositol-3-kinase (PI3-K)/protein kinase B (AKT) pathway is associated with all three major radiotherapy resistance mechanisms in NSCLC: intrinsic radiosensitivity, tumor proliferation and tumor cell hypoxia, which are described in **chapter 2**. The PI3-K/AKT signaling pathway is a key regulator of normal and cancerous growth and cell fate decisions such as proliferation, invasion, apoptosis, and induction of hypoxia-related proteins. Expression of pAKT is an independent prognostic indicator of clinical outcome in retrospective lung cancer studies. Activation of this pathway can be the result of stimulation of receptor tyrosine kinases (such as epidermal growth factor (EGFR) or vascular endothelial growth factor (VEGF)) or mutations or amplifications of PI3-K or AKT itself. Furthermore this cascade can be upregulated by radiotherapy. Data on treatment modulating hypoxia in NSCLC are limited. Blocking the PI3-K/AKT pathway through EGFR inhibition improves radiosensitivity and can affect tumor growth by various mechanisms such as inhibition of neo-angiogenesis via VEGF. Besides this, EGFR-independent activation of PI3-K/AKT commonly occurs leading to treatment resistance. Further prospective studies are needed to quantify the activation status of this pathway which may help to select patients who could benefit from combining targeted therapy with radiotherapy or chemotherapy.

Histology-specific glucose metabolism and the tumor microenvironment in relation to ^{18}FDG-PET

Tumor cells predominantly rely on glycolysis with the production of lactate instead of mitochondrial oxidation even in the presence of oxygen (Warburg effect or aerobic glycolysis). To support the necessary high rate of glycolysis an increased transport of glucose

is needed which is facilitated by upregulation of glucose transporters (GLUT). To counteract cellular acidification upregulation of monocarboxylate transporters (MCT) and carbonic anhydrase IX (CAIX) are needed for subsequent lactate and H+ transport out of the cell. GLUT, MCT and CAIX are all mediated by the hypoxia-inducible factor 1 (HIF-1) pathway in hypoxic conditions. In **chapter 3 and 4** differences in glucose metabolism in adeno- and squamous cell NSCLCs were quantified using the hypoxia and glycolysis-related markers GLUT1, CAIX, MCT1, MCT4 as well as [18]fluoro-2-deoxyglucose positron emission tomography ([18]FDG-PET) imaging. Furthermore, the spatial distribution of these markers in relation to the tumor vasculature was examined. In 111 patients with a curative resection for stage I, II or IIIa NSCLC, pre-treatment [18]FDG uptake was quantified by calculating maximum standardized uptake value (SUVmax) and total lesion glycolysis (TLGmax). Metabolic marker expression, measured by immunofluorescent staining and qPCR and vascular density were determined in 90 fresh frozen tumor resection specimens and patients were retrospectively evaluated for disease free survival. mRNA and protein expression of metabolic markers, except MCT4, and [18]FDG-uptake were higher in squamous cell NSCLC than in adenocarcinomas and adenocarcinomas were better vascularized. In squamous cell carcinoma GLUT and MCT4 expression increased with increasing distance from the vasculature whereas in adenocarcinomas upregulation of MCT4 was already found at closer distance from the vessels. Adenocarcinomas had a worse disease free survival (DFS) compared to squamous cell carcinomas (p=0.016). High glucose consumption assessed by GLUT1, SUVmax or TLGmax was associated with a worse DFS only in adenocarcinomas. Our findings suggest a different metabolism for adeno and squamous cell NSCLC and indicate that adenocarcinomas exhibit glycolysis under normoxic conditions close to the vessels whereas squamous cell carcinomas are exposed to diffusion-limited hypoxia resulting in a very high anaerobic glycolytic rate. Although squamous cell NSCLCs have a higher [18]FDG-uptake, generally considered as a poor prognostic factor, adenocarcinomas had a higher metastatic potential and a worse DFS. The prognostic potential of [18]FDG-PET should be interpreted in relation to histology in NSCLC.

Nuclear imaging as a tool in distinguishing synchronous tumors from metastatic disease

In **chapter 5** the potential of [18]FDG-PET to discriminate metastatic disease from second primary lung tumors was investigated. A simultaneous second primary lung cancer occurs in 1-8% of lung cancer patients. Second primary cancers presenting in lung cancer patients are often (70%) tobacco related, including the upper aero digestive tract, the uroepithelium and colorectum. We hypothesized that SUVs of metastatic tumors in the lung approach the SUV of the primary tumor and that SUVs from two primary tumors differ to a greater extend. We found a significantly larger delta SUV between two tumors in patients presenting with synchronous primary cancers as compared to patients with metastatic disease involving the lungs. For the optimal cut-off of delta SUV=41%, both sensitivity and specificity were 81%. The odds of a second primary was 18.4 times higher in patients with a delta SUV >41%. This

suggests that SUVs from ^{18}FDG-PET images can be helpful in differentiating metastatic disease from second primary tumors in patients with synchronous pulmonary lesions.

Endosonography as a diagnostic tool in lung cancer patients and possibilities for guiding individualized treatment

In patients with lung cancer enlarged or ^{18}FDG-PET positive adrenal glands are suspect for distant metastasis. The positive predictive value of CT (62%) and ^{18}FDG-PET (82%) are limited. To prevent that patients are withheld a possible curative treatment, tissue proof is needed. The aim of the study described in **chapter 6** was to assess the sensitivity of EUS-FNA for left adrenal gland (LAG) metastases in lung cancer patients with a suspect LAG based on imaging. In a group of 85 patients the incidence of a LAG metastasis was 62%. Benign adrenal tissue was found in 29% of patients. Sensitivity for the detection of LAG metastasis and negative predictive value for EUS-FNA were at least 86% and 70% respectively. EUS-FNA is considered a sensitive, safe and minimally invasive technique for the detection of left adrenal metastases in NSCLC patients with a suspect (enlarged and/or ^{18}FDG-PET positive) LAG based on imaging.

Molecular diagnostics

In lung cancer treatment molecular testing for epidermal growth factor *(EGFR)* and *KRAS* mutations is of increasing importance to guide targeted therapy. Endosonography has proven to be of importance, and has been widely implemented in lung cancer diagnosis and staging. For this reason we examined the diagnostic yield and applicability of molecular testing for *KRAS* and *EGFR* mutations in cytological specimens obtained by EUS-FNA or EBUS-TBNA. This is described in **chapter 7**. Patients with EUS- or EBUS-guided FNA for lung adenocarcinoma were selected. Both smears and cellblocks were considered suitable for molecular analysis when >40% of the aspirated cells were tumor cells. The average amount of tumor cells in 35 patients was 72% ± 23%. Molecular analysis could be reliably performed in 77% of patients. Mutation analysis showed *KRAS* in 37% and *EGFR* in 7% of patients. Thus, molecular analysis for *KRAS* and *EGFR* mutations can be performed in cytological specimens from EUS- and EBUS-guided FNA.

General discussion

This thesis is the result of collaboration between different disciplines: radiation oncology, nuclear medicine, pathology, genetics and pulmonary medicine. The studies focus on tumor microenvironment and especially markers of glucose metabolism reflecting the microenvironment, FDG-PET imaging was applied as a biomarker, reflecting the tumor as a whole but at the expense of spatial resolution. Together, these approaches provide information on tumor metabolism in a complimentary way. Differences in tumor microenvironment, imaging and histology have been demonstrated, which pose questions for further research. Another challenge is to derive pathologic and molecular information from cytological specimens, obtained by minimally invasive procedures. This thesis supplies new information on multimodality diagnostics, taking another step towards personalizing treatment of lung cancer patients.

Hypoxia and tumor glucose metabolism

Warburg was the first who observed aerobic glycolysis as a characteristic of cancer cells more than 80 years ago. It has long been regarded as a primitive and insufficient manner for tumor cells to produce their energy and it was believed that it arose from mitochondrial defects in their inability to effectively oxidize glucose.[1] Advances in cancer metabolism research however have shown how aerobic glycolysis supports the anabolic requirements associated with cell growth and proliferation.[2, 3]

Non-proliferating differentiated cells rely on oxidative phosphorylation to produce ATP. In conditions with limited growth factor en nutrient supplies these cells adopt a catabolic metabolism focused on maximizing ATP production: lipids and amino acids are used for energy production if enough oxygen is available and neglected cells will undergo autophagy. In the presence of abundant nutrients and growth factor stimulation cells adapt an anabolic metabolism with production of lipids, proteins and nucleotide synthesis. Cancer cells can also use strategies to decrease ATP production while increasing ATP consumption, which is necessary to sustain glycolytic flux. In cancer cells, signaling pathways downstream of growth factor receptors can be constitutively activated in the absence of extracellular growth factors. Traditionally, in response to growth factor signaling, increased transcription and translation decreases ATP: ADP ratio with subsequent glucose uptake for glycolysis and oxidative phosphorylation. Nowadays, strong evidence supports the hypothesis that growth factor signaling directly influences glucose uptake leading to biomass production and transcription/translation independent of ATP availability. Proliferating cells do use their mitochondria and still derive a fraction of ATP through oxidative phosphorylation but mitochondrial enzymes are abundantly used for synthesis of anabolic precursors.[2]

Most proto-oncogenes and tumor suppressor genes encode components of signaling pathways. Their role in carcinogenesis has traditionally been attributed to their ability to

regulate the cell cycle and sustain proliferative signaling; altered metabolism was seen as an adaptation to meet the increased anabolic demands of a proliferating cell. Metabolites themselves however can be oncogenic by altering cell signaling and blocking cellular differentiation. Altered metabolism has attained the status of a core hallmark of cancer.[2]

This thesis offers new insight in differences in glucose metabolism between different histologies. Adenocarcinomas seem to exhibit glycolysis under normoxic conditions close to the vessels whereas squamous cell carcinomas are exposed to diffusion-limited hypoxia resulting in a high anaerobic glycolytic rate. The adenocarcinomas had a worse disease free survival and a higher metastatic potential. The question remains why squamous cell carcinomas with a high rate of glucose metabolism had a more favorable prognosis as compared to adenocarcinomas. High MCT4 expression and resulting lactate levels in the proximity of the vessels, which was seen in the adenocarcinomas, may create a tumor microenvironment that is favorable for tumor cell migration.

Molecular imaging

Molecular imaging technologies, such as PET using [18]FDG, enable noninvasive metabolic marker detection. The higher rate of glycolysis and subsequent higher glucose uptake by tumor cells is one of the reasons why [18]FDG-PET is useful as an imaging biomarker in solid tumors.[4] As [18]FDG uptake in tumor cells is multifactorial, high [18]FDG uptake, however, is not a direct surrogate marker for tissue hypoxia. This might be true when under hypoxic conditions aerobic glycolysis (Pasteur effect) leads to more glucose uptake by GLUT transporters, but enhanced glucose uptake could also be linked to regions with high proliferation and thus high energy demands.[4] Furthermore, glycolysis under normoxic conditions is a hallmark of malignant tumors.

The advantage of [18]FDG-PET lies in the fact that it has become a well-established tool in cancer diagnosing and staging. [18]FDG-PET has proven its great clinical value in the work up of NSCLC. It has been widely implemented in staging algorithms. The rate of detection of unanticipated metastases has been reported up to 18% in clinical stage I and II patients.[5] Its value as a prognostic indicator in NSCLC is also clear. High [18]FDG uptake is associated with worse survival in NSCLC.[6, 7, 8]

This thesis demonstrates that [18]FDG uptake was higher in squamous cell carcinomas when compared to adenocarcinomas. Adenocarcinomas however had a worse prognosis with a similar [18]FDG -uptake. Interpretation of [18]FDG -PET in relation to glucose metabolism, prediction of prognosis and exploitation in treatment strategies, should therefore be done in relation to histology. Furthermore, [18]FDG-PET can be a valuable tool in discriminating between metastasis and second primary tumors. Assuming that tumors with a shared clonal origin (as in metastases) often behave similarly and have common histological features, [18]FDG-uptake could help characterize synchronous pulmonary lesions. In our cohort a certain cut-off value enabled us to distinguish between different tumors. In future studies this could be prospectively validated by comparison with tissue samples.

Patients with an enlarged [18]FDG-PET positive LAG had a great likelihood of adrenal metastases. Yet, to avoid that patients are withheld possible curative treatment tissue proof is warranted. In this cohort with a high chance of malignancy we found LAG metastases in 62% of patients using EUS-FNA. In this study not all patients underwent [18]FDG-PET in the workup. It could be of interest to apply measurement of deltaSUV between LAG lesions and the primary tumor in future research.

Nowadays, research is focused on the value of [18]FDG-PET in predicting therapy response and treatment outcome. The challenge lays in predicting response early during treatment when treatment schedules can be adjusted on an individual patient basis to reduce unnecessary toxicity or switch to other strategies.

Minimal invasive staging techniques

Endosonography has proven its usefulness in diagnosis and staging lung cancer patients. EUS was commercially first available in 1998 and EBUS in 2004 and already they are crucial in lung cancer staging algorithms. A lot of research has been done and their value has been proven in lymph nodes identified as pathological by radiologic or nuclear imaging (enlarged or [18]FDG-PET positive) and small or [18]FDG-PET negative nodes. Also, results have been compared to cervical mediastinoscopy for EUS alone, EBUS alone or combined ultrasound. A systematic review and meta-analysis on EUS in mediastinal staging showed a sensitivity of 90% and NPV of 78% in pathologically enlarged lymph nodes (>1cm). For smaller lymph nodes this was 58% and 81% respectively.[9] Meta-analyses on EBUS have shown a sensitivity of 85-93%.[10, 11, 12] Combining EBUS and EUS was sensitive in 93% with a NPV of 97% which is very high when compared to a NPV of 89% for mediastinoscopy which has been considered the gold standard.[13] In the radiological normal mediastinum this was 68-76% and 91-94% respectively.[14]

The ASTER trial (prospective multicenter randomized trial) compared cervical mediastinoscopy with combined EUS and EBUS (CUS) versus cervical mediastinoscopie (CM) alone in patients with lung cancer and enlarged or PET positive mediastinal/hilar nodes or a centrally located tumor. Sensitivity for the detection of mediastinal metastases was 80% for CM and 94% for CUS (p=0.04) with a NPV of 86% for CM and 93% for CUS. The number of futile thoracotomies was lower in the CUS arm (7% v 18%, p=0.009) and complications were comparable. The number needed to treat, to detect mediastinal metastases with CM after a negative CUS, was 11.[15]

Other indications are diagnosing primary tumors in lung cancer patients,[16, 17] diagnosing metastases of other solid tumors and,[18] as is shown in this thesis, the detection of LAG metastases. In patients with enlarged and/or PET positive LAG a metastasis of lung cancer was proven in 62% of patients, in 2% another malignancy was found and 29% had benign adrenal tissue. In 5.9% FNA was non-diagnostic. EUS-FNA of the LAG was proven to be a safe and minimally invasive method for the detection of LAG metastases.

Molecular diagnostics and targeted therapy

In the last decade progress has been made in systemic treatment for NSCLC. Treatment approaches are becoming more individualized tailored therapies, which is especially the case for adenocarcinoma or large cell carcinoma. Emerging evidence suggests that histology might be prognostic or predictive of clinical outcome as was reviewed by Hirsh and coworkers.[19] A consistent link between histology and treatment outcome was established for EGFR kinase inhibitors.[19] Significant differences in survival with respect to histology have also been shown in first line chemotherapy with pemetrexed.[20] Recently, treatment standards for NSCLC have shifted from one based on histology to one that incorporates molecular subtypes. This is especially the case for lung adenocarcinomas. Driver mutations that result in constitutionally active mutant proteins mostly occur in oncogenes such as EGFR HER2KRAS, ALK, BRAF, PIK3CA, AKT1, ROS1, NRAS and MAP2K1. Driver mutations are mutually exclusive except for PIK3CA, which can occur together with EGFR or KRAS mutations. Lung adenocarcinomas carrying these driver mutations are sensitive to various targeted therapies leading to substantial clinical benefit.[21] Examples are tyrosine kinase inhibitors like gefitinib and erlotinib in EGFR positive patients and crizotinib in patients with EML4-ALK or ROS1 fusions.[19, 22]

To date half of all NSCLCs harbor no known clinically relevant oncogenic driver.[21] During the last decade new targets in NSCLC have emerged but very few advances were made in squamous cell lung cancer (SCC). First line chemotherapy still is the standard treatment in SCC. Potential future molecular targets in SCC are fibroblast growth factor receptor 1 (FGFR1 22% of SCC), discoidin domain receptor 2 (DDR2 4%), BRAF (2%), PIK3CA (mutations 2-3 % and 33% amplification), AKT1 (1%), MET (1%), EML4-ALK fusion (1%).[23]

During treatment drug resistance invariably emerges. In 37 patients with an EGFR mutation treated with EGFR TKis and acquired drug-resistance repeat biopsies were performed. All tumors retained their activating EGFR mutations and some acquired known mechanisms of resistance including *EGFR* T790M mutation or *MET* gene amplification or others like mutations in the *PIK3CA* gene. In 14% of cases histology transformed to small cell lung cancer (SCLC) sensitive to normal cytotoxic treatment.[24] When progression is seen on repeat imaging it is important to question whether the tumor has become resistant to the current target inhibition and this may demand repeat tissue to guide further treatment decisions.

Most molecular analyses are performed on histological material. The challenge lays in improvement of techniques that are suitable for cytology as in patients with advanced NSCLC this is often what is available. When new material is needed repeat minimally invasive exams like EUS, EBUS or ultrasound or CT guided punctures are relative patient friendly methods. In this thesis it was shown that samples obtained with EUS or EBUS were suitable for molecular analysis in 77% of cases. Further insight in metabolic cancer processes offers the opportunity to selectively target altered metabolism pathways.

Future prospects

This thesis reflects a multidisciplinary attitude in research concerning tumor metabolism and also a personal interest in endosonography as an interventional and oncologic pulmonary physician. The strength in future research lays in this multidisciplinary commitment where non-invasive and invasive techniques meet. Future research could continue to explore differences in metabolism in adeno and squamous cell lung cancer. Non-invasive measurement of tissue lactate in the same group of NSCLC patients could help us to further substantiate our hypothesis that adenocarcinomas rely on aerobic glycolysis with up regulation of MCT4 near the vessels. One would expect that higher lactate levels possibly lead to a greater metastatic potential. Quantification of ^{18}FDG-PET uptake in adenocarcinomas and squamous cell carcinomas in relation to the effect of adjuvant chemotherapy treatment could be an interesting question of a national prospective adjuvant chemotherapy study in operated NSCLC patients (NVALT 8). The difference shown in ^{18}FDG-PET uptake between synchronous primary tumors and metastases in a retrospective analysis could be prospectively validated in a study in which ^{18}FDG-PET and histology are compared. This could also be done for NSCLC patients suspected of LAG metastases. The value of ^{18}FDG-PET as a predictive factor in patients with stage III NSCLC treated with concurrent chemoradiotherapy early during treatment is currently investigated in a prospective study (early response measurement in NSCLC).

References

1. Warburg O, Posener K, Negelein E. Ueber den stoffwechsel der tumoren. In: Warburg O, editor. Constable, London; 1930.

2. Ward PS, Thompson CB. Metabolic reprogramming: a cancer hallmark even Warburg did not anticipate. Cancer Cell 2012;21:297-308.

3. Teicher BA, Linehan WM, Helman LJ. Targeting cancer metabolism. Clinical Cancer Research 2012;18:5537-5545.

4. Busk M, Horsman MR, Jakobsen S, et al. Cellular uptake of PET tracers of glucose metabolism and hypoxia and their linkage. Eur J Nucl Med Mol Imaging. 2008;35:2294-2303.

5. Silvestri GA, Gould MK, Margolis ML et al. Noninvasive staging of non-small cell lung cancer: ACCP evidenced-based clinical practice guidelines (2nd edition). Chest 2007;132:178S-201S.

6. Vansteenkiste JF, Stroobants SG, Dupont PJ, De Leyn PR, Verbeken EK, Deneffe GJ, et al. Prognostic importance of the standardized uptake value on (18)F-fluoro-2-deoxy-glucose-positron emission tomography scan in non-small cell lung cancer: an analysis of 125 cases. Leuven Lung Cancer Group. J Clin Oncol 1999;17:3201-3206.

7. de Geus-Oei LF, van der Heijden HF, Corstens FH, et al. Predictive and prognostic value of FDG-PET in nonsmall-cell lung cancer: a systematic review. Cancer 2007;110:1654-1664.

8. Liao S, Penney BC, Wroblewski K, et al. Prognostic value of metabolic tumor burden on 18F-FDG PET in nonsurgical patients with non-small cell lung cancer. Eur J Nucl Med Mol Imaging 2012;39:27-38.

9. Micames CG, McCrory DC, Pavey DA, Jowel PS, Gress FG. Endoscopic ultrasound-guided fine-needle aspiration for non-small cell lung cancer staging. A systematic review and meta-analysis. Chest 2007;131:539-548.

10. Gu P, Zhao YZ, Jiang, LY, Zhang W, Xin Y, Han BH. Endobronchial ultrasound-guided transbronchial needle aspiration for staging of lung cancer: a systematic review and meta-analysis. Eur J Cancer 2009;45:1389-1396.

11. Adams K, Shah PL, Edmonds L, Lim E. Test performance of endobronchial ultrasound and transbronchial needle aspiration biopsy for mediastinal staging in patients with lung cancer: systematic review and meta-analysis. Thorax 2009;64:757-762.

12. Varela-Lema L, Fernandez-Villar A, Ruano-Ravina A. Effectiveness and safety of endobronchial ultrasound-transbronchial needle aspiration: a systematic review. Eur Respir J 2009;33:1156-1164.

13. Wallace MB, Pascual JM, Raimondo M, Woodward TA, McComb BL, Crook JE, et al. Minimally invasive endoscopic staging of suspected lung cancer. JAMA 2008;299:540-546.

14. Szlubowski A, Zielinski M, Soja J, Annema JT, Sosnicki W, Jakubiak M, et al. A combined approach of endobronchial and endoscopic ultrasound-guided needle aspiration in the radiologically normal mediastinum in non-small cell lung cancer staging: a prospective trial.

Eur J Cardiothorac Surg 2010;37:1175-1179.

15. Annema JT, van Meerbeeck JP, Rintoul RC, Dooms C, DeschepperE, de Leyn P, et al. Mediastinoscopy vs endosonography for mediastinal nodal staging of lung cancer: a randomized trial. JAMA 2010;304:2245-2252.

16. Annema JT , Veseliç M, Rabe KF. EUS-guided FNA of centrally located lung tumours following a non-diagnostic bronchoscopy. Lung Cancer 2005;48:357-61.

17. Tournoy KG, Rintoul RC, van Meerbeeck JP, Carrol NR, Praet M, Buttery RC, et al. EBUS-TBNA for the diagnosis of central parenchymal lung lesions not visible with a routine bronchoscopy. Lung Cancer 2009;63:45-49.

18. Peric P, Schuurbiers OCJ, Veseliç M, Rabe KF, van der Heijden HFM, Annema JT. Transoesophageal endoscopic ultrasound-guided fine-needle aspiration for the mediastinal staging of extrathoracic tumors: a new perspective. Ann Oncol 2010;21:1468-1471.

19. Hirsch FR, Spreafico A, Novello S, et al. The prognostic and predictive role of histology in advanced non-small cell lung cancer: a literature review. J Thorac Oncol. 2008;3:1468-1481.

20. Al-Saleh K, Quinton C, Ellis PM. Role of pemetrexed in advanced non-small-cell lung cancer: meta-analysis of randomized controlled trials, with histology subgroup analysis. Curr Oncol. 2012;19:e9-e15.

21. Pao W, Hutchinson KE. Chipping away at the lung cancer genome. Nature Medicine 2012;18:349-351.

22. Kwak EL, Bang YJ, Camidge DR, Shaw AT, Solomon B, Maki RG, et al. Anaplastic lymphoma kinase inhibition in non-small cell lung cancer. NEJM 2010;363:1693-1703.

23. Perez Moreno P, Brambilla E, Thomas R, Soria JC. Squamous cell carcinoma of the lung: molecular subtypes and therapeutic opportunities. Clin Cancer Rese 2012;18:2443-2451.

24. Sequist LV, Waltman BA, Diad-Santagata D, Digumarthy S, Turke AB, Fidias P et al. Genotypic and histological evaluation of lung cancers acquiring resistance to EGFR inhibitors. Sci Transl Med 2011;3:75ra26.

Chapter 9

Samenvatting en discussie

Samenvatting

Longkanker is één van de meest dodelijke vormen van kanker. De meeste patiënten hebben een gevorderd stadium bij presentatie resulterend in een 5-jaars overleving van slechts 16%. De TNM classificatie is tot heden nog steeds de belangrijkste prognostische indicator. Deze classificatie biedt echter geen informatie over biologisch gedrag van tumoren en geeft geen verklaring voor de kans op recidief binnen een groep patiënten in een bepaald ziektestadium. Histologie speelt een belangrijke rol met betrekking tot het gedrag van de tumor en het resultaat van de behandeling in subgroepen van patiënten met niet-kleincellige longkanker (NSCLC). In dit proefschrift werden facetten van het tumor micromilieu bestudeerd die van belang zijn bij radio- en chemotherapieresistentie. Het ging hierbij vooral om hypoxie- en glycolyse gerelateerde markers, in relatie tot beeldvorming met ^{18}FDG-PET en histologie. Binnen de longziekten heeft endo-echografie haar rol bewezen in de mediastinale diagnostiek van longkankerpatiënten. De waarde van endo-echografie begeleide fijne naald aspiratie (EUS-FNA) bij het opsporen van metastasen in de linker bijnier (LAG), een voorkeursplaats voor metastasering van longkanker, werd onderzocht. Bovendien werd de rol van endo-echografie met betrekking tot moleculaire analyse van materiaal verkregen met EUS-FNA of endobronchiale echografie begeleide transbronchiale naald aspiraties (EBUS-TBNA) bestudeerd.

Radiatie resistentiemechanismen bij het niet-kleincellige longcarcinoom

De phosphatidylinositol-3-kinase (PI3-K) / proteïne kinase B (AKT) pathway is gerelateerd aan drie belangrijke radiotherapie resistentie mechanismen in NSCLC: intrinsieke stralingsgevoeligheid, tumor proliferatie en tumorcel hypoxie. Dit wordt beschreven in **hoofdstuk 2**. De PI3-K/AKT signalering pathway speelt een zeer belangrijke rol bij de regulering van normale en kwaadaardige groei en bij processen in de cel leidend tot proliferatie, invasie, apoptosis en inductie van hypoxie gerelateerde eiwitten. Expressie van pAKT is een onafhankelijke prognostische indicator in retrospectieve longkanker studies. Activering van deze pathway kan worden veroorzaakt door stimulatie van receptor tyrosine kinases (zoals epidermale groeifactor (EGFR) of vascular endothelial growth factor (VEGF)) of mutaties danwel amplificaties van PI3-K of AKT. Bovendien kan deze cascade worden gestimuleerd door radiotherapie. Gegevens over therapieën gericht op modulatie van hypoxie zijn beperkt bij longkanker patiënten. Blokkade van de PI3-K/AKT pathway door EGFR inhibitie verbetert de stralingsgevoeligheid en kan de groei van de tumor beïnvloeden door verschillende mechanismen zoals remming van neo-angiogenese onder invloed van VEGF. Daarnaast treedt EGFR onafhankelijke activering van PI3-K/AKT geregeld op leidend tot therapieresistentie. Er zijn prospectieve studies nodig die de activeringsstatus van deze pathway kwantificeren en die kunnen helpen bij de selectie van patiënten die mogelijk profiteren van 'targeted therapy' in combinatie met radiotherapie of chemotherapie.

Histologie specifiek glucose metabolisme en tumor micromilieu in relatie tot [18]FDG-PET

De activeringsstatus van PI3-K/AKT wordt beïnvloed door verschillende aspecten van het tumor micromilieu zoals de beschikbaarheid van zuurstof en nutriënten. Tumorcellen maken voornamelijk gebruik van glycolyse (hetgeen leidt tot productie van lactaat) in plaats van mitochondrieële oxidatie, zelfs in aanwezigheid van zuurstof (Warburg effect of aërobe glycolyse). Om voldoende energie te verkrijgen, is een hoge mate van glycolyse nodig en dus een verhoogde behoefte aan glucosetransport. Dit wordt ondersteund door opregulatie van glucose transporters (GLUT). Om vervolgens cellulaire verzuring tegen te gaan is opregulatie van monocarboxylate transporters (MCT) en koolzuuranhydrase IX (CAIX) nodig voor transport van lactaat en H+ de cel uit. GLUT, MCT en CAIX worden gereguleerd door de hypoxia-inducible factor 1 (HIF-1) pathway onder hypoxische omstandigheden. In **hoofdstuk 3 en 4** zijn verschillen in glucose metabolisme in adeno- en plaveiselcel longcarcinomen gekwantificeerd aan de hand van hypoxie en glycolyse gerelateerde markers GLUT1, CAIX, MCT1, MCT4 en [18]fluoro-2-deoxyglucose positron emissie tomografie ([18]FDG-PET). Bovendien werd de aanwezigheid van deze markers in relatie tot de tumor vascularisatie onderzocht. Bij 111 patiënten met een curatieve resectie voor stadium I, II of IIIa NSCLC werd de diagnostische [18]FDG-opname gekwantificeerd door het berekenen van de maximale gestandaardiseerde opname (SUVmax) en de totale lesie glycolyse (TLGmax). Metabole marker expressie, gemeten met immunofluorescentie en qPCR en vasculaire dichtheid werden bepaald in 90 fresh frozen tumor resectie preparaten en patiënten werden retrospectief geëvalueerd voor ziekte vrije overleving. mRNA en eiwit expressie van metabole markers, met uitzondering van MCT4, en [18]FDG-opname waren hoger bij longkanker patiënten met een plaveiselcelcarninoom dan met een adenocarcinoom. Adenocarcinomen waren rijker gevasculariseerd. In plaveiselcelcarcinoom nam de expressie van GLUT en MCT4 toe met toenemende afstand van de vasculatuur terwijl in de adenocarcinomen opregulatie van MCT4 juist op kortere afstand van de vaten aanwezig was. Patiënten met een adenocarcinoom hadden een slechtere overleving (DFS) in vergelijking tot patiënten met een plaveiselcelcarcinoom (p = 0.016). Hoge glucose consumptie, vastgesteld met GLUT1, SUVmax of TLGmax was alleen bij patiënten met een adenocarcinoom geassocieerd met een slechtere overleving (DFS). Onze bevindingen suggereren een verschil in metabolisme tussen adeno- en plaveiselcel longcarcinomen en doen vermoeden dat adenocarcinomen gebruik maken van glycolyse in de nabijheid van de vaten onder normoxische omstandigheden en dat plaveiselcel carcinomen blootstaan aan diffusie gelimiteerde hypoxie resulterend in een hoge anaerobe glycolyse. Hoewel plaveiselcel carcinomen een hogere [18]FDG-opname lieten zien wat over het algemeen beschouwd wordt als een slechte prognostische factor, hadden patiënten met een adenocarcinoom vaker metastasen en een slechtere overleving (DFS) in deze studie. Dit suggereert dat de prognostische waarde van [18]FDG-PET moet worden geïnterpreteerd in relatie tot histologie in niet-kleincellige longkanker patiënten.

Nucleaire beeldvorming bij het onderscheiden van synchrone tumoren en gemetastaseerde ziekte.

De rol van [18]FDG-PET bij de discriminatie van gemetastaseerde ziekte en tweede primaire longkanker tumoren werd onderzocht in **hoofdstuk 5**. Een synchrone tweede primaire longkanker treedt op bij 1-8% van de longkankerpatiënten. Tweede primaire kankers in longkankerpatiënten zijn vaak (70%) tabak gerelateerd en behelzen tumoren van de bovenste luchtwegen en spijsverteringskanaal, urinewegen en darmkanker. Onze hypothese was dat SUV waardes van gemetastaseerde tumoren in de long de SUV waarde van de primaire tumor zou benaderen en dat SUV waardes van twee primaire tumoren in een grotere mate verschillend zouden zijn (delta SUV). We vonden een aanzienlijk grotere delta SUV tussen twee tumoren bij patiënten die zich presenteerden met synchrone primaire kanker in vergelijking tot patiënten met longmetastasen. Voor de optimale cutt-of waarde van delta SUV zijnde 41%, was de gevoeligheid en specificiteit 81%. De kans op een tweede primaire tumor was 18.4 keer hoger bij patiënten met een delta SUV > 41%. Dit suggereert dat SUV waardes verkregen middels [18]FDG-PET van waarde kunnen zijn bij het onderscheiden van gemetastaseerde ziekte en tweede primaire tumoren bij patiënten met synchrone long laesies.

De rol van endo-echografie in de diagnostiek van longkankerpatiënten en de mogelijkheden voor therapie op maat.

Vergrote of [18]FDG-PET positieve bijnieren bij patiënten met longkanker zijn verdacht voor metastasering. De positief voorspellende waarde van CT (62%) en [18]FDG-PET (82%) zijn beperkt. Om te voorkomen dat patiënten een mogelijk curatieve behandeling wordt onthouden is weefsel bewijs nodig. Het doel van de studie omschreven in **hoofdstuk 6** was het bepalen van de sensitiviteit van EUS-FNA bij het aantonen van een metastase in de linker bijnier (LAG) bij longkankerpatiënten met een verdachte linker bijnier op de CT en/of [18]FDG-PET. In een groep van 85 patiënten was de incidentie van een linker bijnier metastase 62%. Goedaardig bijnier weefsel werd gevonden bij 29% van de patiënten. De sensitiviteit voor het aantonen van een metastase in de linker bijnier middels EUS-FNA en de negatief voorspellende waarde waren ten minste 86% en 70% respectievelijk. EUS-FNA wordt beschouwd als een sensitieve, veilige en minimaal invasieve techniek voor de detectie van linker bijnier metastasen in niet-kleincellige longkanker patiënten met een verdachte (vergrote en/of [18]FDG-PET positieve) linker bijnier.

Moleculaire diagnostiek

In de behandeling van longkankerpatiënten zijn moleculaire testen naar epidermale groeifactor *(EGFR)* en *KRAS* mutaties van toenemend belang voor targeted therapy. Endo-echografie heeft zijn waarde bewezen en is op grote schaal geïmplementeerd bij de diagnostiek en stadiering van longkankerpatiënten. Daarom onderzochten we in **hoofdstuk 7** de diagnostische opbrengst en de toepasbaarheid van moleculaire diagnostiek voor *KRAS*

en *EGFR* mutaties in cytologische monsters verkregen met EUS-FNA of EBUS-TBNA. Longkanker patiënten met een adenocarcinoom gediagnosticeerd met EUS of EBUS werden geselecteerd. Uitstrijkjes en cell blocks werden geschikt beschouwd voor moleculaire analyse wanneer > 40% van de cellen bestond uit tumorcellen. Het gemiddelde aantal tumorcellen in 35 patiënten was 72% ± 23%. Moleculaire analyse kon op betrouwbare wijze worden uitgevoerd bij 77% van de patiënten. Mutatie analyse toonde *KRAS* bij 37% en *EGFR* bij 7% van de patiënten. Moleculaire analyse naar *KRAS* en *EGFR* mutaties in cytologische monsters verkregen met EUS-FNA en EBUS-TBNA is haalbaar.

Algemene discussie

Dit proefschrift is het resultaat van een multidisciplinaire samenwerking tussen de afdelingen radiotherapie, nucleaire geneeskunde, pathologie, genetica, thoracale chirurgie en longziekten. De focus richt zich op het tumor micromilieu, met in het bijzonder glucose metabolisme, en FDG-PET als biomarker van de tumor op macroniveau waarmee complementaire informatie over het tumor metabolisme wordt verkregen. Tumor micromilieu, beeldvormende technieken en histologie komen samen en bieden een vertrekpunt voor verder onderzoek. Daarnaast werd onderzoek gedaan naar het verkrijgen van pathologische en moleculaire diagnostiek uit cytologische monsters, verkregen door minimaal invasieve procedures. Dit proefschrift draagt bij aan translationeel onderzoek en zet hopelijk een stap in de richting van (targeted/personalized) behandeling van longkankerpatiënten op maat.

Hypoxie en glucose metabolisme in de tumor

Meer dan 80 jaar geleden beschreef Warburg als eerste onderzoeker aërobe glycolyse als kenmerk van kankercellen. Lange tijd zag men dit als een primitieve en insufficiënte manier van energieproductie door tumorcellen en er werd verondersteld dat dit te maken had met een mitochondriale stoornis om effectief glucose te oxideren.[1] Onderzoek naar kanker metabolisme heeft aangetoond dat aërobe glycolyse nuttig is voor de verhoogde behoefte aan energie bij celgroei en proliferatie.[2, 3]

Normale niet delende cellen maken gebruik van oxidatieve fosforylatie voor de productie van ATP. Onder omstandigheden met een beperkte aanwezigheid van groeifactoren en voedingstoffen is er sprake van een katabole stofwisseling gericht op het verbeteren van ATP productie: lipiden en aminozuren worden gebruikt voor de energieproductie in aanwezigheid van voldoende zuurstof en gedepleerde cellen ondergaan autophagie. In aanwezigheid van een overvloed aan voedingsstoffen en groeifactoren is er een anabool metabolisme met de productie van lipiden, eiwitten en nucleotiden. Kankercellen zijn in staat ATP productie te verlagen terwijl de ATP consumptie toeneemt wat noodzakelijk is

voor het onderhouden van glucose influx. In kankercellen kunnen signalering pathways downstream van de groeifactor receptoren geactiveerd blijven in afwezigheid van extracellulaire groeifactoren. Er werd altijd gedacht dat er als gevolg van respons op groeifactoren een verhoogde transcriptie en translatie optreedt met daling van de ATP: ADP verhouding waardoor glucose opname plaatsvindt voor glycolyse en oxidatieve fosforylering. Er zijn inmiddels sterke aanwijzingen die de hypothese ondersteunen dat groeifactor signalering rechtstreeks leidt tot glucose opname en biomassaproductie, transcriptie en translatie onafhankelijk van de beschikbaarheid van ATP. Delende cellen gebruiken hun mitochondria deels voor het onttrekken van ATP door middel van oxidatieve fosforylering maar mitochondriale enzymen worden voornamelijk gebruikt voor de synthese van anabole precursors.[2]

De meeste proto-oncogenen en tumor suppressor genen coderen voor componenten van signalering pathways. Hun rol in de carcinogenese is traditioneel toegeschreven aan het vermogen om de celcyclus te reguleren en het onderhouden van proliferatieve signalering; wijzigingen in het metabolisme werden gezien als adaptatie aan de verhoogde anabole behoeften van een delende cel. Metabolieten zelf kunnen echter ook oncogeen zijn door verandering van de cel signalering en door blokkade van celdifferentiatie. Dit wordt tegenwoordig gezien als een wezenlijke eigenschap van kankercellen.[2]

Dit proefschrift biedt nieuwe inzichten in verschillen in glucose metabolisme tussen verschillende soorten niet-kleincellige longkanker. Adenocarcinomen lijken gebruik te maken van glycolyse onder normoxische omstandigheden, dichtbij de vaten terwijl plaveiselcel carcinomen meer blootgesteld zijn aan diffusie gelimiteerde hypoxie wat resulteert in een hoge anaërobe glycolyse. Patiënten met een adenocarcinoom hadden een slechtere ziekte vrije overleving en vertoonden meer metastasen. Vraag blijft waarom patiënten met een plaveiselcelcarcinoom met een hoge mate van glucose metabolisme een betere prognose hadden dan patiënten met een adenocarcinoom. Mogelijk leidt hoge MCT4 expressie en verhoogde lactaatconcentratie nabij de bloedvaten in de adenocarcinomen tot een relatief gunstig tumor micromilieu dat aanzet tot tumorcel migratie en metastasering.

Moleculaire Imaging

Moleculaire imaging technologieën, zoals [18]FDG-PET, kunnen worden ingezet als een non-invasieve methode voor het kwantificeren van de metabole status van een tumor. [18]FDG-PET wordt door toegenomen glycolyse en glucose opname door tumorcellen als een waardevolle imaging biomarker gezien in solide tumoren.[4] [18]FDG opname in tumorcellen is multifactorieel bepaald en dus staat verhoogde [18]FDG opname niet direct gelijk aan weefsel hypoxie. [18]FDG-opname zou als een surrogaat marker voor weefsel hypoxie kunnen gelden indien onder hypoxische omstandigheden aerobe glycolyse tot meer glucose opname via de glucose transporters leidt (Pasteur effect). Echter verhoogde glucose opname door de cel kan ook optreden in gebieden met een hoge proliferatie en dus meer behoefte aan

energie.[4] Bovendien is glycolyse in normoxische omstandigheden een wezenlijk kenmerk van kwaadaardige tumoren.

[18]FDG-PET heeft als voordeel dat het breed geïmplementeerd is in de diagnostiek en stadiering van kanker en van grote klinische waarde is gebleken bij de work-up van patiënten met longkanker. Studies hebben laten zien dat [18]FDG-PET bij 18% van de patiënten met een klinisch stadium I en II onverwacht afstandsmetastasen aantoont.[5] Daarnaast is [18]FDG-PET een prognostische indicator bij niet kleincellige longkanker. Hoge [18]FDG opname is geassocieerd met een slechtere overleving in patiënten met niet-kleincellige longkanker.[6, 7, 8]

In dit proefschrift wordt getoond dat [18]FDG opname hoger is in de plaveiselcel carcinomen in vergelijking met adenocarcinomen. Met dezelfde [18]FDG-opname hadden patiënten met een andeocarcinoom echter een slechtere prognose. Dit maakt aannemelijk dat de interpretatie van [18]FDG-PET met betrekking tot glucose metabolisme, als prognostische indicator en ter verkenning van behandel strategieën, in relatie tot histologie zou moeten gebeuren. Daarnaast lijkt [18]FDG-PET een waardevol hulpmiddel in het onderscheiden van metastasen en tweede primaire tumoren. [18]FDG-opname zou kunnen helpen bij het karakteriseren van synchrone tumoren in de long, ervan uitgaande dat tumoren met een gedeelde clonale oorsprong (zoals bij metastasen) zich vaak op dezelfde manier gedragen en gemeenschappelijke histologische kenmerken hebben. In ons cohort bleek het mogelijk om op grond van een bepaalde cut-off waarde onderscheid te maken tussen tweede primaire tumoren en gemetastaseerde ziekte. In toekomstig onderzoek zou dit verder prospectief gevalideerd kunnen worden door een vergelijking te trekken met weefsel diagnostiek.

Patiënten met een vergrote [18]FDG-PET positieve linker bijnier hebben een hoge suspectie op bijniermetastasen. Echter, om te voorkomen dat patiënten een mogelijk curatieve therapie onthouden wordt, is het noodzakelijk om de metastase PA bevestigd te krijgen. In ons cohort van patiënten met een hoge vooraf kans op maligniteit werden metastasen in de linker bijnier in 62% van de patiënten aangetoond door EUS-FNA. Helaas ondergingen niet alle patiënten in deze studie een [18]FDG-PET in de diagnostische work-up. Het zou interessant kunnen zijn om in een nieuwe studie deltaSUV metingen tussen de primaire tumor en de [18]FDG-PET positieve linker bijnier te vergelijken met resultaten van de EUS-FNA van de bijnier.

Tegenwoordig focust klinisch onderzoek met [18]FDG-PET zich onder andere meer op het voorspellen van therapierespons en uitkomst van behandeling. Er ligt een uitdaging in het voorspellen van respons op therapie vroegtijdig tijdens het behandeltraject waardoor de behandel strategie kan worden aangepast voor de individuele patiënt en mogelijk onnodige toxiciteit van een ineffectieve behandeling wordt voorkomen.

Minimaal invasieve stadiërings technieken

Endo-echografie heeft zijn nut in de diagnostiek en stadiëring van longkankerpatiënten inmiddels ruim bewezen. EUS en EBUS zijn sinds 1998 en 2004 commercieel beschikbaar en inmiddels cruciaal in longkanker stadiërings algoritmen. Er is veel onderzoek gedaan dat de

inzetbaarheid van EUS en/of EBUS bij pathologische lymfeklieren geïdentificeerd met CT en/of PET (vergrote of ^{18}FDG-PET positieve klieren) en kleine of ^{18}FDG-PET negatieve lymfeklieren ondersteund. De resultaten zijn ook vergeleken met de gouden standaard: de cervicale mediastinoscopie voor EUS alleen, EBUS alleen en in patiënten die CUS ondergingen (gecombineerde EUS en EBUS). Een systematische review en meta-analyse naar de waarde van EUS bij de mediastinale stadiering van longkankerpatiënten toonde een sensitiviteit van 90% en een negatief voorspellende waarde (NPV) van 78% in pathologisch vergrote lymfeklieren (> 1 cm). Voor kleinere lymfklieren was de sensitiviteit 58% en de NPV 81%.[9] Meta-analyses naar de waarde van EBUS bij de mediastinale diagnostiek van longkankerpatiënten laten een sensitiviteit van 85-93% zien.[10, 11, 12] Combinatie van EBUS en EUS had een sensitiviteit van 93% met een NPV van 97% welke zeer hoog is in vergelijking met een NPV van 89% voor de mediastinoscopie die wordt beschouwd als de gouden standaard.[13] Bij patiënten met een radiologisch onverdacht mediastinum was dit 68-76% en 91-94% respectievelijk.[14]

In de ASTER trial (een prognostische multicenter gerandomiseerde trial) werd de cervicale mediastinoscopie voorafgegaan door gecombineerde EUS en EBUS (CUS) vergeleken met een cervicale mediastinoscopie (CM) alleen bij patiënten met longkanker met vergrote en/of ^{18}FDG-PET positieve mediastinale/hilaire klieren danwel een centrale tumor. De sensitiviteit voor de detectie van mediastinale metastasen was 80% voor de cervicale mediastinoscopie versus 94% voor CUS (p = 0.04) met een NPV van 86% voor de cervicale mediastinoscopie en 93% voor CUS. Het aantal zinloze thoracotomieën was lager in de CUS arm (7% v 18%, p = 0.009) en complicaties waren vergelijkbaar. Het aantal patiënten dat nodig was om een mediastinale metastase vast te stellen met een cervicale mediastinoscopie na een negatieve CUS bedroeg 11.[15]

Andere indicaties voor endo-echografie liggen in de diagnostiek van primaire tumoren in longkankerpatiënten, [16, 17] het diagnosticeren van metastasen van andere solide tumoren[18] en zoals blijkt uit dit proefschrift, het aantonen van een metastase in de linker bijnier. Bij patiënten met een vergrote en/of ^{18}FDG-PET positieve linker bijnier werd een metastase van longkanker bewezen bij 62% van de patiënten, in 2% werd een andere maligniteit gevonden en bij 29% van de patiënten werd goedaardig bijnier weefsel aangetroffen. Bij 5,9% van de patiënten bleek EUS-FNA geen representatief weefsel en dus geen diagnose op te leveren. Met deze studie werd bevestigd dat EUS-FNA van de linker bijnier een veilige en minimaal invasieve methode is voor het vaststellen van bijnier metastasen bij patiënten met longkanker.

Moleculaire diagnostiek en targeted therapy

In het laatste decennium is vooruitgang geboekt bij de systemische behandeling van patiënten met niet-kleincellige longkanker. Behandel strategieën worden steeds meer een therapie op maat hetgeen tot dusver met name het geval is voor adenocarcinoom of grootcellig carcinoom. Er is bewijs dat histologie mogelijk prognostisch of predictief is voor

de klinische uitkomst. Dit is na te lezen in een review door Hirsch en collega's.[19] Een consistent verband tussen histologie en uitkomst van behandeling is vastgesteld voor EGFR tyrosine kinase remmers.[19] Verschillen in de overleving met betrekking tot histologie werd ook aangetoond voor eerste lijns chemotherapie behandeling met pemetrexed.[20] Recentelijk zijn behandelschema's voor patiënten met niet-kleincellige longkanker verschoven van louter histologie gebaseerde behandeling naar behandeling gestuurd door moleculaire eigenschappen. Dit is momenteel vooral het geval voor longkankerpatiënten met een adenocarcinoom. Meestal is er sprake van driver gen mutaties in het oncogen (dat leidt tot ongebreideld actieve eiwitten) zoals EGFR, HER2, KRAS, ALK, BRAF, PIK3CA, AKT1, ROS1, NRAS en MAP2K1. Dit soort driver gen mutaties komen niet gezamenlijk voor met uitzondering van PIK3CA mutaties die tegelijk met EGFR of KRAS mutatie kunnen optreden. Longkanker patiënten met een adenocarcinoom met dergelijke mutaties zijn mogelijk sensitief voor targeted therapy met een substantiële klinische winst. [21] Voorbeelden zijn tyrosine kinase-remmers zoals gefitinib en erlotinib in EGFR positieve patiënten en crizotinib bij patiënten met EML4-ALK of ROS1 fusies.[19, 22]

Tot op heden heeft de helft van alle niet-kleincellige longkankers geen bekend klinisch relevant oncogen.[21] De laatste jaren zijn er nieuwe targets gevonden bij longkanker maar met name voor het plaveiselcel carcinoom is dit nog beperkt. Eerste lijns chemotherapie is nog steeds de standaard behandeling voor longkanker patiënten met een plaveiselcel carcinoom (pcc). Potentiële toekomstige moleculaire targets bij plaveiselcel carcinomen zijn fibroblast groeifactor receptor 1 (FGFR1 22% van de pcc), discoidin domein receptor 2 (DDR2 4%), BRAF (2%), PIK3CA (mutaties 2-3% en amplificatie bij 33%), AKT1 (1%), MET (1%), EML4-ALK fusie (1%).[23]

Tijdens de behandeling ontstaat er eigenlijk altijd geneesmiddel resistentie. Bij 37 patiënten met een EGFR mutatie behandeld met een EGFR tyrosine kinase remmer en verworven resistentie werd een hernieuwde biopsie uitgevoerd. Alle tumoren behielden hun activerende EGFR mutaties en enkele verkregen een bekend resistentie mechanismen zoals *EGFR* T790M mutatie of *MET* amplificatie en overige verworven mutaties zoals bij het *PIK3CA* gen. Bij 14% van de patiënten was er een histologische transformatie opgetreden naar kleincellige longkanker (SCLC) gevoelig voor de gebruikelijke chemotherapie.[24] Wanneer progressie wordt gezien bij hernieuwde beeldvorming moet overwogen worden of er resistentie is opgetreden tegen de huidige targeted therapy en kan hernieuwde weefselafname worden overwogen om verdere behandel beslissingen te sturen.

De meeste moleculaire analyses worden uitgevoerd op histologisch materiaal. De uitdaging ligt in de verbetering van technieken die geschikt zijn voor onderzoek op cytologisch materiaal. In patiënten met gevorderde longkanker is vaak alleen cytologie voorhanden. Wanneer nieuw tumor materiaal nodig is bij gevorderde longkanker, is minimaal invasieve diagnostiek zoals EUS, EBUS en echografische danwel CT geleide punctie een relatief patiënt vriendelijke methode. In dit proefschrift werd aangetoond dat cytologisch materiaal verkregen met EUS of EBUS zich goed leent voor moleculaire analyse in 77% van

onderzochte monsters. Verder inzicht in metabole kanker processen biedt de mogelijkheid om selectief gerichte therapie in te zetten.

Toekomstperspectief

Dit proefschrift weerspiegelt een multidisciplinaire kijk op onderzoek naar tumor metabolisme en toont ook een persoonlijke interesse in endo-echografie als interventie en oncologisch longarts. De kracht van toekomstig onderzoek ligt in een multidisciplinaire samenwerking waarbij non-invasieve (beeldvormende) en invasieve technieken bij elkaar komen. Toekomstig onderzoek zou verschillen in het metabolisme tussen adeno- en plaveiselcel longcarcinomen verder kunnen exploreren. Non-invasieve meting van weefsel lactaat in dezelfde groep van longkanker patiënten zou onze hypothese kunnen ondersteunen dat adenocarcinomen gebruik maken van aërobe glycolyse met op regulatie van MCT4 in de nabijheid van de vaten. Men zou kunnen verwachten dat hogere lactaat concentraties het risico op metastasering vergroten. Kwantificering van [18]FDG-PET opname in adenocarcinomen en plaveiselcel carcinomen in relatie tot het effect van adjuvante chemotherapie behandeling zou een interessante subvraag kunnen zijn van een nationale prospectieve studie naar het effect van adjuvante chemotherapie in patiënten geopereerd aan lonkanker (NVALT 8). Het verschil in [18]FDG-PET opname tussen synchrone primaire tumoren en metastasen in onze retrospectieve analyse zou prospectief gevalideerd kunnen worden in een vervolgstudie welke [18]FDG-PET opname en histologie vergelijkt. Dit zou ook gedaan kunnen worden in longkankerpatiënten met een mogelijke bijniermetastase. De waarde van [18]FDG-PET als een voorspellende factor vroeg tijdens behandeling van patiënten met stadium III NSCLC behandeld met concurrent chemoradiotherapie wordt momenteel onderzocht in een prospectieve studie (early response measurement bij NSCLC).

Referenties

1. Warburg O, Posener K, Negelein E. Ueber den stoffwechsel der tumoren. In: Warburg O, editor. Constable, London; 1930.

2. Ward PS, Thompson CB. Metabolic reprogramming: a cancer hallmark even Warburg did not anticipate. Cancer Cell 2012;21:297-308.

3. Teicher BA, Linehan WM, Helman LJ. Targeting cancer metabolism. Clinical Cancer Research 2012;18:5537-5545.

4. Busk M, Horsman MR, Jakobsen S, et al. Cellular uptake of PET tracers of glucose metabolism and hypoxia and their linkage. Eur J Nucl Med Mol Imaging. 2008;35:2294-2303.

5. Silvestri GA, Gould MK, Margolis ML et al. Noninvasive staging of non-small cell lung cancer: ACCP evidenced-based clinical practice guidelines (2nd edition). Chest 2007;132:178S-201S.

6. Vansteenkiste JF, Stroobants SG, Dupont PJ, De Leyn PR, Verbeken EK, Deneffe GJ, et al. Prognostic importance of the standardized uptake value on (18)F-fluoro-2-deoxy-glucose-positron emission tomography scan in non-small cell lung cancer: an analysis of 125 cases. Leuven Lung Cancer Group. J Clin Oncol 1999;17:3201-3206.

7. de Geus-Oei LF, van der Heijden HF, Corstens FH, et al. Predictive and prognostic value of FDG-PET in nonsmall-cell lung cancer: a systematic review. Cancer 2007;110:1654-1664.

8. Liao S, Penney BC, Wroblewski K, et al. Prognostic value of metabolic tumor burden on 18F-FDG PET in nonsurgical patients with non-small cell lung cancer. Eur J Nucl Med Mol Imaging 2012;39:27-38.

9. Micames CG, McCrory DC, Pavey DA, Jowel PS, Gress FG. Endoscopic ultrasound-guided fine-needle aspiration for non-small cell lung cancer staging. A systematic review and meta-analysis. Chest 2007;131:539-548.

10. Gu P, Zhao YZ, Jiang, LY, Zhang W, Xin Y, Han BH. Endobronchial ultrasound-guided transbronchial needle aspiration for staging of lung cancer: a systematic review and meta-analysis. Eur J Cancer 2009;45:1389-1396.

11. Adams K, Shah PL, Edmonds L, Lim E. Test performance of endobronchial ultrasound and transbronchial needle aspiration biopsy for mediastinal staging in patients with lung cancer: systematic review and meta-analysis. Thorax 2009;64:757-762.

12. Varela-Lema L, Fernandez-Villar A, Ruano-Ravina A. Effectiveness and safety of endobronchial ultrasound-transbronchial needle aspiration: a systematic review. Eur Respir J 2009;33:1156-1164.

13. Wallace MB, Pascual JM, Raimondo M, Woodward TA, McComb BL, Crook JE, et al. Minimally invasive endoscopic staging of suspected lung cancer. JAMA 2008;299:540-546.

14. Szlubowski A, Zielinski M, Soja J, Annema JT, Sosnicki W, Jakubiak M, et al. A combined approach of endobronchial and endoscopic ultrasound-guided needle aspiration in the radiologically normal mediastinum in non-small cell lung cancer staging: a prospective trial.

Eur J Cardiothorac Surg 2010;37:1175-1179.

15. Annema JT, van Meerbeeck JP, Rintoul RC, Dooms C, DeschepperE, de Leyn P, et al. Mediastinoscopy vs endosonography for mediastinal nodal staging of lung cancer: a randomized trial. JAMA 2010;304:2245-2252.

16. Annema JT , Veseliç M, Rabe KF. EUS-guided FNA of centrally located lung tumours following a non-diagnostic bronchoscopy. Lung Cancer 2005;48:357-61.

17. Tournoy KG, Rintoul RC, van Meerbeeck JP, Carrol NR, Praet M, Buttery RC, et al. EBUS-TBNA for the diagnosis of central parenchymal lung lesions not visible with a routine bronchoscopy. Lung Cancer 2009;63:45-49.

18. Peric P, Schuurbiers OCJ, Veseliç M, Rabe KF, van der Heijden HFM, Annema JT. Transoesophageal endoscopic ultrasound-guided fine-needle aspiration for the mediastinal staging of extrathoracic tumors: a new perspective. Ann Oncol 2010;21:1468-1471.

19. Hirsch FR, Spreafico A, Novello S, et al. The prognostic and predictive role of histology in advanced non-small cell lung cancer: a literature review. J Thorac Oncol. 2008;3:1468-1481.

20. Al-Saleh K, Quinton C, Ellis PM. Role of pemetrexed in advanced non-small-cell lung cancer: meta-analysis of randomized controlled trials, with histology subgroup analysis. Curr Oncol. 2012;19:e9-e15.

21. Pao W, Hutchinson KE. Chipping away at the lung cancer genome. Nature Medicine 2012;18:349-351.

22. Kwak EL, Bang YJ, Camidge DR, Shaw AT, Solomon B, Maki RG, et al. Anaplastic lymphoma kinase inhibition in non-small cell lung cancer. NEJM 2010;363:1693-1703.

23. Perez Moreno P, Brambilla E, Thomas R, Soria JC. Squamous cell carcinoma of the lung: molecular subtypes and therapeutic opportunities. Clin Cancer Rese 2012;18:2443-2451.

24. Sequist LV, Waltman BA, Diad-Santagata D, Digumarthy S, Turke AB, Fidias P et al. Genotypic and histological evaluation of lung cancers acquiring resistance to EGFR inhibitors. Sci Transl Med 2011;3:75ra26.

Dankwoord

Dit proefschrift is een afronding van een periode maar ik zie het ook als een mooie basis voor verdere multidisciplinaire samenwerking binnen de thoracale oncologie. ik wil iedereen die heeft bijgedragen hartelijk danken en een paar mensen in het bijzonder.

Allereerst wil ik mijn dank uitspreken aan alle patiënten die de basis gevormd hebben voor de studies in dit proefschrift. Tijdens mijn werk binnen de keten longoncologie en longchirurgie word ik geregeld geconfronteerd met de persoonlijke verhalen van mijn patiënten. Deze verhalen zijn stuk voor stuk speciaal en maken dat er met velen een persoonlijke band ontstaat tijdens het vervolg op de polikliniek. Dat maakt de beleving van mijn dagelijkse werk bijzonder en ik hoop dat de studies in dit proefschrift en in de toekomst een bijdrage kunnen leveren aan het verbeteren van de vooruitzichten van longkankerpatiënten.

Prof. Richard Dekhuijzen, dank voor je ondersteuning en vertrouwen tijdens mijn wetenschappelijke vorming en de vorming tot de medisch specialist die ik nu ben. Je weet me altijd goed te helpen bij het vinden van de 'rode draad'. Ik heb je steun en betrokkenheid immer erg gewaardeerd: dank hiervoor.

Promotoren Prof. Hans Kaanders, Prof. Wim Oyen, Prof. Richard Dekhuijzen en copromotoren Jan Bussink en Erik van der Heijden, ik heb de verschillende uurtjes die we samen hebben doorgebracht om te brainstormen over de onderzoekslijnen steeds erg fijn gevonden. De multidisciplinaire inbreng en jullie enthousiasme hebben me enorm geholpen bij de totstandkoming van dit proefschrift. Ook de vele researchbesprekingen met Jan Bussink, Erik van der Heijden en Lioe-Fee de Geus-Oei waren erg waardevol en hielpen me zeer om op gang te blijven.

Tineke Meijer, hartelijk dank voor de samenwerking. Het was inspirerend om gezamenlijk de studies die voortkwamen uit de weefselbank longtumoren te doen. Nog veel succes bij de afronding van je eigen proefschrift.

Analisten op het lab van de radiotherapie en bij de nucleaire geneeskunde ook bedankt voor jullie ondersteuning bij de analyses en geduldige uitleg! Monika Looijen bedankt voor je hulp bij de analyse van de PA coupes.

Jouke Annema, ik wil jou hartelijk danken voor je hulp bij de opleiding tot 'endo-echografist'. Ik heb het zeer gewaardeerd dat je me eigen hebt gemaakt in de wereld van EUS en EBUS. De samenwerking op wetenschappelijk gebied kwam als vanzelf en je steun hierbij was ontzettend fijn. Het gaf me de kans om in dit proefschrift ook iets te laten zien

van mijn bijzondere 'hobby' endo-echografie.

Erik van de Heijden, jou wil ik speciaal bedanken voor al je steun. Naast de researchbesprekingen, was het fijn om met je te kunnen sparren. Ook door het overnemen van uren patiëntenzorg op het endo-echoprogramma en de preoperatieve poli longchirurgie maakte je het voor me mogelijk om ruimte en tijd te creëren voor mijn onderzoek. Je hebt tijdens mijn opleiding in belangrijke mate bijgedragen aan mijn liefde voor de endo-echografie en de longoncologische zorg. Samen met jou, Miep van der Drift en Chantal Smits- van der Graaf is de longoncologie in het Radboud UMC goed op de kaart gekomen. Ik vind dat we een ontzettend leuk en enthousiast team vormen en hoop op een langdurige, plezierige en vruchtbare samenwerking samen met onze verpleegkundig specialisten. De multidisciplinaire samenwerking met onze partners binnen de thoracale oncologie heeft een goede en bovenal erg prettige basis om ons verder te ontwikkelen binnen de patiëntenzorg en wetenschappelijk onderzoek.

Nicolle Peters, ik ben ontzettend blij geweest met jouw komst. Als verpleegkundig specialist neem je me veel werk uit handen. Je bent een ontzettend lief en betrokken mens. Ons enthousiasme voor de thoracale chirurgie werkt volgens mij synergistisch en ik hoop dat we nog lang samen mogen werken aan het blijvend optimaliseren van de longchirurgische patiënten zorg.

Dit proefschrift was nooit tot stand gekomen als ik niet een goede balans had gevonden tussen werk, wetenschap en privéleven. Door lekker te sporten lukt het om mijn hoofd leeg te maken. Ook de gezellige activiteiten met mijn vrienden uit Abcoude, Dick en Marije en de vele spontane borrels, BBQs, concerten, tripjes naar Milaan, Madrid en Maastricht met de buurtjes uit de straat houden het leven aangenaam.

Pap en mam, jullie ontzettend bedankt voor jullie steun. Door jullie opvoeding ben ik wie ik ben. Jullie hebben me geleerd om respect te hebben voor de mens en hebben me altijd gestimuleerd in de dingen die ik doe. Ik kijk met warme gevoelens terug naar mijn jaren thuis en waardeer jullie betrokkenheid en steun nog steeds. Ik hou van jullie!

Bart en Claudine, ik heb jullie gevraagd als paranimfen omdat ik het fijn vind dat jullie op deze dag bij me staan. Eigenlijk is dit altijd al het geval geweest: jullie staan altijd voor me klaar en dat is een fijn gevoel! Dank je wel.

Lieve Pim, ontzettend bedankt voor je steun en eindeloze geduld met mij. Zonder jou was dit nooit gelukt. Ik ben ontzettend blij dat we elkaar 25 jaar geleden ontmoet hebben. Dat is ook een mijlpaal die we dit jaar vieren. Bij jou voel ik me nog altijd een meisje en ik vind het supergezellig met jou! En Sophie en Max, jullie zijn echt de kroon op mijn leven. Jullie zijn twee schatten van kinderen en ik hou superveel van jullie!

Curriculum Vitae

Olga CJ Schuurbiers is geboren op 28 april 1970 in het Radboud Ziekenhuis te Nijmegen. In 1988 behaalde zij haar VWO diploma in Nijmegen. Ze studeerde een jaar psychologie en behaalde haar propedeuse aan de Katholieke Universiteit Nijmegen omdat ze was uitgeloot voor de studie geneeskunde. In 1989 startte zij alsnog met de studie geneeskunde. In het kader van de studie werd een onderzoekstage gedaan bij de afdeling pathologie in samenwerking met de gynaecologie. Dit betrof een update van de Nederlandse registratie clear cell adenocarcinoom van de vagina en cervix bij DES dochters en niet DES dochters. In 1996 werd het artsexamen cum laude behaald.

Vanaf 1996 werkte zij als arts-assistent in een verpleeghuis van de Dubois Stichting te Venlo waarbij zij werkzaam was op de somatische en psychogeriatrische afdeling, de somatische dagbehandeling en in het verpleeghuis voor jongeren (de Witte Steen). Na hier met veel plezier en toewijding gewerkt te hebben, startte zij in 1998 als arts-assistent niet in opleiding op de afdeling longziekten van het VieCuri Medisch Centrum te Venlo. Zij solliciteerde voor de opleiding tot longarts bij de afdeling longziekten in het Universitair Medisch Centrum Nijmegen waar zij in 1999 enkele maanden heeft gewerkt als arts-assistent niet in opleiding tot de start van de interne vooropleiding in 2000 in het Catharina Ziekenhuis te Eindhoven. Van 2002 – 2006 werd de opleiding tot medisch specialist vervolgd in het Universitair Medisch Centrum Nijmegen waarna zij vanaf 1 januari 2006 deel uitmaakte van de medische staf longziekten. Wegens haar interesse in de longoncologie werd er onder begeleiding van prof. dr. Richard Dekhuijzen samen met de afdeling radiotherapie, prof. dr. Hans Kaanders en nucleaire geneeskunde, prof. dr. Wim Oyen, een basis gelegd voor multidisciplinair oncologisch onderzoek hetgeen geleid heeft tot dit proefschrift. Tevens werd in dit samenwerkingsverband een studie opgestart naar early response measurement bij patiënten met stadium III longkanker die behandeld worden met concurrent chemoradiotherapie, welke inmiddels geanalyseerd wordt en tevens de basis vormde voor een vervolgstudie voor deze patiënten categorie.

Als medisch specialist ligt haar focus en hart ook bij de thoracale oncologie en in het bijzonder bij de thoracale chirurgie en thoracale endoscopie/echografie. Zij is nauw betrokken, samen met haar oncologisch georiënteerde collega longartsen, binnen de keten thoracale oncologie. Ze ontwikkelde/optimaliseerde het zorgpad thoracale chirurgie waarbij een sterke affiniteit bestaat voor optimalisatie van kwaliteit, logistiek en patiëntveiligheid. Daarnaast volgde zij in 2006 gedurende enkele maanden een training in EUS en later ook EBUS bij Jouke Annema aan het Leids Universitair Medisch Centrum. De thoracale endoscopie en echografie worden vanaf december 2005 uitgeoefend in nauwe samenwerking met Erik van de Heijden binnen het Endo-Echocentrum Nijmegen.

Ze leerde haar echtgenoot Pim Siebers op het eindexamen feest van de middelbare school kennen in 1988. Ze wonen samen sinds 1991. Zij hebben twee schatten van kinderen: Sophie (2002) en Max (2005). Sinds 2006 zijn ze gelukkig getrouwd.

Bibliography

Jan Theys, Sanaz Yahyanejad, Roger Habets, Paul Span, Ludwig Dubois, Kim Paesmans, Bo Kattenbeld, Jack Cleutjens, Arjan J. Groot, Olga C.J. Schuurbiers , Philippe Lambin, Jan Bussink, Marc Vooijs. High NOTCH activity induces radiation resistance in non small cell lung cancer. Radiother Oncol.2013; doi:pii:S0167-8140(13)00299-5.10.1016.

Ad F. Verhagen, Olga C. J. Schuurbiers, Monika G. Looijen-Salamon, Stefan M. van der Heide, Henry A. van Swieten and Erik H. F. M. van der Heijden. Mediastinal staging in daily practice: endosonography, followed by cervical mediastinoscopy. Do we really need both? Interact Cardiovasc Thorac Surg. 2013; doi: 10.1093/icvts/ivt302.

Usmanij EA, de Geus-Oei LF, Troost EGC, Peters-Bax L, van der Heijden HFM Kaanders JHAM, Oyen WJG, Schuurbiers OCJ, Bussink J.[18]F-FDG-PET early response evaluation of locally advanced Non-Small Cell Lung Cancer treated with concomitant chemo-cadiotherapy. J Nucl Med. 2013 Sep;54(9):1528-34.

Ingrid J Kleiss, Ad F T M Verhagen, Jimmie Honings, Olga C J Schuurbiers, Henricus F M van der Heijden, Henri A M Marres. Tracheal surgery for benign tracheal stenosis: our experience in 63 patients. Clin Otolaryngol. 2013 Aug;38(4):343-7.

Mourisse J, Liesveld J, Verhagen AFTM, van Rooij G, van der Heide SM, Schuurbiers OCJ, van der Heijden HMF. Efficiency, Efficacy and Safety of EZ-Blocker compared to Left-sided Double-Lumen Tube for One-lung Ventilation. Anesthesiology. 2013 Mar;118(3):550-61.

Van der Heijden HFM, Looijen-Salamon MG, Schuurbiers OCJ, Bussink J, Ligtenberg MJL. EBUS and EUS guided fine needle aspirations for molecular diagnostic analysis in lung cancer. Thoracic Cancer 2012; 3: 201-206.

Govaert SLA, Troost EGC, Schuurbiers OCJ, de Geus-Oei LF, Termeer A, Span PN, Bussink J. Treatment outcome and toxicity of intensity-modulated (chemo)radiotherapy in stage III non-small cell lung cancer patients. Radiat Oncol 2012;7(1):150.

Meijer TWH, Schuurbiers OCJ, Kaanders JHAM, Looijen-Salamon MG, de Geus-Oei LF, Verhagen AFTM, Lok J, van der Heijden HFM, Rademakers SE, Span PN, Bussink J. Differences in metabolism between adeno- and squamous cell non-small cell lung carcinomas: spatial distribution and prognostic value of GLUT1 and MCT4. Lung Cancer 2012; 76(3):316-23.

Schuurbiers OCJ, Tournoy KG, Schoppers HJ, Dijkman BG, Timmers HJLM, de Geus-Oei LF, Grefte JMM, Rabe KF, Dekhuijzen PNR, van der Heijden HFM, Annema JT. EUS-FNA for the detection of left adrenal metastasis in patients with lung cancer. Lung Cancer 2011;73(3):310-5.

Schuurbiers OCJ, Looijen-Salamon MG, Ligtenberg MJL, van der Heijden HFM. A brief retrospective report on the feasibility of epidermal growth factor receptor and KRAS mutation analysis in transesophageal ultrasound- and endobronchial ultrasound-guided fine needle cytological aspirates. J Thorac Oncol 2010;5(10):1664-7.

Dijkman BG, Schuurbiers OCJ, Vriens D, Looijen-Salamon MG, Bussink J, Timmer-Bonte JNH, Snoeren MM, Oyen WJG, van der Heijden HFM, de Geus-Oei LF. The Role of F-18-FDG-PET in the differentiation between lung metastases and synchronous second primary lung tumors. EJNM 2010;37(11):2037-2047.

Peric R, Schuurbiers OCJ, Veselicx M, Rabe KF, van der Heijden HFM, Annema JT. Transesophageal endoscopic ultrasound-guided fine-needle aspiration for the mediastinal staging of extrathoracic tumors: a new perspective . Ann Oncol 2010;21(7):1468-71.

Schuurbiers OCJ, Kaanders JHAM, van der Heijden HFM, Oyen WJG, Dekhuijzen PNR, Bussink J. The PI3-K/AKT-pathway and radiation resistance mechanisms in non-small cell lung cancer. J Thorac Oncol 2009;4:761-767.

Schuurbiers OCJ, Schermer TR, Dekhuijzen PNR, van Weel C. Tiotropium, a long-acting bronchodilating agent for the treatment of COPD. Ned Tijdschr Geneeskd 2006;150(22):1227-32.

Thunnissen FB, Schuurbiers OCJ, den Bakker MA. A critical appraisal of prognostic and predictive factors for common lung cancers. Histopathology 2006;48(7):779-86.

Hanselaar A, van Loosbroek M, Schuurbiers OCJ, Helmerhorst T, Bulten J, Bernhelm J. Clear cell adenocarcinoma of the vagina and cervix. An update of the central Netherlands registry showing twin age incidence peaks. Cancer 1997;79(11):2229-36.